PHD THESIS

The Action Potential Duration And Repolarization Of The Human Ventricle And Its Relation To The Body Surface ECG

Submitted To University College London, In Part Fulfilment For The Degree Of Doctor Of Philosophy

Primary Supervisor: Professor Pier Lambiase

Secondary Supervisor: Dr Ben Hanson

UCL Institute Of Cardiovascular Science

January 2018

Dr Neil Thomas Srinivasan

BSc, MBChB, MRCP

BHF Clinical Research Fellow

UCL & The Barts Heart Centre

Declaration

I, Neil Thomas Srinivasan confirm that the work presented in this thesis is my own. Where information has been derived from other sources, I confirm that this is indicated in the thesis.

Neil Thomas Srinivasan

Date: 6 January 2018

Abstract

Repolarization dispersion has been associated with increased risk of cardiac arrhythmia in animal studies, but whether it is present in humans and how its manifests on the surface ECG is unknown. This thesis aimed to bridge the gap between our basic cellular and intracardiac understanding of cardiac electrical activity with the surface ECG focusing specifically on cardiac repolarization and the surface ECG.

Restitution studies in humans with structurally normal and abnormal hearts were performed, looking at transmural and regional gradients of repolarization. The data were then analysed to assess the association of intracardiac repolarization with the surface T-wave. Finally a novel non-invasive ECG (ECGI) was used to study the electrical substrate in patients with arrhythmogenic right ventricular cardiomyopathy (ARVC).

In normal human heart restitution studies epicardial APD was shorter than endocardial APD, with smaller differences in the apicobasal orientation. It was found that, local repolarization times in the right and left ventricle occur along the upslope of the body surface T-wave in leads V1-V3 and V5,V6 and Lead-I respectively; and the difference between the end of the upslope in V1 and V6 provides a good representation of right to left dispersion of repolarization.

In patients with structurally abnormal hearts myocardial scar, regardless of pathology, resulted in prolonged APD compared to normal healthy tissue diminishing transmural gradients of APD and resulting in localised transmural dispersion of repolarization.

Finally ECGI characterised the electrophysiological substrate in ARVC, demonstrating prolonged APD in these patients compared to control patients. ECGI was able to demonstrate the presence of electrophysiological changes before changes were visible on cardiac MRI.

In conclusion, this work shows that APD gradients are present in the intact human heart, and can be demonstrated both using contact electrophysiological mapping and on methods that incorporate the body surface ECG.

Table Of Contents

Table Of Figures

Grants And Ethics Applications Relating To This Thesis

Grants

Utilisation of Advanced High Density Surface ECG Mapping to Improve Diagnosis & Ablation Outcomes in Inherited Cardiovascular Disease & Complex Arrhythmia Patient.

BHF Clinical Research Training Fellowship - FS/14/9/30407

I wrote the application for this grant under the guidance of my primary and secondary supervisors. I responded to the reviewers comments with a rebuttal and was awarded this nationally competitive funding to complete my thesis.

Utilisation of Advanced High Density Surface ECG Mapping to Improve Diagnosis & Ablation Outcomes in Inherited Cardiovascular Disease & Complex Arrhythmia Patient - BRC200 rev/CM/PL/ 101320

I wrote the application for this grant and was awarded £77,544 to purchase the ECGI research system.

Ethical Applications

Dynamic Conduction-Repolarisation Interactions in Ventricular Arrhythmogenesis: The role of the autonomic nervous system & ion channel function in human and murine hearts - 10/H0715/19 - IRAS ID 38478

I wrote the ethical application for this study and performed substantial amendments to enable me to perform my research in normal hearts and in patients with ventricular tachycardia. I was interviewed by the research ethics committee as part of the process.

Multi-Lead ECG analysis of ventricular depolarization and repolarization characteristics of inherited cardiac diseases - 14/LO/0360 - IRAS ID 144257

I wrote the ethical application for this study and performed substantial amendments to enable me to perform my research using ECGI. I was interviewed by the research ethics committee as part of the process. I have subsequently made further amendments which have enabled our team to perform this research in other centers.

Acknowledgements

The work described in this thesis was generously supported by the British Heart Foundation through the award of a Clinical Research Training Fellowship.

Primary academic thanks must go to Professor Pier Lambiase for his excellent supervision throughout. Without his shared enthusiasm for this mechanistic research project, this would never have got off the ground. His continued unyielding support throughout has been an inspiration. My "wing-man" Dr Michele Orini, who shared many late nights with me debating APD heterogeneity in the ventricle, among other things, and flew round the world with me to do the work and present at conferences. It was the best time of our lives. Thanks also to Professor Peter Taggart, an honour to work with a godfather of the field. Nurses, Carolyn Brennan and Eileen Firman for their help and guidance while sharing an office with me for three years. Those were great days I shall always cherish, and taught me many of life's wisdoms. A special thanks to all the clinical staff at the old "Heart Hospital" and The Barts Heart Centre for helping perform the cath lab work, with a special mention to Dr Ron Simon who did almost all the restitution studies with me. A kind hearted man who clearly shares a passion for research. We always forget the nurses and physiologists who stayed late and suffered through endless restitution curves, and they deserve a special mention. Too many to name individually. Finally a thanks to Christopher Andrews and Dr Yoram Rudy for their collaboration in the ARVC ECGI project, it was a wonderful experience to work in Washington University St Louis, and an honour to get to personally meet and know the great Dr Rudy; a man who's ground breaking computer model I worked on over fifteen years ago. I never thought I would get to meet or work with him, and to share a paper with him is a true honour. One of the greats. Stefania Rosmini and Heerajnarain Bulluck did the MRI work for that study, and should be thanked and congratulated for their excellent work and team play.

Finally, and most importantly, to my beloved wife Julie who put up with all of this and not seeing me. Thank you for your patience, your kindness, your love and support. To Rufus for staying up at every night writing this with me in-between bottle feeds. Mum, Dad, Aunties, Uncles, Grandparents, particularly the late great Professor Colleen Srinivasan and Roger Flory both taken from us too soon. This wet's on you!!

Publications and Abstracts Derived From This Thesis

Publications

Electrical and Structural Substrate of Arrhythmogenic Right Ventricular Cardiomyopathy Determined Using Noninvasive Electrocardiographic Imaging and Late Gadolinium Magnetic Resonance Imaging.
Christopher M. Andrews*; **Neil T. Srinivasan***; Stefania Rosmini; Heerajnarain Bulluck; Michele Orini; Sharon A. Jenkins; Antonis Pantazis; William J. McKenna,; James C. Moon; Pier D. Lambiase; Yoram Rudy. Circ Arrhythm Electrophysiol. 2017;10:e005105. DOI: 10.1161/CIRCEP.116.005105.

Disease Severity and Exercise Testing Reduce S-ICD Left Sternal ECG Screening Success in Hypertrophic Cardiomyopathy
Neil T. Srinivasan, Kiran H. Patel, Kashif Qamar, Amy Taylor, Marco Bacà, Rui Providência, Maria Tome-Esteban, Perry Elliott, Pier D. Lambiase.
In press Circulation EP. Circ Arrhythm Electrophysiol. 2017 Apr;10(4). pii: e004801. doi: 10.1161/CIRCEP.117.004801.

Gaining approval for clinical research.
Cobb V, **Srinivasan N**, Lambiase P·Br J Hosp Med (Lond). 2016 Jul;77(7):414-8. doi: 10.12968/hmed.2016.77.7.414.

Ventricular Stimulus Site Influences Dynamic Dispersion of Repolarization In The Intact Human Heart.
Neil T. Srinivasan, Michele Orini, Ron B. Simon, Rui Providência, Fakhar Z. Khan, Oliver R. Segal, Girish G. Babu, Richard Bradley, Edward Rowland, Syed Ahsan, Anthony W. Chow, Martin D. Lowe, Peter Taggart and Pier D. Lambiase. Am J Physiol Heart Circ Physiol. 2016 Sep 1;311(3):H545-54. doi:10.1152/ajpheart.00159.2016. Epub 2016 Jul 1.

Abstracts

105Investigation of the transmural action potential duration and repolarization properties of scar borderzone in patients undergoing ventricular tachycardia ablation .
NT Srinivasan M Orini R Providencia C Martin M Dhinoja R Hunter MD Lowe F Khan PD Taggart RJ Schilling PD Lambiase. EP Europace, Volume 19, Issue suppl_1, 1 October 2017, Pages i45, https://doi.org/10.1093/europace/eux283.099

25First evidence that differences in the t-wave upslope of the body surface ECG reflect right to left dispersion of repolarization in the intact human heart
NT. Srinivasan, M. Orini, R. Providencia, RB. Simon, MD. Lowe, OR. Segal, AW. Chow, RJ. Schilling, R. Hunter, PD. Taggart, PD Lambiase .October 2017Europace 19(suppl_1):i11-i11. DOI10.1093/europace/eux283.034

80Relationship of conduction velocity and conduction velocity dynamics to bipolar voltage and drivers in atrial arrhythmia. S Honarbakhsh, RJ Schilling, M Orini, **NT Srinivasan**, R Providencia, E Keating, M Finlay, A Chow, MJ Earley, PD Lambiase, RJ Hunter. October 2017Europace 19(suppl_1):i35-i35. DOI10.1093/europace/eux283.075

93Impact of QTc formulae in the prevalence of short and long corrected QT intervals in a young adult cohort. Rui Providencia **Neil Srinivasan** Nabeela Karim Shohreh Honarbakhsh MJ Ferreira L Goncalves Eloi Marijon Pier Lambiase. EP Europace, Volume 19, Issue suppl_1, 1 October 2017, Pages i40, https://doi.org/10.1093/europace/eux283.088

117Investigation of the transmural APD properties of scar borderzone in patients undergoing ventricular tachycardia ablation
NT. Srinivasan, M. Orini, R. Providencia, C. Martin, M. Dhinoja, R. Hunter, MD. Lowe, F. Khan, PD. Taggart, RJ. Schilling, PD. Lambiase. Europace (2017) 19 (suppl_3): iii12.DOI:https://doi.org/10.1093/ehjci/eux135.006

P1793Impact of QTc formulae in the prevalence of long corrected QT interval and impact on risk of Long QT Syndrome
R. Providencia, **N. Srinivasan**, N. Karim, S. Honarbakhsh, MJ. Ferreira, L. Goncalves, PD. Lambiase. Europace (2017) 19 (suppl_3): iii396.DOI:https://doi.org/10.1093/ehjci/eux161.102

P1022Differences in the upslope of the body surface ECG-Twave reflect dispersion of repolarization in the intact human heart
NT. Srinivasan, M. Orini, R. Providencia, RB. Simon, MD. Lowe, OR. Segal, AW. Chow, RJ. Schilling, R. Hunter, PD. Taggart, PD Lambiase. Europace (2017) 19 (suppl_3): iii219.DOI:https://doi.org/10.1093/ehjci/eux151.203

32 Global high density mapping of re-entry vulnerability index aids risk stratification and identifies sites of arrhythmia initiation in brugada syndrome and ARVC. Claire Martin, Michele Orini, **Neil Srinivasan,** Justine Bhar-Amato, Anthony Chow, Martin Lowe, Ron Simon, Peter Taggart, Pier Lambiase. Heart 2017;103:A25-A26.

Novel Repolarisation Metric Predicts Arrhythmia Origin And Clinical Events In ARVC And Brugada Syndrome
Claire Martin, Michele Orini, **Neil Srinivasan**, Justine Bhar-
Amato, Shohreh Honarbakhsh, Anthony Chow, Martin Lowe, Ron Simon, Perry Elliott, Peter Tagga rt, Pier Lambiase. doi: https://doi.org/10.1101/123422. Europace (2017) 19 (suppl_3): iii35.

FIrst Evidence That Differences In The Upslope Of The Body Surface Ecg Reflect Dispersion Of Depolarisation In The Intact Human Heart .Neil T. Srinivasan, Michele Orini, Rui Providencia, Ron Simon, Martin Lowe, Oliver R. Segal, Anthony W. Chow, Richard J. Schilling, Ross J. Hunter, Peter Taggart, and Pier D. Lambiase, C-PO02-11. Heart Rhythm, Vol. 14, No. 5, May Supplement 2017

First Evidence Thar Surface Tpeak-Tend Correlate with Right to Left and Transmural Repolarization in the Intact Human Heart. Srinivasan et al.. 2016 (Poster Abstract Heart Rhythm Society Conference San Francisco)

Disease Severity and Exercise Testing Reduce S-ICD ECG Screening Success in Hypertrophic Cardiomyopathy. Srinivasan et al.. 2016. (Poster Abstract Heart Rhythm Society Conference San Francisco)

Eligibility of hypertrophic cardiomyopathy patients for subcutaneous ICD: results of postural and exercise ECG screening. **Srinivasan et al.**.2015. (Poster abstract HRC Confernce Birmingham UK)

Dynamic transmural activation recovery interval gradients exceed apico-basal gradients in the intact human heart. Srinivasan et al..2015 (Oral abstract HRS Confernce Birmingham UK)

E**ligibility of hypertrophic cardiomyopathy patients for subcutaneous ICD: results of postural and exercise ECG screening. Srinivasan et al.**.2015. (Oral Abstract at Europace/ Cardiostim Confernce Milan)

Transmural activation recovery interval gradients exceed apico-basal gradients in the intact human heart. Srinivasan et al..2015. (Poster Abstract at Europace/ Cardiostim Confernce Milan)

Dynamic transmural activation recovery interval gradients exceed apico-basal gradients in the intact human heart. Srinivasan et al..2015. (Oral Abstract at Heart Rhythm Society Conference Boston)

Chapter 1

Introduction

1.1. General Introduction

An estimated 180,000-300,000 sudden cardiac deaths (SCD) occur in the United States annually (Chugh et al. 2008; Adabag et al. 2010). Worldwide sudden and unexpected cardiac death is the most common cause of demise, accounting for >50% of all cardiovascular deaths (Adabag et al. 2010; Zipes et al. 2006). In the majority of SCD cases, ischemic heart disease (IHD) is the underlying cardiovascular cause(Rea & Page 2010; Adabag et al. 2010; Estes 2011; Zipes et al. 2006). The accepted definition of SCD is that it occurs within one hour of onset of symptoms in witnessed cases, and within 24-hours of last being seen alive when it is unwitnessed (Adabag et al. 2010). The majority if cases are unwitnessed, with ventricular fibrillation(VF) being the final underlying mechanism (Myerburg et al. 2009; Rea & Page 2010; Adabag et al. 2010; Estes 2011; Zipes et al. 2006).

Despite the decline in mortality from IHD over the several decades due to improved primary and secondary preventative strategies, the incidence of SCD as a proportion of overall cardiovascular deaths has increased (Adabag et al. 2010). This is because in-hospital mortality has declined more rapidly (Adabag et al. 2010), highlighting the need for better primary prevention strategies(Figure 1.).

A major advance in the prevention of SCD has been the development of the implantable cardioverter-defibrilator (ICD) (Nanthakumar et al. 2004). The secondary prevention trials (trials in survivors of cardiac arrest), AVID (Antiarrhythmics versus Implantable Defibrillators) (AVID Investigators 1997), CIDS (Canadian Implantable Defibrillator Study) (Connolly et al. 2000) and CASH (Cardiac Arrest Study of Hamburg) (Kuck et al. 2000), have demonstrated significant improvements in survival rates with ICD implantation compared to drug therapy in this patient population.

The MADIT (Multicenter Automatic Defibrillator Implantation Trial) (Moss et al. 1996) and MUSTT (Multicenter Unsustained Tachycardia Trial) (Buxton et al. 1999) studies enrolled patients post myocardial infarction (MI), comparing primary prevention with an ICD against standard medical therapy, in patients with a reduced ejection fraction(EF; <35% and <40% respectively) plus either documented or induced ventricular tachycardia(VT) and demonstrated a 58-59% relative risk reduction in death. Subsequently MADIT II(Moss et al. 2002), showed a 28% relative risk reduction in 2 year

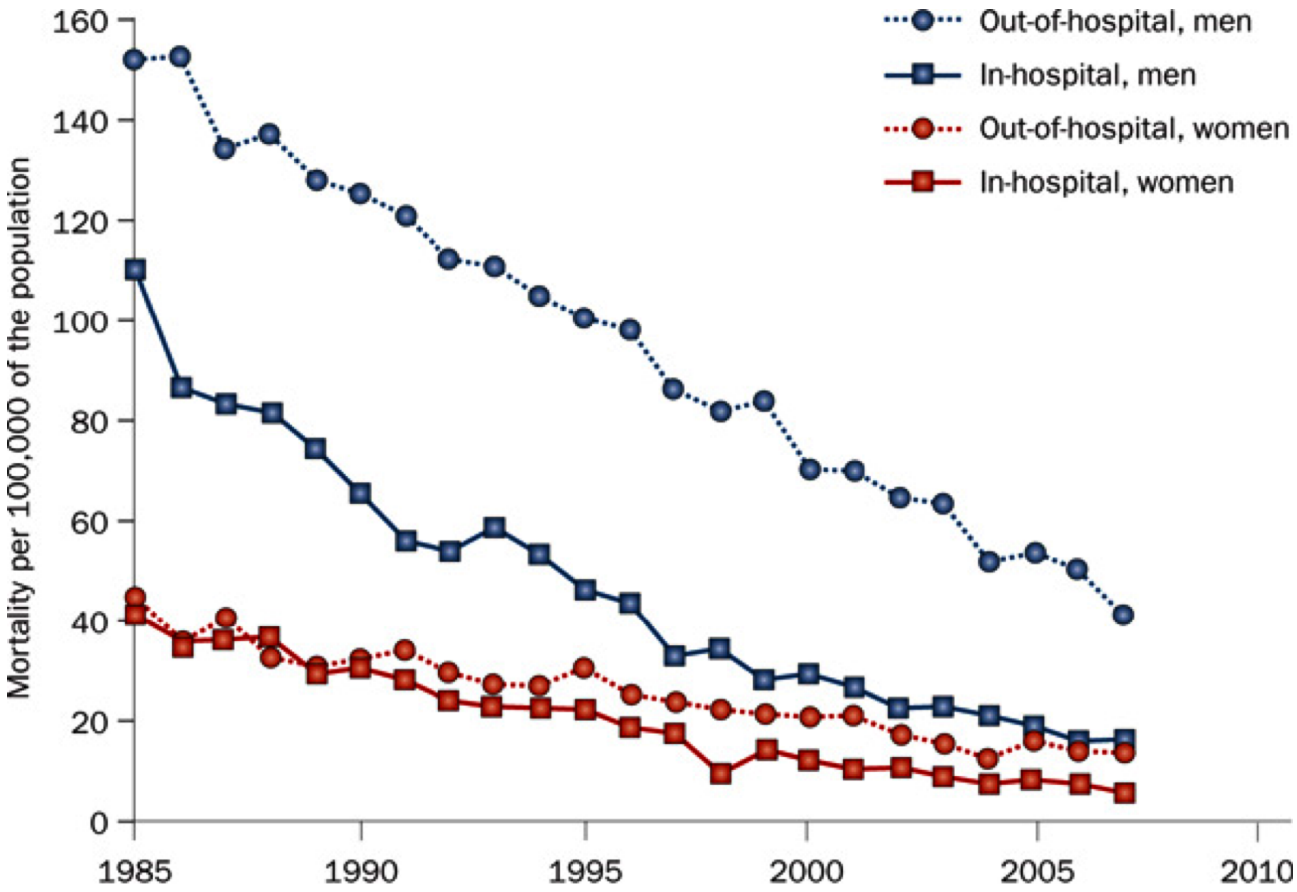

Figure 1. Trend in in-hospital and out-of hospital cardiovascular mortality, in people living in Minneapolis-St Paul, MN, USA. Reprinted from Adabag et al.(Adabag et al. 2010). With permission from Springer Nature.

mortality in post-MI patients with an EF<30% without the requirement for documented or induced VT. The DEFINITE (Defibrillators In Non-Ischemic Cardiomyopathy Treatment Evaluation) (Kadish et al. 2004) study compared the benefit of ICD against standard therapy in patients with heart failure, EF ≤35% and PVC's or non-sustatined (NSVT), demonstrating a strong trend towards reduced mortality with ICD. While in the Sudden Cardiac Death in Heart Failure Trial (SCD-HeFT) (Bardy 2005), which enrolled patients with both ischemic and non-ischemic cardiomyopathy with New York Heart Association (NYHA) class II or III and EF ≤35%, showed a benefit of ICD when compared ICD to standard medical therapy.

What is interesting within these primary prevention trials is that apart from a low EF no other significant major risk predictor's have identify who will benefit form an ICD. The major studies have

used an EF cut-off between ≤30-40%, however the median populations within these studies tend to have far lower EF's, and subgroup analysis of patients closer to the cut-off often shows no clear benefit (Moss et al. 2001; Bardy 2005; Moss et al. 2002; Moss et al. 1996; Myerburg et al. 2009). Additionally in the "high-risk" population studies such as MADIT II (Moss et al. 2002) and SCD-HeFT (Bardy 2005), <40% of patients received appropriate ICD shock therapy during the first 4 years of follow-up.

It is evident is that we have only targeted a subgroup of patients in whom, the incidence of events is high and therefore they have been labeled as "high-risk"(Figure. 2A). The challenge for clinicians lies in the fact that most episodes of SCD occur in individuals who, have no known cardiac disease, are not perceived high risk by traditional measures, or as a first presentation of an undiagnosed underling cardiac condition. (Figure. 2B) (Myerburg et al. 2009). Thus, the vast majority of SCDs occur in patients who are at "low risk" (Myerburg et al. 2009). Although the incidence within this group of patients is low, they cumulatively account for the greatest number of events (Figure. 2A). Additionally the indications for primary prevention in less common conditions such as Hypertrophic Cardiomyopathy (HCM), Arrhythmogenic Right Ventricular Cardiomyopathy (ARVC), Long-QT syndrome (LQT), Brugada Syndrome (BrS), and Early Repolarization (ER) remain less clear, with few if any definite risk markers beyond patient symptoms (Myerburg et al. 2009; Priori et al. 2013).

The sole reliance on reduced EF as a marker of risk is therefore imprecise (Buxton 2005; Moss 2005; Buxton et al. 2007; Myerburg et al. 2009), particularly in less well defined patient populations. There is a need for both patient specific and dynamic risk markers of SCD. Electrocardiographic (ECG) markers such as QRS-duration (N. C. Wang et al. 2008), QT-variability (Haigney et al. 2004), heart rate variability/turbulence (Bauer et al. 2006; Barthel et al. 2003), post ectopic turbulence (Mäkikallio et al. 2005), non-sustained VT (Mäkikallio et al. 2005), signal-averaged ECG (Gold et al. 2000), and microvolt T-wave alternans (Bloomfield et al. 2004; Gold et al. 2000) have all been investigated, but have yet to demonstrate themselves as clear clinical risk predictive tools with significant predictive value. Recent work has demonstrated that dynamic differences in the T-wave of the paced ECG can predict risk of VT (Nicolson et al. 2012).

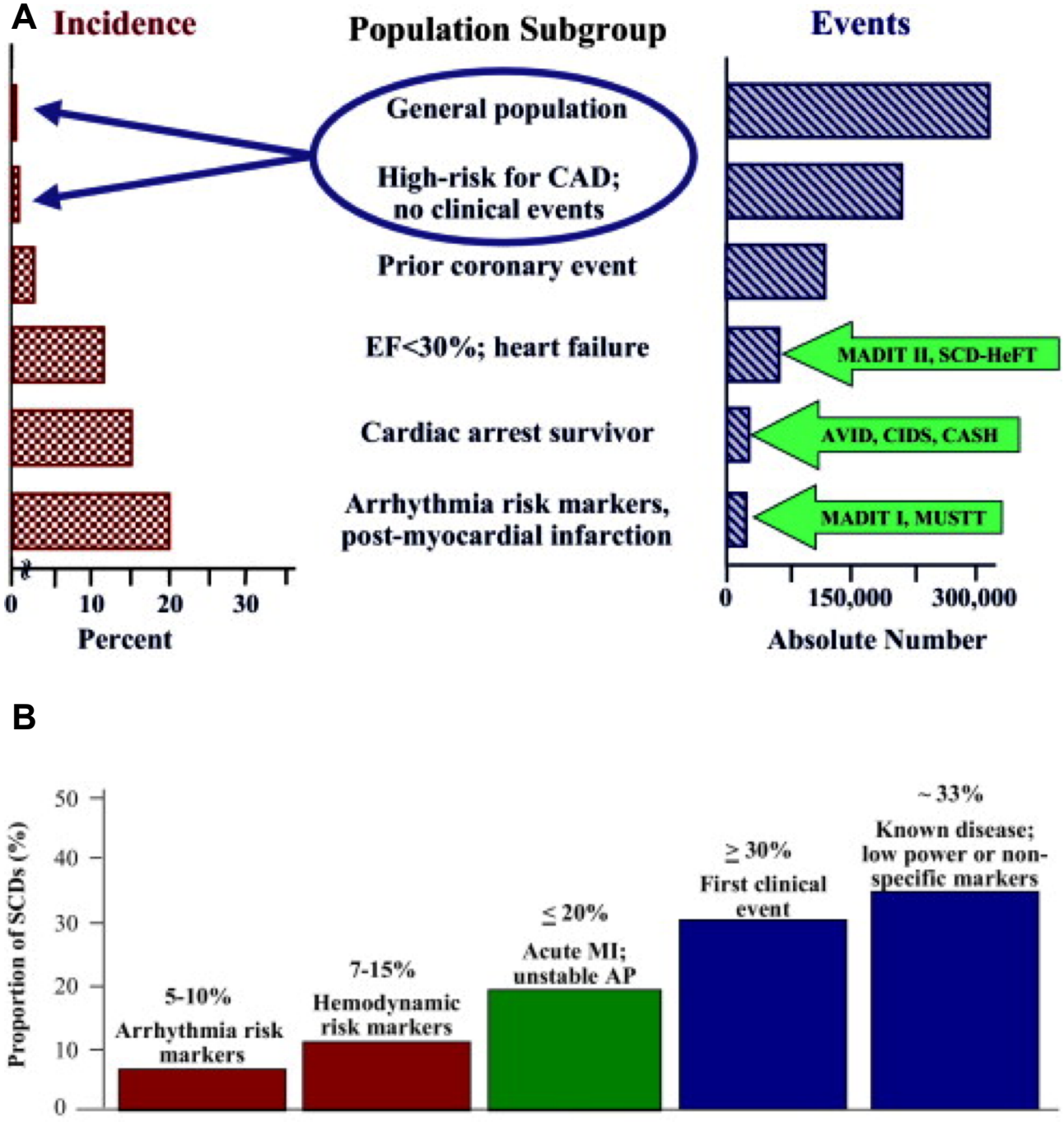

Figure 2. A. Incidence and total annual event burden for general adult population, based on population subgroups. The majority of trials have involved patients post MI, survivors of cardiac arrest, or ejection fraction (EF) <30% where the incidence is high, but event rates overall are low. B. Clinical status of patients at the time of sudden cardiac death (SCD). Almost two-thirds of patients present as a first clinically manifest event or in the settings of a known disease without traditionally identified risk markers. Repprinted from Myerburg et al. (Myerburg et al. 2009). With permission from Elserver.

The underlying mechanism of SCD is thought to be VF. The mechanism and basis for the initiation and sustaining of VT/VF has been the subject of much study since the work of Mines (Mines 1914; Mines 1913) and Mayer (Mayer 1906). Extensive research has focused on the cellular and ionic electrophysiological mechanisms, that govern the various tissues within the heart, and their role in arrhythmogenesis (Zaitsev et al. 2003; Antzelevitch et al. 1998; Conrath & Opthof 2006; Salama & Choi 2007; Di Diego et al. 2002; Kondo et al. 2004; Pastore et al. 2006; Hayashi et al. 2008; Garfinkel et al. 1997; Antzelevitch et al. 2009; Glukhov et al. 2012; Yan & Antzelevitch 1998; Cohen et al. 1976). Fundamentally normal and abnormal cardiac conduction represents an interaction between depolarization sequences of the heart, the repolarization sequences and their interplay with the structural and electrical heterogeneity of the tissue which can lead to the re-excitation or 're-entry' of the excitatory wave.

Clinically, our understanding of electrophysiologic mechanisms has expanded vastly over the past 40 years (Chow et al. 2004; Stevenson et al. 1997; Stevenson & Soejima 2007; Anon 2013; Taggart et al. 2003; Garfinkel et al. 1997). This has lead to the development of advanced ablation strategies for a variety of cardiac arrhythmias. Additionally the work of Rosenbaum and colleagues (Rosenbaum et al. 1982; Schwartz et al. 2009; Laurita et al. 1996) has contributed greatly to explain the relation of the surface electrocardiogram (ECG) to the electrical processes within the heart. However, there remains a discord in our understanding of basic cellular electrophysiological mechanisms linking the intracardiac and surface electrical parameters recorded clinically.

This thesis seeks to bridge the gap between our basic cellular and intracardiac understanding of cardiac electrical activity with the surface ECG. I will focus specifically on repolarization characteristics of the heart and their relation to the surface ECG, in order to identify new potential biomarkers of cardiac risk.

Chapter 2

Literature Review

2.1. Basic Cardiac Cellular Electrophysiology

The mammalian heart is an electromechanical pump to the systemic and pulmonary circulation, that is controlled by a coordinated sequence of electrical impulses (Grunnet 2010).The function of these impulses is the rapid activation of groups of cells, with the capacity to respond to changes in heart rate and autonomic tone (Nerbonne & Kass 2005). The experiments of Burton-Sanderson (Burdon-Sanderson 1884) with the capillary electrometer in frog and tortoise heart captured these impulses as the cardiac action potential(Figure. 3).

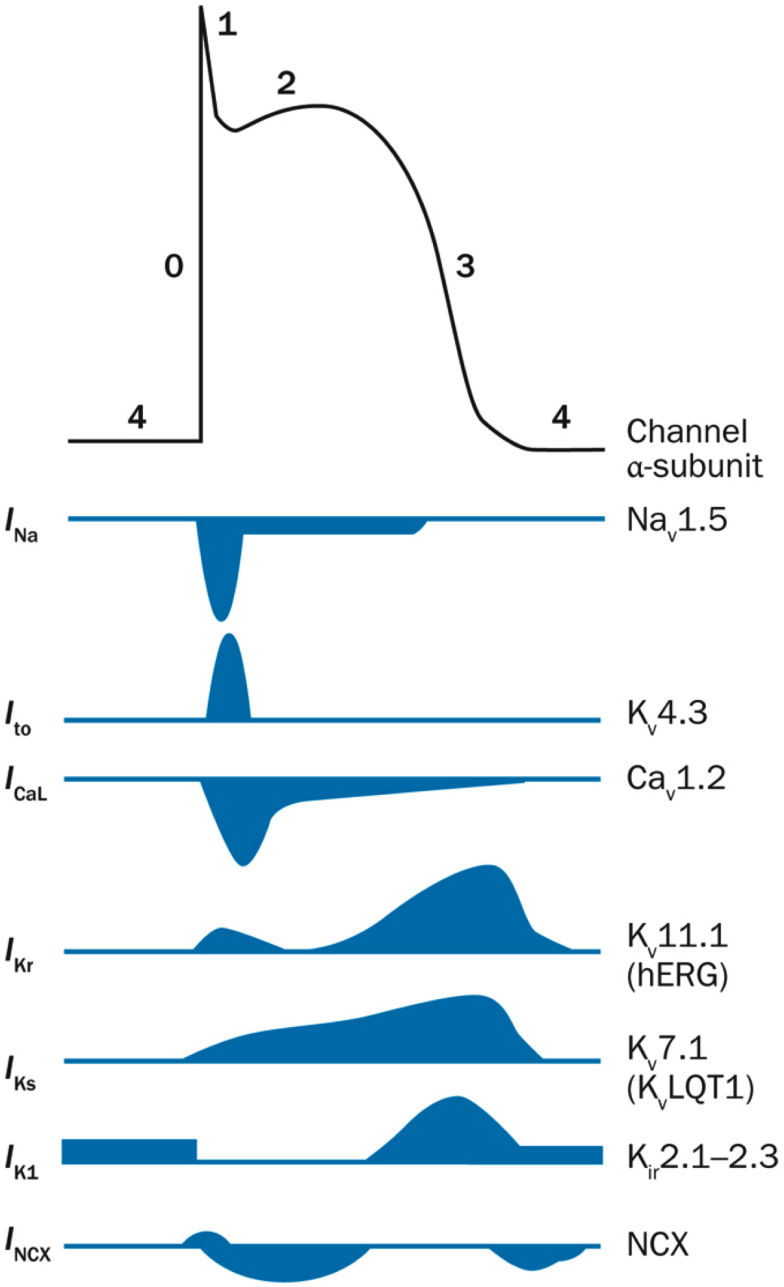

Figure 3. Phases of the cardiac action potential (top, black) with contributing ion channel currents (bottom, blue) and channel subunits (right). Reprinted from Gurnnet (Grunnet 2010). With permission from John Wiley and Sons.

The cardiac action potential begins at Phase 4, where the resting membrane potential is thought to be between -75mV and -90mV. This is then followed by the rapid depolarization (Phase 0), initiated by activation of the voltage-gated Na+ channel (Nav1.5) (Fozzard & Hanck 1996; Yu & Catterall 2003; M. Liu et al. 2014), encoded by the SCN5A gene. The Nav1.5 channel is activated at a membrane potential of around -55mVm. The activation is fast and steeply voltage sensitive(Fozzard & Hanck 1996), giving rise to rapid voltage-dependent activation within a few milliseconds (Stühmer et al. 1989; Grant & Starmer 1987). This results in a rapid influx of Na+ into the cell to depolarize it. The peak Na+ current is important for proper cardiac signalling. It should also be noted that the voltage range for both activation and inactivation of Nav1.5 overlap, resulting in a "window" current of persistent Na+ (Attwell et al. 1979).

The rapid depolarization and influx of sodium into the cell is followed by Phase 1 of the cardiac action potential, where a transient or partial repolarization occurs. This phase occurs due to activation of the transient outward voltage-gated K+ channel (Ito) (Grunnet 2010). There are two types of Ito current, Ito-fast, and Ito-slow (Xu 1999; Guo et al. 1999), named after their recovery from inactivation. Both are rapidly activated and inactivated. Activation begins at membrane potentials of -30mV and above. Ito-fast is encoded by the KCND2(Kv4.2) and KCND3(Kv4.3) genes, while Ito-slow is encoded by the KCNA4 gene(Kv1.4) (Grunnet 2010).

Following this the Phase 2 or plateau phase of the cardiac action potential takes place. This phase is characterised by activation of voltage gated Ca2+ with a subsequent influx of Ca2+ into the cell. The influx of calcium causes excitation contraction coupling, and a subsequent calcium induced calcium release from the intracellular stores of the sarcoplasmic reticulum (Bers 2002). There are two types of voltage-gated calcium channels, the L-Type and T-type(Bean 1985). L-type channels have large single channel conductance, are long lasting currents and are activated at membrane potentials above -20mV to -30 mV(Nilius et al. 1985). Once they are activated, they are inactivated slowly over hundreds of milliseconds(Bean 1985). Only the L-type is thought to be present in human myocardium(Perez-Reyes 2003). The majority of L-type channels are encoded by the CACNA1C gene which translates the Cav1.2 protein(α-subunit) (Grunnet 2010). Additionally the Na+/Ca2+ exchanger(NCX), which

exchanges 3 Na+ for 1 Ca2+ is also active during the initial part of Phase 2. This channel serves to pump Ca2+ out of the cell from within the cell, but is reversed at a membrane potential of about -30mV, thus causing transient influx during Phase 2 of the action potential and contributing the net gain of Ca2+(Figure. 4) (Bers 2002; Grunnet 2010).

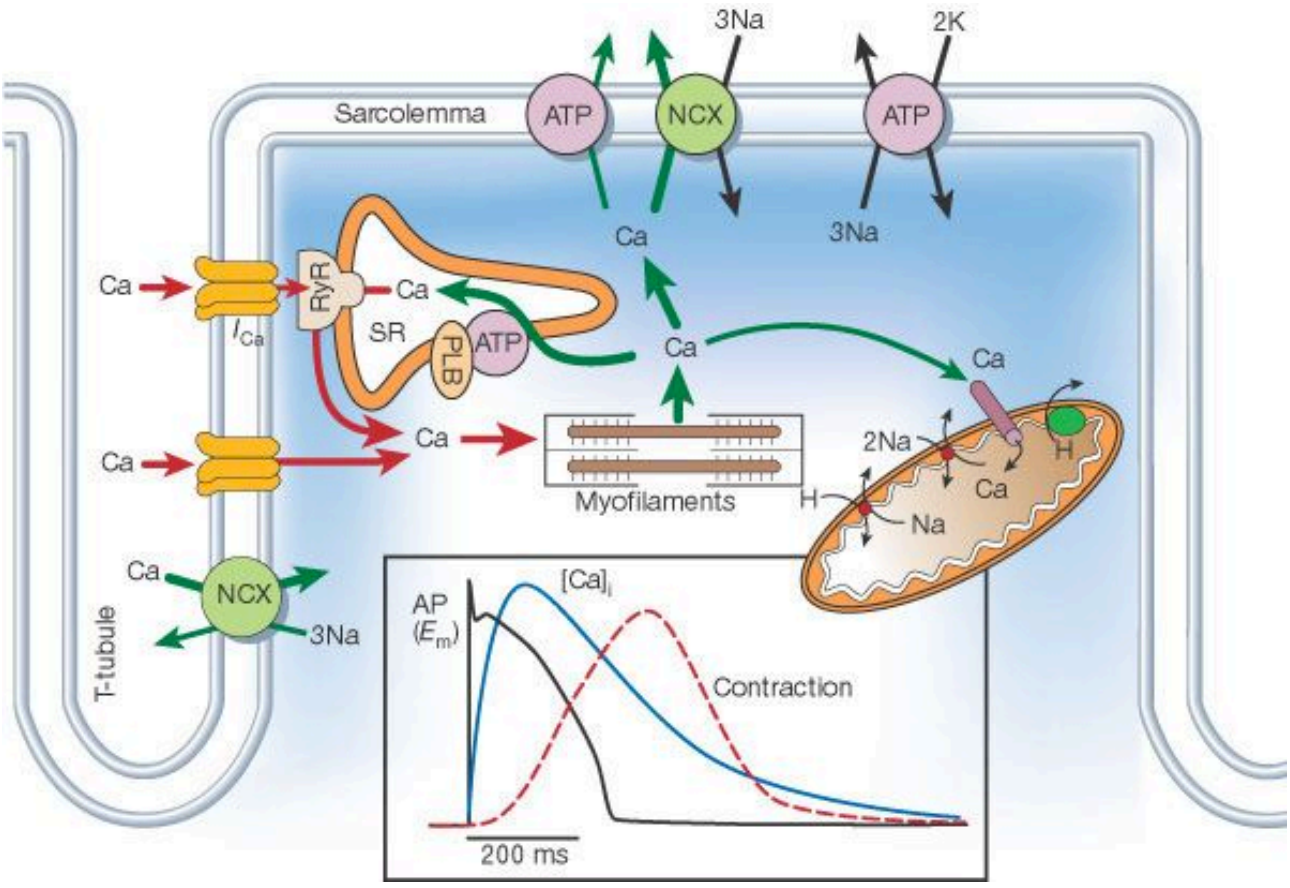

Figure 4. Calcium handling within the heart. Reprinted from Bers (Bers 2002). With permission from Springer Nature.

The return of the cell membrane potential to its resting state occurs in phase 3, as a consequence of inactivation of voltage and Ca2+ dependent Ca2+ channels and the increased conduction of K+ channels. The three main potassium channels responsible for human cardiac repolarization are IKr, IKs and IK1. Their expression within the myocardium is heterogenous, and influenced by heart rate and parasympathetic/sympathetic activity. IKs displays slow activation (Horie et al. 1990), IKr rapid activation (Sanguinetti 1990), while IK1 is an inward rectifier channel which is voltage independent

(Varro et al. 1993; Dhamoon & Jalife 2005). IKr (Kc11.1) has a pore forming α-subunit coded for by the KCNH2 gene while the two different β-subunits KCNE1 and KCNE2 play an important interactive role (Sanguinetti & Tristani-Firouzi 2006). IKs is formed by the assembly of proteins from the KCNQ1 gene (Kc7.1 pore forming protien) and KCNE1 (Grunnet 2010).

IKs is thought to be expressed heterogenously within the heart, with possible evidence of a transmural gradient (Akar 2002). Sympathetic activity may up regulate the activity of IKr although conversely a reduction in current is seen at the subsequent high heart rates due to fewer channels having time to reach their active state (Hua 2004). Additionally IKr is also reduced at slow heart rates. At faster heart rates and increased sympathetic tone IKs, with its slow deactivation kinetics, will accumulate (Diness et al. 2006). Additionally IKs appears to display volume loading sensitivity properties (Grunnet et al. 2003). Several other potassium channels are thought to play a role in the repolarization phase of the action potential, notably IK_{ATP} which is primarily active in states of cellular ischemia and or hypoxia, and is inhibited by normal levels of cellular ATP, thus becoming active during ATP depletion (Isomoto & Kurachi 1997). When activated this channel conducts potassium into the cell through the whole of phase 0-3, causing a triangulation of the action potential (Grunnet 2010).

The return from the end of Phase 3 to the resting membrane potential, is defined as Phase 4 of the action potential. Clinically this is noted as the diastolic interval. Although there is little charge movement during this phase, not all ion channels are closed. Indeed pore forming potassium channels and the slowly deactivating IKr and IKr remain open during this phase, perhaps as a protective mechanism against delayed-after-depolarization (DAD) (Grunnet 2010). Additionally Phase 4 has an important interactive effect on the subsequent depolarization (Phase 0), as Na+ and Ca2+ channels involved in depolarization are inactivated in a time and voltage dependent manner. Therefore a longer time spent in Phase 4 and the greater the hyperpolarization the more Na+ and Ca2+ channels available to elicit the subsequent action potential (Grunnet 2010).

2.2. Cellular Mechanisms Of Arrhythmia

Arrhythmias are abnormal cardiac rhythms that occur outside the normal expected sequence of cardiac impulse generation and propagation. The two major requisites for initiation of an arrhythmia are the presence of a trigger and a substrate.

Common triggering events for arrhythmia are enhanced automaticity and afterdepolarizations (Figure. 5A). Enhanced automaticity occurs when a region of myocardium known as an ectopic focus; outside of the sinus node (SAN) and atrioventricular (AVN); generates a cardiac impulse. At a cellular level enhanced automaticity is caused by an increased sympathetic drive or abnormal remodelling of ion channels (Imanishi & Surawicz 1976). It should be noted that the repolarization reserve of the ventricle plays an important role in this phenomenon. In conditions of hypokalemia, the open probability of Ikr and Ik1 is decreased, providing less hyperpolarizing capacity to withstand the depolarization in abnormal automaticity (Grunnet 2010), and the same is true in mutations that decrease the activity of these channels. In addition Ito is also affected by hypokalemia (Wang et al. 2004).

Afterdepolarizations occur outside of regular phase 0 depolarization and can be either early, occurring in phase 2 or 3, or delayed, where they occur in phase 4. Early afterdepolarizations (EADs), occur due to the release from inactivation of the voltage-gated L-type Ca2+ channel at a membrane potential sufficiently depolarized to allow reactivation of these channels (Grunnet 2010; Ming et al. 1994; Zeng & Rudy 1995). Conditions of prolonged repolarization with a reduced repolarization velocity, promote the release of the L-type Ca2+ channel from inactivation, and therefore promote the occurrence of EAD's (Hirano et al. 1992). EAD's are therefore more common during bradycardia when the APD is prolonged, in long-QT syndrome at high heart rates and with increased sympathetic drive (Shimizu et al. 1991; Volders et al. 1997). Delayed afterdepolarizations (DADs) occur due to the NCX co-transporter working in a forward mode such that 3 Na+ enters the cell in exchange for 1 Ca2+. This net gain of positive ions results in depolarization of the cell. Excessive forward activity of NCX during the diastolic interval, occurs in response to increased intracellular Ca2+, commonly as consequence of spillover from the sarcoplasmic reticulum (Marban et al. 1986). DADs have to be sufficiently large in

amplitude in order reach the threshold for triggering an action potential. It is thought that DAD's occur in the mid-myocardial region of the ventricular myocardium (Liu & Antzelevitch 1995; Antzelevitch et al. 1991), which has a lower density of IKs than the endocardium and the epicardium and thus a lower reserve of outward current to prevent the net inward current.

In order for a trigger to initiate a propagated arrhythmia, it must ally with a substrate that permits this propagation. To obtain unintended and continued propagation of a wave of electrical impulse the trigger must re-excite or reenter tissue that has already been excited, but is now again in a state of excitability. Re-entry can occur in either anatomical or functional methods. A typical mechanism of an anatomical re-entry would be scar tissue or accessory electrical pathways within the tissue, which serves as a substrate in which unidirectional conduction block occurs in one direction and subsequent unidirectional conduction and reentry into the tissue (Figure. 5B). Within these anatomical loops/or circuits there are often regions of specific differential conduction velocity, which permits recycling of the current loop when initiated at appropriate timing intervals.

Functional reentry, also relies on these fundamental principles of unidirectional block and reentry, but occurs without an anatomical barrier. Sustaining it requires an electrical circuit that is long enough and with the appropriate velocity characteristics, such that when the depolarization wave subsequently reaches its origin it is no longer in a refractory state. Thus the leading wavefront, impinges on its tail, traveling through partially refractory tissue, while keeping a central core refractory, through constant bombardment from the circulating wavefront. This theory is known as the leading circle principle of reentry (Allessie et al. 1976, Allessie et al. 1977) and crucial to this phenomenon is the wavelength (WL) and path length. WL is the product of the refractory period (RP) and conduction velocity (CV) (Figure. 5C). If the path length is shorter than the WL the propagating impulse will meet its origin in a refractory state. Therefore shorter WL's are more likely to initiate reentry, by favouring the development of multiple reentrant circuits and subsequently fibrillation.

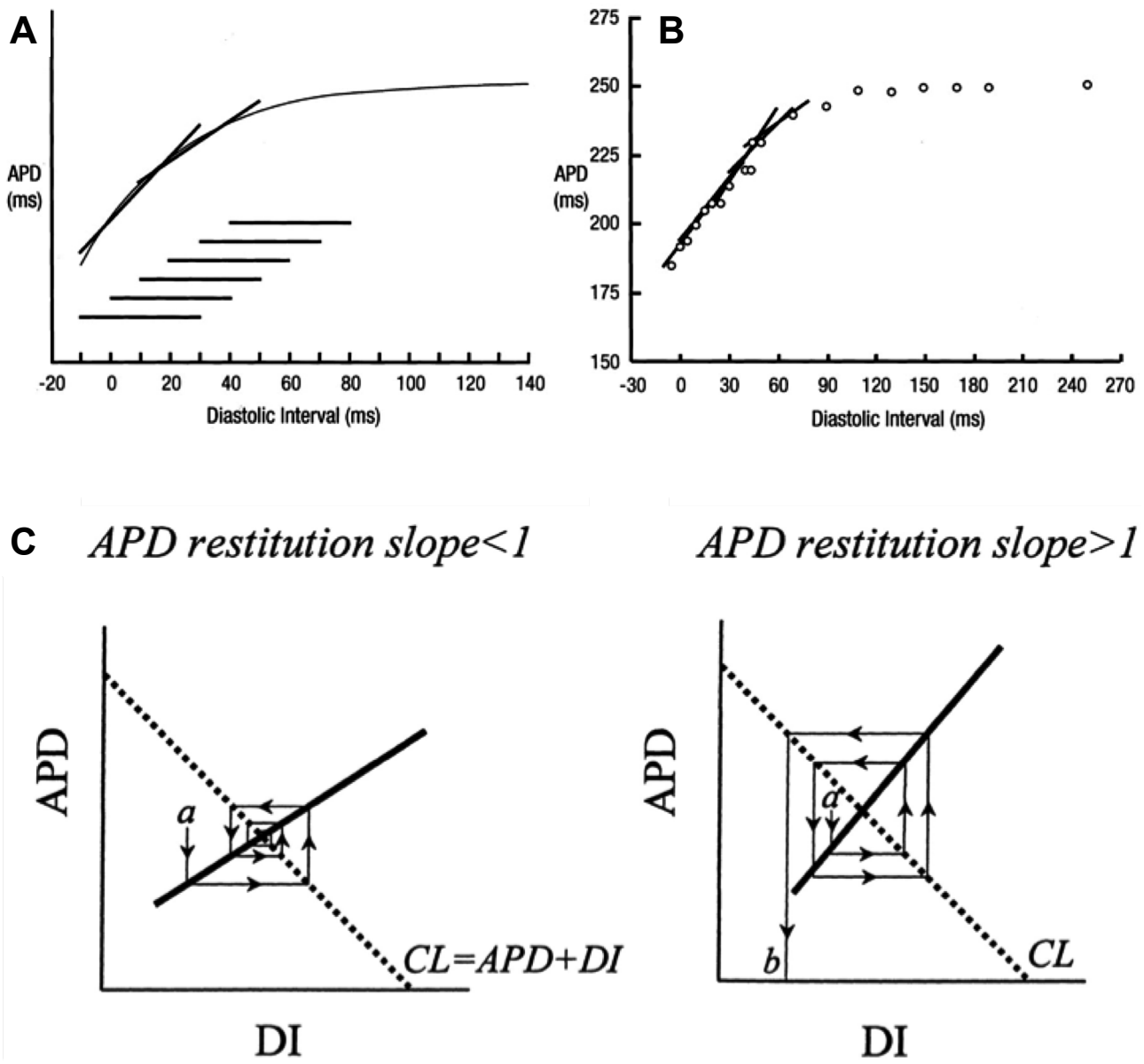

Figure 6. Cardiac Restitution. Example of a cadiac restitution curve made by collection of various recorded S2 extra-stimuli points (open circles in B). **A**. Curves are fit with a monotonic exponential to display shape. The steep portion of the restitution curve is measured using piecewise linear regression of 40ms disastolic intervval windows, with the steepest curves shown in **B**. **C**. cobweb diagram displaying how restitution curve steepness >1 is theoretically arrhythmogenic. APD and DI equilibrate at the interetction of the of the restitution curve (solid line) with the dotted line (defined by the relationship APD+DI=CL). When restitution slope <1, shortening DI results in smaller changed in APD enabling establishment of equilibrium, when the slope is >1 small changes in DI result in large changes in APD, which then produces a large change in DI, amplifying ossicilations, causing conduction failure, and wave break along the spiral wave. Reprinted from Taggart et al. (Taggart et al. 2003), and Weiss et al.(Weiss et al 1999). With permission from Wolters Kluwer Health, Inc.

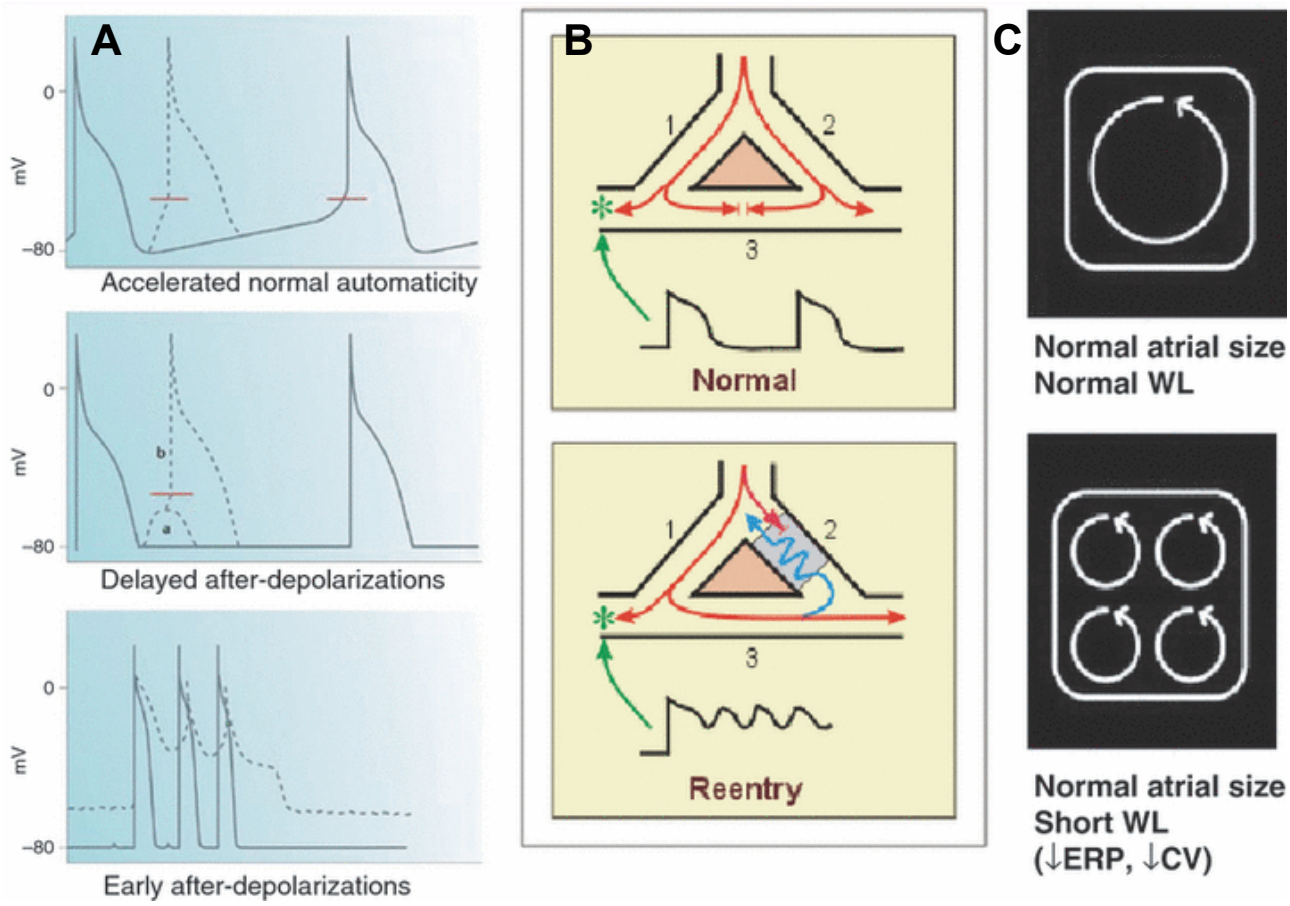

Figure 5. A. Schematic of monophasic action potential recording, showing examples of accelerated automaticity, delayed after-depolarizations and early after-depolarizations. **B**. Anatomical re-entry around a fixed obstacle with regions of differential conduction and repolarization properties. **C**. Functinal re-entry in the atrium with the wavefront impinging on its tail due to short wavelength. Reprinted from Gurnnet (Grunnet 2010). With permission from John Wiley and Sons.

The leading circle concept, is based on impulse propagation properties in one-dimension. It would be expected that cardiac sodium channel blocker administration would be pro-arrhythmic, due to decrease of RP and CV (Grunnet 2010). However, these drugs are useful anti-arrhythmics in many cases. To explain these properties and the three dimensional nature of arrhythmia, the spiral wave or rotor concept has also emerged, in which the excitatory wave forms a rotor or rotating source. The rotor forms because the wave cannot move in the refractory wake of the previous wave, and therefore moves in the opposite direction and adjacent regions as they recover (Zipes, Jalife & Stevenson 2017). Thus

the inner tip circulates around an excitable core, which has a slow upstroke velocity of phase 0. This tip follows a complex course, radiating waves to the surrounding tissue while giving rise to so called daughter waves, that can result in chaotic electrical activity (Zipes, Jalife & Stevenson 2017). This form of reentry does not require inhomogeneities of refractory periods, but can be modified by anisotropy, heterogeneous myocardium and anatomical obstacles.

Other forms of reentry include "figure-of-8 reentry", reflection and anisotropic reentry. In "figure-of-8 reentry" two excitation wavefronts trace through a central common pathway through a region of slow conduction, followed by exit in both clockwise and anticlockwise directions around this region which now forms a line of functional block, before re-entering (Zipes, Jalife & Stevenson 2017). In reflection the excitatory wave travels through an area of conduction delay, before returning to return along the same path (Zipes, Jalife & Stevenson 2017).

Anisotropic reentry deserves special mention, because anisotropic orientation of cardiac fibers is a normal feature of cardiac tissue, which can be accentuated in disease. Functional resistance to impulse propagation occurs depending on the fiber orientation, with faster conduction in the longitudinal axis of the fiber orientation, in line with the cellular gap junctions. This is further amplified by the localised differences in membrane refractoriness, in adjacent areas. Additionally electrical heterogeneity of channel expression, conduction and repolarization exists within the heart (Antzelevitch & Dumaine 2011). Notably there is experimental evidence to suggest that Ito is more prominent in the ventricular epicardium than the endocardium, leading to an exaggerated phase 1 notch and dome (Li et al. 1998). Additionally Ito current density is thought to be larger in the right ventricular (RV) sub-epicardium compared to the left ventricular (LV) sub-epicardium causing right to left differences (Di Diego et al. 1996). IKs is also thought to show a lower current density in the sub-epicardium (Liu et al. 1995), as well as displaying a RV to LV difference, with less current density in the LV (Volders et al. 1999). Additionally heterogeneity of $I_{Na/Ca}$ and I_{Na} may also exist (Zygmunt et al. 2000; Antzelevitch 2000).

Whether this electrical heterogeneity is present in humans is a matter of significant debate(Conrath & Opthof 2006). It has been suggested that the ventricle can be divided into endocardial, mid-myocardial and epicardial, layers, with action potential recordings from the mid myocardium being longer than

those recorded in the epicardium and endocardium (Antzelevitch & Dumaine 2011). Due to these differences, namely reduced IKs and a sustained late I_{Na} (Antzelevitch & Dumaine 2011) there is reduced repolarization capacity of mid-myocardium. Additionally dispersion of repolarization has also been documented in an apico-basal and right to left direction within the heart (Conrath & Opthof 2006). These dispersions can provide an important substrate for initiation of unidirectional block and reentry, particularly in response to changes to heart rate, where regional failure of APD adaptation due to ion channel heterogeneity, particularly in disease, can lead to rate related, or beat-to-beat variability which can accentuate inhomogeneity and lead to reentry (Thomsen et al. 2004).

2.3. Cardiac Restitution

Experimental studies have demonstrated that ventricular arrhythmias are commonly triggered by closely coupled extra beats that are capable of triggering reentry. The adaptation of cardiac action potential in response to an extra stimulus at a different coupling interval to the steady-state is termed cardiac restitution (Figure. 6A&B) (Franz 2003). The electrical restitution curve (ERC) was first described in experiments by Bass (Bass 1975). In general the action potential (APD) restitution curve tends to show a shortening of APD as the diastolic interval shortens my addition of an extra stimulus (S2).

The shape of the restitution curve is often modelled as a monotonic or single-exponential (Watanabe et al. 1995), however its shape in humans is far more complex, being characterised by a steep early phase, that reaches a maximum at a diastolic interval (DI) of 50ms, followed by a hump or downward turn, before achieving a flatter plateau phase(Franz et al. 1983). Though there is much debate with regard to the presence of the hump, the APD curve is at least bi-phasic or tri-phasic. Much interest has been generated as to why there should be an initial steep slope to the curve. Studies by Garfinkel et al (Garfinkel et al. 2000), in pig wedge preparation, have suggested that flattening of this early steep portion of the curve can prevent ventricular fibrillation. It has been hypothesised that a steep initial restitution slope >1, will promote or amplify electrical alternates, either of the T-wave or APD, and promote wave break which can lead to fibrillation (Weiss et al. 2000; Garfinkel et al. 1997; Weiss et al. 1999). With steeper curves, small changes in DI, create large changes in APD, which leads to APD/ electrical alternans, wave break and VF (Figure 6C.). In both human and animal studies, T-wave alternans is thought to be a surface electrical marker of vulnerability to VF (Pastore et al. 1999).

The steep portion of the restitution curve is also of interest, due to the concept of the 'vulnerable window', to re-entry (Franz 2003). The steep portion of the ERC is related to the rapid recovery of from inactivation of the fast voltage-gated Na+ channel (Nav1.5). Regional heterogeneity in the recovery of this channel produces a window in which spatial dispersion of conduction velocity in the ventricle exists, favouring reentry. This heterogeneity may occur due to abnormal recovery of this

channel itself, due to intrinsic mechanisms within the myocardium that cause this, or abnormal dispersion in the repolarization of the ventricle which alters the timeframe in which rapid phase 4 reactivation of the channel occurs. In humans and animal studies this window has also been shown to related both to dispersion of the refractory period and therefore phase 3 of the APD (Fabritz et al. 1994; Moubarak et al. 2000). Thus a dynamic interplay between activation recovery and repolarization play a significant role in governing the risk of lethal ventricular arrhythmia (Weiss et al. 2002; Garfinkel et al. 2000)

When abrupt changes in heart rate occur, physiologic adaptation of APD develops, with 40% of the adaptive shortening or lengthening of APD occurring within 5 seconds (Franz et al. 1988; Franz 2003). The effect of rate dependent APD shortening at a constant new cycle length(CL), is the reciprocal lengthening in DI, and a leftward shift of the curve for any given new increased heart rate (Franz et al. 1988; Franz et al. 1983). The function of this leftward shift is to move the point at which APD operates away from the steep portion of the curve (Franz 2003; Franz et al. 1983), and thus the vulnerable window. In addition the restitution curve becomes flatter at faster cycle lengths, which may be protective from arrhythmogenesis(Franz 2003). Thus the concept of steeper initial slopes of restitution being arrhytmogenic, is of some debate. Despite experimental evidence suggesting that flattening the curve is protective (Garfinkel et al. 2000) against VF, theoretically a steep initial slope allows quicker APD escape from steep portion of the slope. While flat slopes would result in a foreshortened refractory period, thus losing the protective effect afforded by this. Indeed there is much debate with regard to the principle of slopes >1 promoting fibrillation. In human studies of patients with EF <40%, a restitution slope of >1 did not predict risk of ventricular arrhythmias (Narayan et al. 2007).

2.4. Cellular Mechanisms Of Restitution

The cellular mechanisms for restitution follow a similar pattern to the cellular mechanisms of APD generation. The activation of the voltage-gated Na+ channel (Nav1.5), are largely responsible for the initial steep phase of the restitution curve, however, with increasing prematurity, APD becomes foreshortened, due to incomplete activation of this channel (Bode et al. 2002; Koller et al. 1995). The incomplete activation on Nav1.5, results in a slow upstroke and reduced peak amplitude (or overshoot), with in failure of activation of inward calcium currents which serve to prolong the APD (Bode et al. 2001; Koller et al. 1995). In addition with increasing prematurity of extra stimuli, the lingering conductance of Iks, Ikr and Ik1 (Delmar et al. 1991), prevent full reactivation of significant numbers of Nav1.5, a concept known as stimulus response latency (Koller et al. 1995), further abbreviating APD and ultimately causing the refractory period.

Calcium cycling also plays an important role in the shape of the restitution curve, particularly with regard to the hump and flat portion. During the flat portion of the curve, a sufficiently prolonged DI allows, filling of the calcium stores in the sarcoplasmic reticulum(SR). Thus when calcium enters the cell at longer DIs, during phase 2 of the action potential, there is a greater release of calcium which via a negative feedback loop on the ryadonine-to-dihydropyridine(DHP)-sensitive receptor is inhibitory to the L-type calcium channel (Bers 2002). This results in a shortening of phase 2 of the APD and a decrease in phase 2 area(Bers 2002). As DI begins to shorten the SR has had less time to fill, and therefore releases less calcium. Less SR release at shorter DI's results in less inhibition of the L-type calcium channel from the DHP receptor, greater Ica-L current, and therefore a longer phase 2 of APD. This phenomenon is thought to account for early peak and subsequent tail-off or hump in the restitution curve.

It should also be noted that given longer DI's result in greater calcium release from the SR stores, they also result in greater contractile force. Thus shorter DI's result in diminished contractile force as the SR stores have been inadequately filled. Full recovery of SR calcium stores and therefore SR calcium release therefore only occurs at DI's of 500ms or CL 800ms (Bean et al. 1985).

Finally as mentioned previously, the potassium channels Ikr, Iks and Ik1 play a role in the repolarization phase of the cardiac action potential. The activation of these currents therefore also causes an initial curtailment of APD in the restitution curve during the tail-off after the initial peak. At longer cycle lengths Ikr and Iks become inhibited (Franz 2003). Clinically this is seen as an increased propensity for torsades de pointes, following bradycardia or pauses. During cardiac restitution, this is demonstrated as an gradual lengthening of the APD beyond the level of the initial peak and hump phase, due to a gradual decrease in inward potassium current conductance at longer cycle lengths.

2.5. The Monophasic Action Potential And The Electrogram

The relationship between the cellular electrical behaviour of the myocardial tissue, characterised by the coupled action potentials of a series of connected cells, to the surface ECG has been the subject of intense study and debate. True action potential recordings are only recorded on individual cells by placement of a glass-microelectrode into individual cells (Ino et al. 1988; Hoffman et al. 1959). These so called transmembrane-action-potentials (TAPs) are only suitable for in vitro studies and of uncoupled tissue and though important in understanding basic cellular mechanisms do not always translate into useful clinical applications. Monophasic action potential (MAP) recording however, can reproduce the high fidelity of TAP recordings, in the beating heart, in order to study the activation and repolarization characteristics of a localised region of myocardium.

Original MAP recordings such as those recorded by Burdon-Sanderson in frog heart (Burdon-Sanderson 1884) involved inducing injury to part of the epicardial myocardial tissue, and placing two electrodes, one on the injured site of the tissue and one on the intact myocardium to make recordings of potential electrical difference; hence the term injury current. These recordings are different to the multiphasic deflections made by recordings made in intact human myocardium where no injury is made, such as those often recorded in the cardiac electrophysiology laboratory. This technique was subsequently refined to cause injury by suction electrodes, and the first MAPs recorded using this method in humans were performed by Krosgren et al (Korsgren et al. 1966).

In view of the controversy regarding whether the injury method was a true recording of the MAP or merely a registration of potential variations within injured tissue the 'contact' electrode method of MAP recording was also performed devised and performed by Jochim et al. (Jochim et al. 1935) mammalian heart. In this method light pressure is applied to the to the tissue with one electrode while the other electrode is merely in contact with the tissue. This work showed not only that the MAP was positive in relation to zero if the pressure electrode was connected to the positive amplifier input (active electrode), but also that the shape and nature of the MAP was related and cause by electrical permutations within the site where pressure was not applied(Figure. 7A) (Jochim et al. 1935).

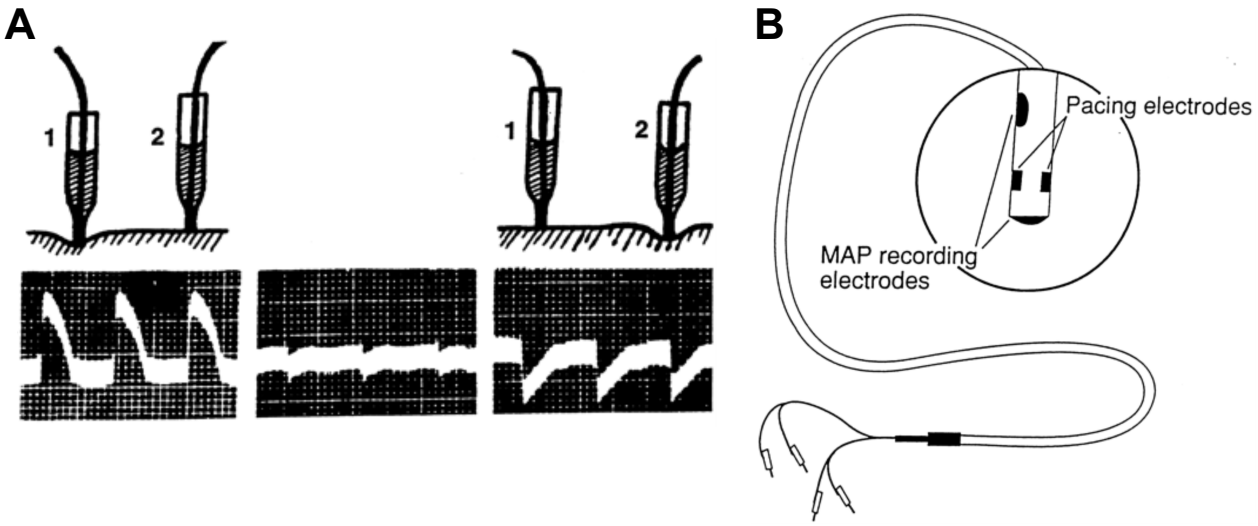

Figure 7. A. Monophasic aciton potential recordings, as performed by Jochim et al., showing the action potential shape is related to pressure, and fixed depolarization of a region of tissue in relation adjacent used as a reference, and that the action potential is positive if the pressure electrode is active (positive electrode, shown as 1 in diagram). **B**. Modern MAP recording electrodes as designed by Franz et al. (Franz et al. 1987; Franz et al. 1991, Franz et al. 1986, Franz et al. 1983). Reprinted from Franz. (Franz 1999). With permission from Oxford University Press.

The contact electrode technique was subsequently pioneered by Franz et al. (Franz et al. 1987; Franz 1991a; Franz et al. 1986; Franz 1983) for human use, and is the safest and most clinically applicable method for direct recording of MAPs in humans, avoiding the risk of embolism and tissue injury(Figure. 7B).

The generation of the MAP via the contact electrode, is related to the number of cells or electromotive generators contributing to it, with greater wall thickness and muscle mass contributing a greater MAP amplitude (Franz & Franz 1999; Franz 1991b), the so called 'volume conductor' hypothesis. Thus the MAP signal results from a current source with individual cells in series. Via the contact electrode MAP, local pressure on the myocardium depolarizes these cells to a membrane potential of -30 to -20 mV, this causes the sodium channels to remain in an inactivated state, as described earlier, rendering this region of tissue unexcitable (Franz & Franz 1999). The surrounding cellular tissue continues to be

depolarized and repolarized in a normal manner against the backdrop of this region with a fixed potential.

Assuming normal intracellular coupling this leads to electrical gradients of current flow across the two sites (Franz & Franz 1999). Thus during late electrical diastole where the normal cellular tissue is at a membrane potential of -90mv compared to the fixed potential of -30 to -20mv of the contact electrode tissue, in the extracellular tissue the current flows from the normal to the depolarized (contact electrode) tissue. This creates a current source from the normal cells and a current sink in the depolarised contact tissue, with a MAP recording that is a steady negative potential (Franz & Franz 1999). During electrical systole the excitation wave moves towards and across the electrically fixed region of the contact electrode. This depolarization wave changes the surrounding membrane potential to +30mv, which reverses the source-sink relationship in at the extracellular surface. On the surface there is a relative negative charge in the normal tissue in relation the contact electrode, with reversal of current flow and a MAP signal which moves in a positive direction, inscribing a phase 0 upstroke and an early phase 1 (Franz & Franz 1999). As the depolarization wave encompasses the MAP contact electrode site and passes it, the resting membrane potential or TAP gradually declines from its peak of +30mv. This results in less of an extracellular gradient with gradual decline in the MAP potential towards the isoelectric line, as a result of a smaller source-sink boundary gradient for current flow from the fixed depolarised contact tissue to the normal tissue. When the intracellular cellular membrane potential falls to the same as the fixed depolarized region the MAP reaches the isoelectric line, at which point further negative fall of the intracellular normal membrane potential results in a reversal of the extracellular gradient towards its original state in electrical diastole (Franz & Franz 1999).

It should be noted that MAPs can be recorded in unipolar and closer-bipolar configuration. In the unipolar configuration, if both electrodes are placed on intact myocardium a surface bipolar recording will be made, if both electrodes are placed on injured, ischemic or depolarized tissue again a MAP will not be seen due to a cancelling out (Franz & Franz 1999). Thus one electrode has to be placed on fixed depolarized tissue and the other on normal active tissue to record a MAP. When a MAP-exploring electrode is connected to an external reference such as 'Wilson's central terminal, again a MAP will be

recorded, but is contaminated by far-field potentials. Thus only a close bi-polar arrangement that creates a MAP that does not extend beyond the region of depolarization, with an indifferent electrode far enough away from the MAP generating current, yet close enough to avoid far field potentials (Olsson et al. 1991; Franz & Franz 1999) is reliable.

2.6. The Surface ECG

The relationship between the electrical repolarization of the heart, recorded either clinically or experimentally as MAPs and TAPs, and the surface electrogram, is poorly understood. The surface T-wave is upright in almost all leads, and concordant to the QRS complex. Yet at a cellular depolarization and repolarization reflect current flow in opposite directions. It has thus been hypothesised that in order for the surface T-wave to be concordant, the wave of repolarization must travel in the opposite direction to the wave of depolarization (Brink & Goodwin 1952).

Experimental studies to confirm such a hypothesis are limited. In dogs, experimental studies have suggested longer repolarization times in the endocardium and the apex, compared to the basal and endocardial regions (Burgess et al. 1972), while implanted electrode arrays, have shown that epicardial extracellular electrode recordings showed predominantly positive depolarization potentials, with the endocardium being more negative, suggesting a transmural unidirectional gradient of earlier epicardial repolarization to endocardial repolarization (Spach & Barr 1975). Others have found a repolarization gradient from the base of the heart base as compared to the apex (Cohen et al. 1976; Watanabe et al. 1985; Autenrieth et al. 1975) . It should also be noted that the repolarization sequence of the ventricle complex, and is related to the sequence of activation (Durrer et al. 1970). True repolarization heterogeneity occurs over a very small region or distance of ventricle. However, peak dispersion of repolarization, regardless of activation sequence, is thought to correlate with the peak of the local T-wave (Autenrieth et al. 1975).

Human studies using contact electrode MAPs (Franz et al. 1987) during sinus rhythm and atrial pacing have shown that the apex is the site of earliest activation and correspondingly the longest APD, while later activating sites had shorter APD. Additionally there was a significant transmural gradient of APD and repolarization with the epicardium repolarizing earlier (Franz et al. 1987). Therefore the sequence of activation also plays a pivotal role in the sequence of repolarization, either through inherent physiological mechanisms or through electronic forces (Rosenbaum et al. 1982).

Thus the surface T-wave is inscribed by a sequence of repolarization electromotive forces, which vary spatially, starting and ending at different times within different regions of the ventricle; and temporally, where regions of myocardium which begin repolarization at similar times display different repolarization time courses. The concept of spatial variation is well known. Cohen et al. (Cohen et al. 1976) recorded intracellular action potentials from the ventricular apex and base of sheep heart and found shorter APD at the apex when compared to the base, and this difference, in action potential was sufficient to explain the T-wave morphology. It should be noted, however, that Cohen et al (Cohen et al. 1976), recorded these differences by taking samples of the tissue from the endocardium of the base and the epicardium of the apical tissue, and this is a significant limitation to any conclusions drawn from this study. Similar differences with a longer repolarization at the base compared to the apex have also been noted in animal studies (Schutz et al. 1931), where subtraction of these electrograms resulted in an electrogram with some characteristics to the T-wave. In addition to apico-basal gradients of repolarization, differences in repolarization from left to right ventricle have also been demonstrated(Cowan et al. 1988), with LV epicardial APD shown to be longer than RV epicardial APD, using MAP recordings. Finally, the presence of transmural dispersion of depolarization has been extensively recorded both in the intact human heart (Cowan et al. 1988), and in isolated wedge preparations (Li et al. 1998; Antzelevitch & Dumaine 2011; Antzelevitch et al. 1991). Notably the work of Antzelevitch and colleagues, has led to the discovery of a sub-population of mid-myocardial cells called M-cells, which display longer APD than endocardial or epicardial cells at slow heart rates or in response to sodium channel blockade (Liu et al. 1993; Antzelevitch et al. 2011; Weissenburger et al. 2000). It has been proposed that this dispersion in repolarization, particularly in relation the the M-cell may play a role in the genesis of the T-wave. However, debate exists as to whether this is a true phenomenon or a function of the cellular preparation of the tissue. Work by Myles et al. (Myles et al. 2010) using optical mapping in a rabbit perfused ventricular free wall wedge preparation have shown that the transmural APD differences are influenced by the wavefront of activation with the longest APD at the site of activation and a shortening of APD along the line of activation, when stimulating from either the endocardium or epicardium highlighting the important role of electronic interactions in more intact tissue preparations, and a lack of transmural APD differences in this study.

Although such work may help to explain the myocardial surface electrogram, by use of a localised subtraction method, the body surface ECG is far more complex entity and is related to the potential differences of limb and precordial leads, which record the electrical activity of the heart conducted through body tissue, that acts as a volume conductor, to the skin surface. Indeed only the work of Franz (Franz et al. 1987), has truly studied the surface ECG in relation to the intact body as a conductor. One of the important findings of that work is the inverse relationship between activation and repolarization, which not only serves to reduce dispersion of repolarization, but also neatly explains the concordance of the normal T-wave, as the repolarization wave travels in the opposite direction to the activation sequence. Thus repolarization is due to an opposite cellular current flow to depolarization, the T-wave will be concordant to the QRS complex on the surface ECG (Franz 2001).

In addition to spatial variation in of APD, temporal variation is another well known phenomenon which may contribute to the genesis of the T-wave. This may occur due to temporal voltage dispersion or temporal "beat-to-beat" dispersion. It is recognised that different localised regions of tissue may display variable repolarization voltage gradient characteristics in Phase 3 of the action potential (Behrens et al. 1998; Behrens et al. 1996), and that this greatest dispersion in repolarization voltage corresponds to the peak of the surface T-wave. It was also shown that the gradients of the different Phase 3 slopes played the greatest part in determining the morphology of the T-wave. "Beat-to-beat" temporal variability, defined as alteration in APD from one beat to the next, is also known as electrical alternans, and can result in surface T-wave alternans. However, this form of variability is similar to spatial variability because of the nonuniform variation APD across the spatial regions of the ventricle that occur.

Finally, much has been learnt regarding the inscription of the surface T-wave from studies pertaining to the concept of cardiac memory. It has long been known, that the APD and the surface T-wave of the heart are governed by the activation sequence and alter over time in relation to a change in activation sequence (Rosenbaum et al. 1982; Rosenbaum et al. 1983; Laurita et al. 1996; Rosen 2009; Ozgen & Rosen 2009). In addition following a period of change in activation sequence, the changes in APD and T-wave morphology remain, regardless of the activation sequence, a concept known as "cardiac-

memory" (Rosen 2009; Ozgen & Rosen 2009). For instance, in the paced ventricle, the T-wave becomes inverted, and when this pacing is stopped the T-wave continues to be inverted. The mechanism of this alteration in APD is thought to be through a mixture of alterations in ion channel trafficking (namely Ito, Ica-l, Ikr and Cx43) and gene transcription, with angiotensin II playing an important modulatory role (Ozgen & Rosen 2009). The net outcome of this however, is a repolarization process that again follows the opposite direction of the activation sequence with early activation sites having a longer APD than late activating sites, resulting in R-T concordance and maintains itself when ventricular pacing is stopped.

2.7. Cardiac Repolarization and Sudden Cardiac Death

Given the well established concepts of a vulnerable window to VF during T-wave shocks, and the knowledge that dispersion of repolarization is associated with risk of ventricular arrhythmia, analysis of the surface ECG for risk markers of cardiac mortality remains an elusive but important goal. QT dispersion, signal-average ECG, heart rate variability and T-wave alternans (Gold et al. 2000; Mäkikallio et al. 2005; Barthel et al. 2003; Bauer et al. 2006; Haigney et al. 2004), have all been purported as potential predictors of ventricular arrhythmia and sudden death. However, none have been shown to be specific or sensitive enough at large scale analysis. This is partly because they lack specificity to the cardiac repolarization process alone and to its dispersion, but also because of inherent issues with the accuracy and usability of these measures.

Additionally T-wave analysis via vector cardiography, using indices such as total cosine R-to-T (which describes the angle of the repolarization wavefront in relation to the depolarization wavefront) and T-loop dispersion have also been studied (Acar et al. 1999; Zabel et al. 2000) and shown to relate to outcome, though their direct relation to repolarization dispersion is unclear. Recently Nicholson et al. (Nicolson et al. 2012) have developed R2I2(Figure. 8), which is a surrogate measure of APD on the surface ECG and found that repolarization heterogeneity of this marker to risk in ischemic cardiomyopathy, however, again this measure fails to take into account the whole of the T-wave, and may therefore omit valuable information regarding the repolarization process and its dispersion. In both experimental and human studies, Tpeak-Tend has been suggested to be a good marker of repolarization dispersion and therefore risk (Yan & Antzelevitch 1998; Panikkath et al. 2011; Castro Hevia et al. 2006). However the accuracy and applicability of such a measurement, particularly in the context of altered T-wave morphology or tachycardia has been called into question.

There is therefore need to further elucidate the underlying mechanisms of the T-wave, both in health and in disease, in order to improve our use of it in the diagnostic management and stratification of our patients.

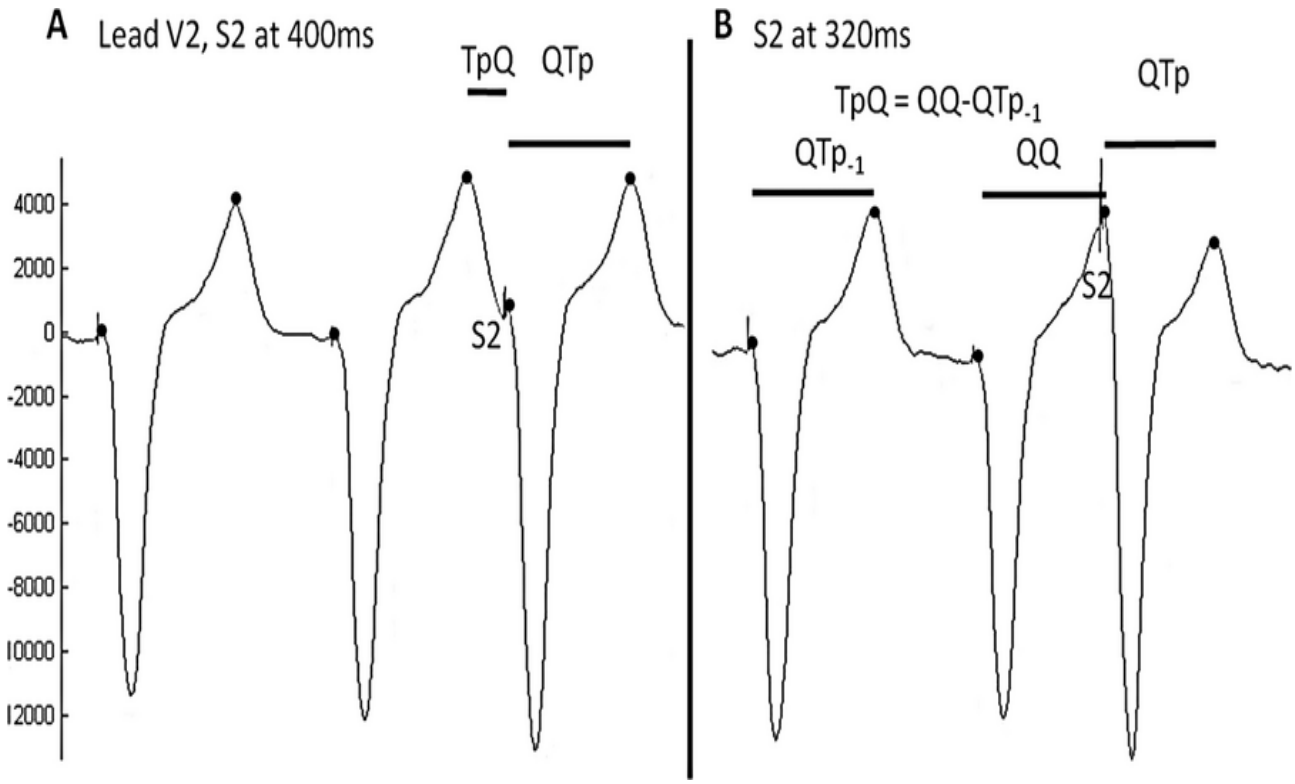

Figure 8. Technique for measuring R2I2 on the surface ECG. Reprinted from Nicolson et al. (Nicolson et al. 2012). With permission from John Wiley & Sons.

Chapter 3

Research Aims and Hypothesis

3.1. General Research Aims

Our understanding of the basic mechanisms that govern the generation of the body surface T-wave is incomplete. Given the failure of current risk prediction models to identify the majority of cases of sudden cardiac death, this thesis seeks to bridge the gap between the basic physiological mechanisms, to the electrical recordings on the surface of the heart. The aim of this thesis is to study these electrophysiological processes and how they translate to the surface ECG in health and disease, in order to define new noninvasive electrocardiographic markers of risk. Importantly most risk markers are based on static and often single time-point analysis of surface electrogram markers. This thesis investigates the dynamic nature of these markers in response to stress, in order to highlight failure of adaptation of repolarization as a key mechanism in the genesis and risk of arrhythmia.

This will be conducted through invasive and non-invasive dynamic stressors. Invasive recordings will be conducted in the cardiac electrophysiology lab, in patients with structurally normal hearts, and patients with at risk of VT/VF (ischemic cardiomyopathy and other cardiomyopathies). Non invasive stress in the form of exercise stress in patients with ARVC, will be performed.

The primary objective of this thesis is to elucidate the normal and abnormal APD properties if the heart and relate this to surface ECG manifestations of abnormal repolarization kinetics in order to develop new mechanistically based markers of SCD risk.

3.2. Research Hypotheses

This thesis will address the following hypotheses:

1. Transmural gradients of APD are present in the normal intact human heart.

2. Transmural and apico-basal gradients of APD play an important role in determining total repolarization time.

3. Disruption of transmural dispersion of APD occurs in disease and results in dispersion of localised total repolarization time.

4. Localised disruption of transmural and apico-basal gradients of APD affects the morphology of the surface ECG T-wave and manifests as changes in Tpeak-Tend.

5. Body surface and non-invasive ECGi mapping is able to identify non-invasive **clinical** markers of disease, before established imaging modalities such as cardiac MRI and CT.

This will be addressed via:

1. Custom designed signal processing methods to analyse activation and repolarization time in high-density "whole-heart" unipolar signals recorded during electrophysiological study (EPS) of the heart.

- To assess the presence of transmural gradients of APD and their role in total repolarization time and repolarization dispersion, in the intact normal human heart and in patients with Ventricular Tachycardia (VT).

2. Correlation of alterations in the intra-cardiac unipolar electrograms with simultaneous surface ECG dynamic changes during dynamic stress in patients with structurally normal hearts.

- To assess the role transmural and apico-basal repolarization gradients play in the formation of the surface T-wave morphology by examining the relationship between changes in intra-cardiac

conduction-repolarization dynamics and surface ECG T wave morphologies, in order to identify new markers of cardiac risk on the surface ECG.

3. Body Surface 256 ECG lead assessment of patients with ARVC utilising the inverse solution to provide epicardial mapping of the heart, in order to try to establish new non-invasive ECG markers of risk. This will be compared with conventional imaging such as MRI and CT to see if electrical markers of disease can identify early disease that is not visible on conventional imaging.

Chapter 4

Methodology

4.1. Recording The Cardiac Signal

As previously described, cellular ionic movements within the myocardial cell underlie the genesis of the of the recordable electrical currents within the myocardium and body surface. True action potential recordings can only be recorded on individual cells by placement of a glass-microelectrode into individual cells (Ino et al. 1988; Hoffman et al. 1959). They are only suitable for in vitro studies. MAPs can reproduce the high fidelity of TAP recordings, in the beating heart, in order to study the activation and repolarization characteristics of a localized region of myocardium. The contact electrode technique pioneered by Franz et al. (Franz et al. 1987; Franz 1991a; Franz et al. 1986; Franz 1983) for human use is the safest and most clinically applicable method for direct recording of MAPs in humans, avoiding the risk of embolism and tissue injury. The goal of this thesis, however, is to relate global "whole-heart" activation and repolarization dynamics to the surface ECG recordings in order to find new markers of cardiac risk. It is, therefore, not feasible or safe to deploy multiple MAP catheters throughout the right and left ventricle, and transmurally to assess this. Additionally measurements made with MAP catheters are highly operator dependent, particularly with regard to myocardial stability and pressure applied to the myocardium to obtain the signal.

In clinical electrophysiology, multipolar catheters are frequently placed in contact with the myocardium in order to gain more global information about the electrical activation of the heart. These catheters record and subtract the potential difference between two closely spaced electrodes in contact with the cardiac surface. This "bipolar" signal gives a clear inscription of the local activation, because the local subtraction process allows for a narrow field of view (Figure. 9B). An individual catheter pole, records the electrical signal generated by a wavefront underneath the electrode (the local event) but also the signal as the electrical activity moves away from the electrode (remote or far-field events; Figure. 9A). In the bipolar configuration the amplitude of the signal induced by the wavefront attenuates by the third power of distance (Durrer & van der Twell 1953; de Bakker & Wittkampf 2010), while using the single pole recording ("unipolar") the signal attenuates by the square of the distance. Therefore bipolar recording attenuates the far field effect, and if the poles are close together this provides accurate assessment of the local activation time. Additionally these electrograms are often filtered, to remove

electrical interference from the room, baseline drift and remote signals, often with a low-pass filter of 30Hz and a high-pass filter 500Hz and a notch filter at 50Hz. Such a configuration, although useful in delineating local activation, also causes loss of the T-wave component of the signal, thus making analysis of ventricular repolarization impossible.

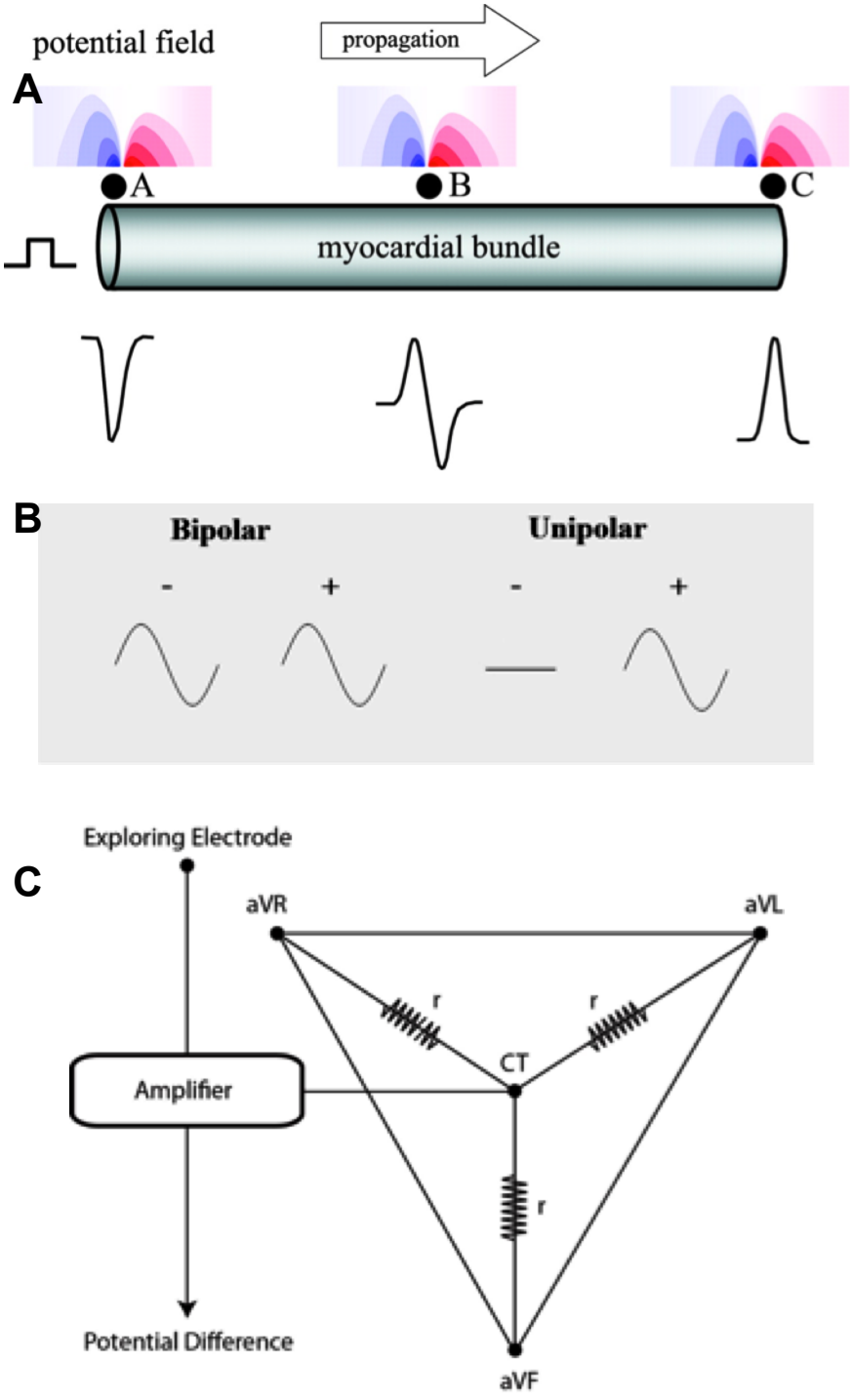

Figure 9. Unipolar and bipolar recording. **A**. Unipolar recording of a propogation of a potential field along a myocardial bundle from a-c, with revorded signal at each site underneath. **B**. Example of bipolar signal vs unipolar signal recording. Bipolar recording uses subtraction of the two signals to negate far-field effects. **C**. Wilson's central terminal used to reference the exploring electrode against in unipolar recording. Reproduced from deBakker et al.(deBakker 2010). With permission from Wolters Kluwer Health, Inc.

Unipolar electrograms record the local electrical activity in contact with the cardiac tissue, in relation to a reference anode with a theoretical zero signal. This is achieved in the cardiac catheterization lab by placing the reference electrode in the blood pool; where there is theoretically zero signal; or by using a mathematical mean of potentials recorded from the surface ECG, known as "Wilsons'Central Terminal"(Wilson et al. 1934; Burger etc al. 1955; Bacharova et al. 2005) (Figure. 9C). The advantage of the unipolar method is that less filtering is usually required and that information about the T-wave is acquired enabling repolarization of the local myocardium to be assessed. As a current wavefront approaches a unipolar electrode a positive deflection is recorded, and as the wavefront moves away a negative potential is recorded(Figure. 9B).

Thus the unipolar electrogram largely contains a monophasic or bi-phasic deflection for the activation wavefront. The deflection is negative at the site of early activation, bi-phasic at the site where activation passes and positive a the site at which activates last(Figure. 9A). Discerning the timestamps on the unipolar electrogram that represent local myocardial activation and repolarization has been the subject of much study and debate. A wealth of evidence supports the use of the minimum derivative of the QRS complex (dV/dt_{min}) to represent the time-point of local activation or upstroke of of the action potential of the myocardial cells underneath the electrode (Janse 1986; Wyatt et al. 1981; Steinhaus 1989a; Haws & Lux 1990; Chen et al. 1991; Anderson et al. 1993). This holds true even in ischemic conditions (Janse 1986), and is potentially more accurate than activation derived on a bi-polar signal, where precise activation may be difficult to pinpoint as deflections may occur due to any potential difference between the two recording electrodes.

Two methods to delineate the local repolarization time on the unipolar T-wave have been proposed. The "Wyatt" method (Wyatt et al. 1981)(Figure. 10A) utilizes the maximum derivative (dV/dt_{max}) of the T-wave, while the"alternative"method (Martinez & Olmos 2005) utilizes the maximum derivative (dV/dt_{max}) of the inverted and the minimum derivative (dV/dt_{min}) on upright the unipolar electrogram (Yue 2005) (Figure. 10B).The time interval between activation time (AT) and repolarization time (RT) on the unipolar electrogram, is known as ARI and is a surrogate marker of local APD (Figure. 10 A&C). The Wyatt method is the most widely utilised method to estimate ARI and there is a clear mechanistic and

physiological basis for using the positive derivative of of the unipolar T-wave, especially given that ionically, repolarization is electrically opposite to depolarization where the negative derivative is taken (Steinhaus 1989b). Although the Wyatt method may possibly underestimate ARI, the alternative method (Chen et al. 1991) results in a significant overestimation (Coronel et al. 2006) (Figure. 10B). Evidence to support the utilization of the alternative method in intracardiac human studies is based on correlations between APD recorded as a monophasic action potential and a unipolar signal derived from non-contact mapping (Yue et al. 2005; Yue 2005; Yue et al. 2004), however in this thesis contact unipolar electrograms are used, which would favour the use of the Wyatt method. Additionally much computational and mathematical modelling work support the use of the Wyatt method as long as the exploring/recording electrode is in close contact with the myocardium (Western et al. 2015; Potse et al. 2009) (Figure. 10 C&D). Thus in this thesis unfiltered unipolar electrogram recordings are used and analysed using the Wyatt method.

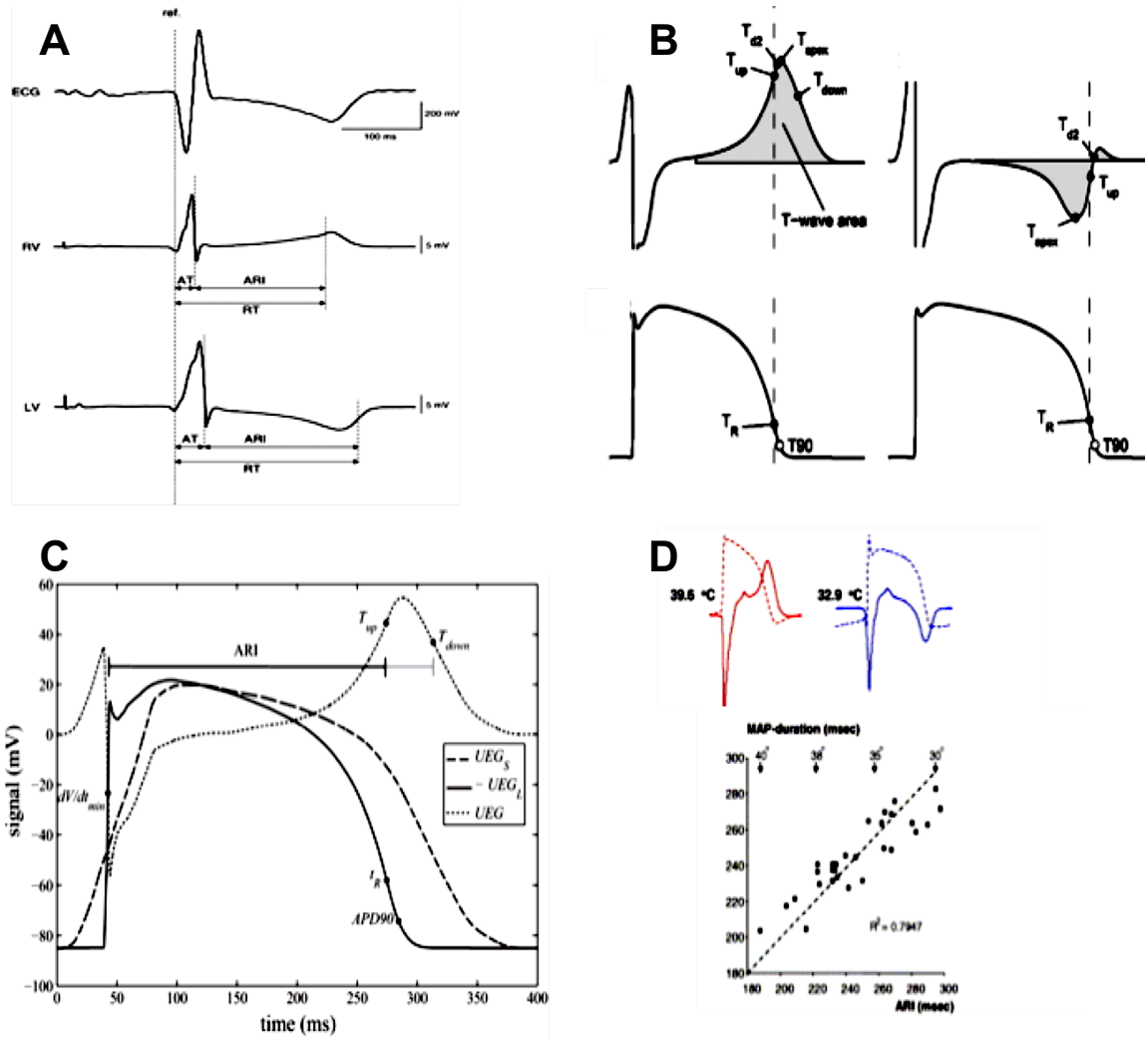

Figure 10. Wyatt vs Alternate Method. **A**. Schematic of the Wyatt method reproduced from Coronel et al. (Coronel et al 2007). Activation time (AT) is defined as the minimum derivative (dV/dT_{min}) of the unipolar QRS complex, while repolarization time (RT) is defined as the maximum derivative (dV/dT_{max}) of the unipolar T-wave. The time between AT and RT, is activation recovery interval (ARI), which is a surrogate marker of action potential duration (APD), as shown in panel B. Modeling studies shown in panel **B&C** reproduced from Potse et al.(Potse et al. 2009) and Western et al. (Western et al 2015), support the use of of the Wyatt method for defining RT. The downslope (dV/dT_{min}) is thought to represent far-field repolarization events, while local repolarization is represented by upslope of the T-wave, as seen in panel **C**. Panel **D** shows evidence from pig studies reproduced from Coronel et al. (Coronel et al. 2006), where the local repolarization defined by monophasic action potential (MAP) recordings corresponds with the Wyatt method (dV/dT_{max} of the unipolar T wave) , with a linear correlation of ARI on the unipolar T-wave and APD on the MAP. With permission from Elserver.

4.2. Cardiac Signal Analysis

Cardiac electrical signals collected from the study were collected and analyzed 'off-line' using custom designed software in MATLAB_R2014a (The MathWorks Inc., Natick, MA, 2014). For each patient 2-4Gb of data were generated. This data was extracted from the LABSYSTEM™ (Figure. 11A) electrophysiology recording system (Bard Limited, Murray Hill, NJ), and analyzed in Matlab. The custom script was designed by our engineer Michele Orini (MO) at UCL, with my assistance in testing for errors and improvements in code. In total 16 scripts, each containing between 1000-4000 lines of Matlab code (Figure. 11B) were constructed to form a graphic user interface (GUI) where data could be imported (Figure 11C).

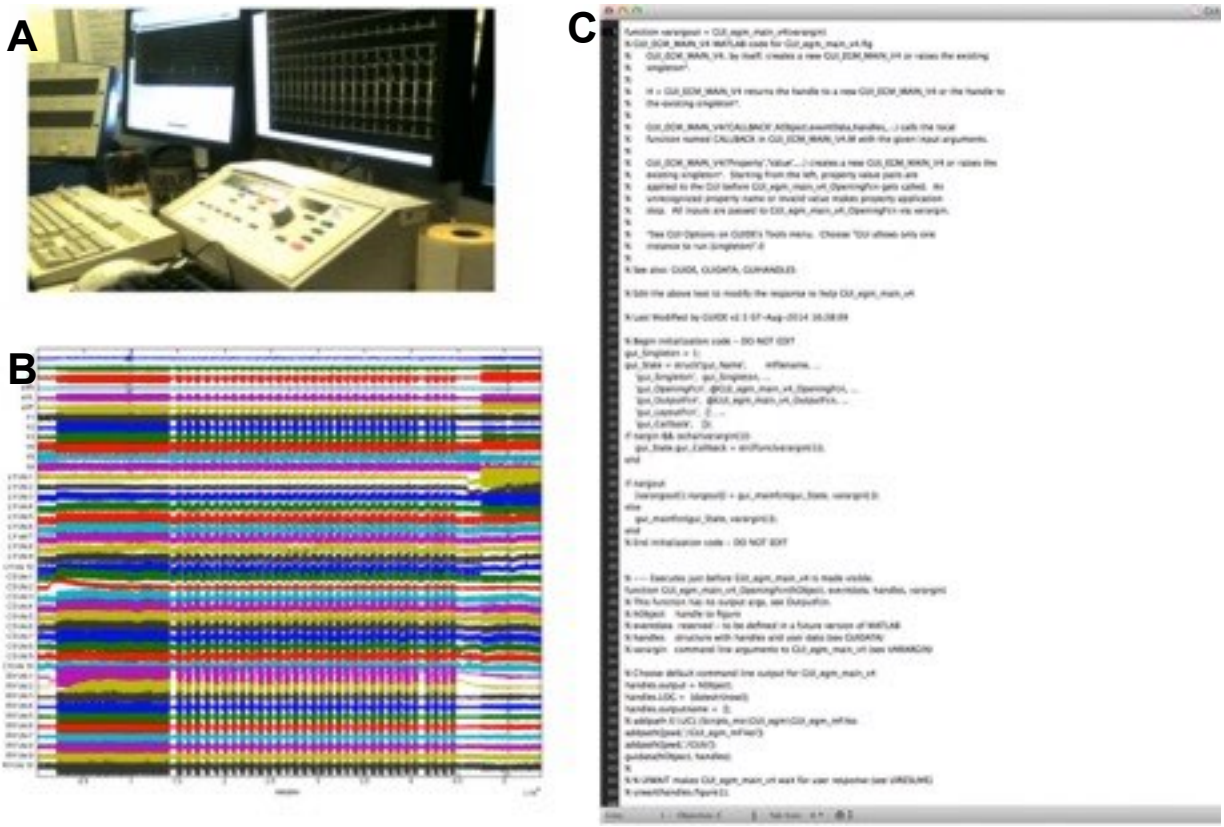

Figure 11. Importing signal for 'off-line' analysis. **A**. Signal recorded in LABSYSTEM™, and then extracted via USB. **B.** Matlab code was created to import the data for analysis and to create a graphic user interface (GUI) to analyse the data. **C.** Import of the data into the GUI to reading and analysis.

The cardiac signal was then analyzed in a semi-automated manner in the GUI (Figure. 12A&B). The GUI, identified AT, RT and calculated ARI(Figure. 11A&B) automatically and this was then checked manually, by myself for errors. The data was then plotted in the matlab GUI and any necessary preliminary fitting of individual patient data, as well as elimination of outliers was performed (Figure. 12C&D).

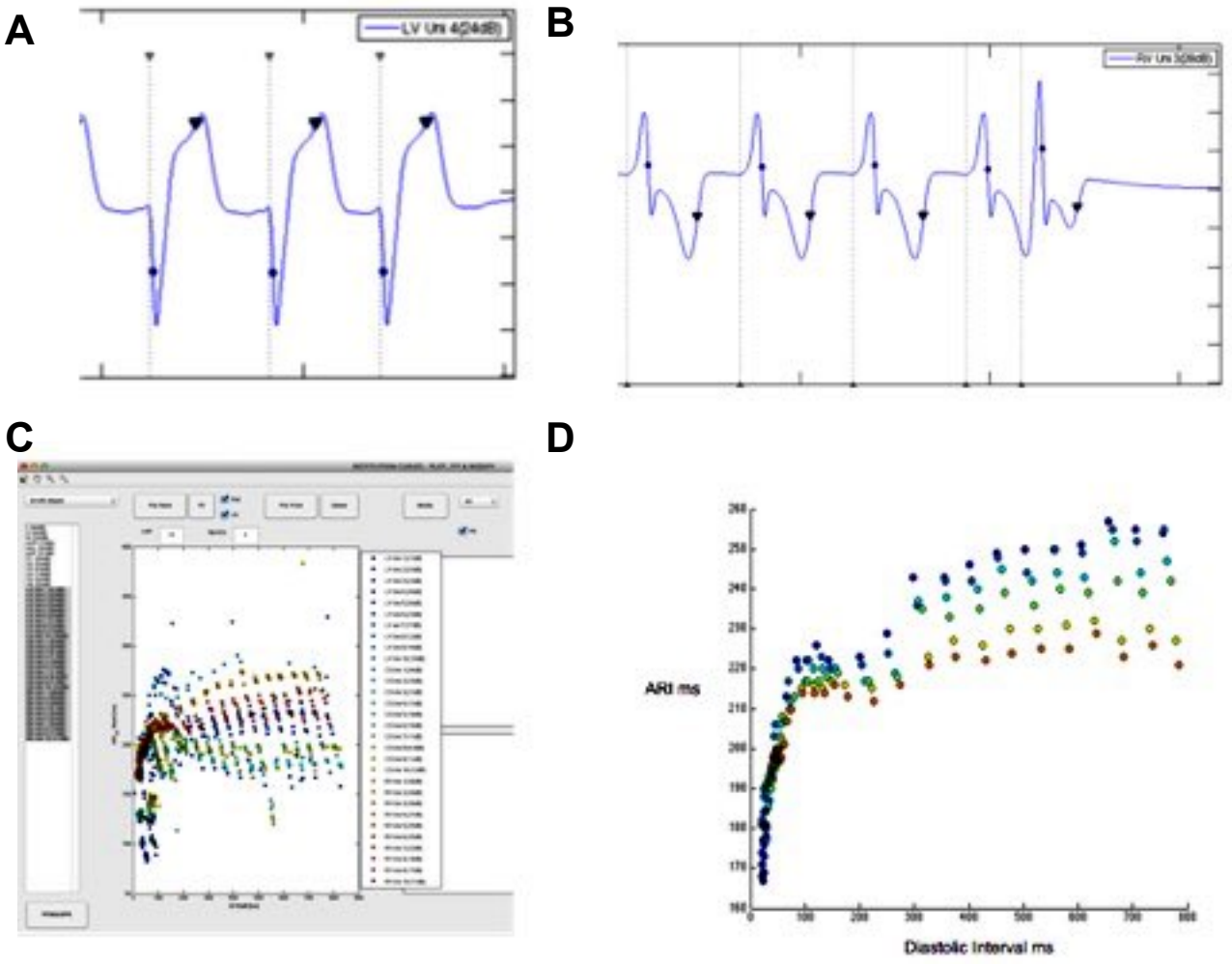

Figure 12. Example of Cardiac Signal Analysis in the GUI. **A&B**. Analysis of a train of restitution, in the GUI. The markers for activation time and repolarization time are calculated automatically, by the Matlab GUI, with manual checking and correction subsequently performed. **C&D**, restitution curves plotted in the GUI with outlier points (seen in **C**), checked for errors and recalculated as necessary, to create the final restitution curve as seen in panel **D**.

4.3. Normal Heart Human Restitution Study

4.3.1. Study Population

Ten patients with structurally normal hearts and preserved left ventricular ejection fraction who were due to undergo electrophysiology study (EPS) for diagnosis of an arrhythmia or ablation of supraventricular tachycardia (SVT) were considered for the study. All patients had normal upright T-waves in the precordial leads and no evidence of latent pre-excitation. Studies were conducted in a post absorptive state. All anti arrhythmic drugs were stopped for 5 days prior to procedure. The Study was approved by the National Research Ethics Committee London - Harrow.

4.3.2. Intracardiac Recording

Following clinical EPS and after any ablation was performed, a decapolar catheter (Response; St. Jude Medical, Minnetonka, MN) was placed in the RV for recording in an apico-basal orientation (Figure. 13A). A steerable decapolar catheter (Inquiry; St. Jude Medical, Minnetonka, MN) was placed on the lateral wall of the LV for recording in an apico-basal orientation in the LV endocardium via the retro-aortic approach and a steerable decapolar catheter (Inquiry; St. Jude Medical, Minnetonka, MN) was placed on the epicardium (Epi) of the LV via the lateral cardiac vein via the coronary sinus for recording transmurally across the LV wall (Figure. 13A). Transmural apposition of the catheters was checked with left anterior oblique (LAO) and right anterior oblique (RAO) fluoroscopy (Figure. 13B). The research protocol did not begin until 20 minutes after the clinical procedure to allow adequate time for isoprelanine which may have been used as part of the clinical procedure to be eliminated.

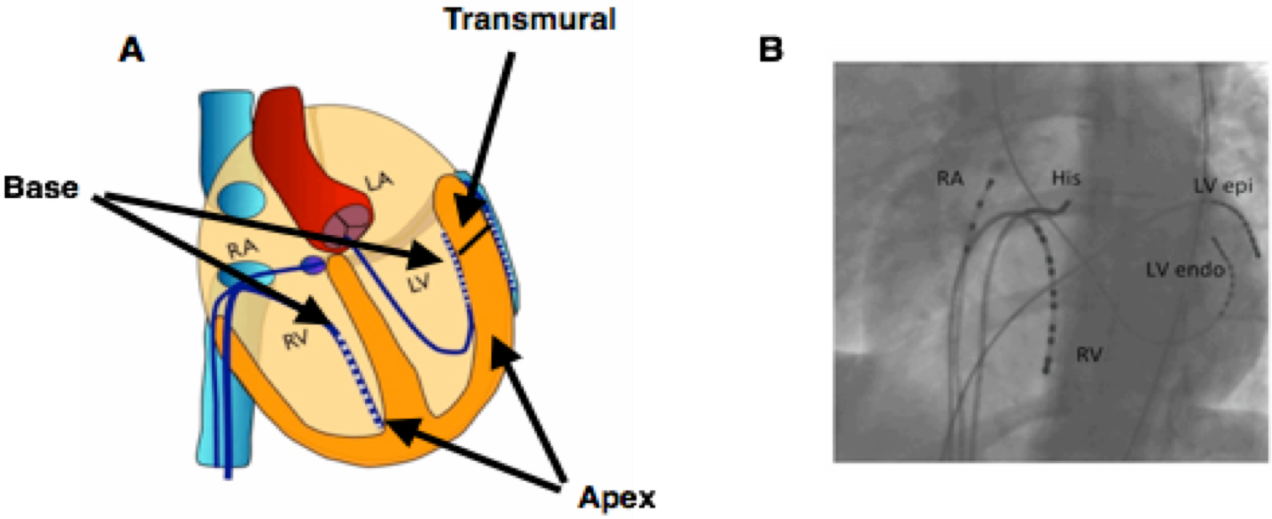

Figure 13. Orientation of catheters in the heart for recording. **A**. Schematic showing positioning of catheters in an apicobasal orientation in the LV and RV endocardium, and transmurally across the LV lateral base via the CS. **B**. Check of catheter position via fluoroscopy. LV - Left Ventricle, RV - right ventricle, RA - Right Atrium, endo - endocardium, epi - epicardium.

4.3.3. Restitution Protocol

For the research study, programmed electrical stimulation was performed at a pulse width of 2ms and a stimulus strength of 2x the diastolic threshold. Restitution was performed by pacing in three separate regions within the heart; the RV apex, the LV endocardium at the base and the LV epicardium at the base, with recording made apicobasally in the RV and LV and transmurally at the base of the LV. The restitution protocol began with pacing the distal pole of the Epi catheter, at the base of the LV, at a Basic Cycle Length (BCL) of 600ms for 3 mins in order to achieve steady state. Following this a restitution protocol was initiated with the delivery of a drive train of 9 beats(S1) BCL 600ms followed by the delivery of an extra stimulus (S2) at a coupling interval (CL) of 1000ms. The S1S2 coupling interval was then decremented in 50ms steps between S2 intervals of 1000 to 400ms, then by 20ms intervals between S2 interval of 400 and 300ms. At 300ms the S2 interval was decremented in 5 ms

steps until effective refractory period (ERP) of the tissue. At ERP an S2 stimulus at 10ms+ERP was applied followed by further decrementing S2 in steps of 2ms to confirm ERP. This protocol was then repeated in the distal pole of the LV catheter at the base of the LV endocardium, and the distal pole of the RV catheter at the apex of the RV endocardium.

We elected to perform a standard S1-S2 restitution protocol rather than a dynamic restitution protocol; where a train of S1 pulses are delivered for a fixed number of beads (often 50 beats), followed by gradual decrement in the S1-S1 interval until 2:1 conduction block occurs, because the dynamic protocol takes a significant period of time and we felt it unethical to the patient to prolong their procedure further with the research protocol.

4.3.4. Activation and Repolarization Time Evaluation

Unipolar electrograms (0.05 - 500 Hz, 2,000-Hz sampling rate) were recorded (Figure 12A&B). Local AT was calculated as the interval from pacing stimulus to the minimum of the first derivative of the unipolar QRS complex (dV/dt_{min}) (Figure 14. A&B) (Coronel et al. 2006). Local RT was defined using the Wyatt method (Coronel et al. 2006), as the maximum the first derivative of the unipolar T-wave. The Wyatt method was chosen because of its firm theoretical and experimental basis. It is established as the most accurate surrogate measure of local RT in the unipolar electrogram in experimental (Wyatt et al. 1981; Coronel et al. 2006; Haws & Lux 1990) and theoretical studies (Potse et al. 2009) (Scacchi et al. 2009), and has been shown to be independent of activation sequence (Haws & Lux 1990). Activation recovery interval (ARI) was used as a surrogate marker of APD and was calculated as RT minus AT. Diastolic interval (DI) was obtained by calculating the local coupling interval as the interval from the activation time after the last beat at basic coupling interval S_2 and activation time after the premature beat S_2 (AT_{S2}- AT_{S1}) and then subtracting the median ARI (ARI_{med}) for the preceding S_1 train after discarding the first three beats. Given that steady state pacing at BCL was performed for 3 minutes, and that the majority of rate adaptation takes place within the first 10-15 beats (Franz 2003), and that pauses between drive trains were the the region of 3-5 beats, we excluded the first 3 beats of

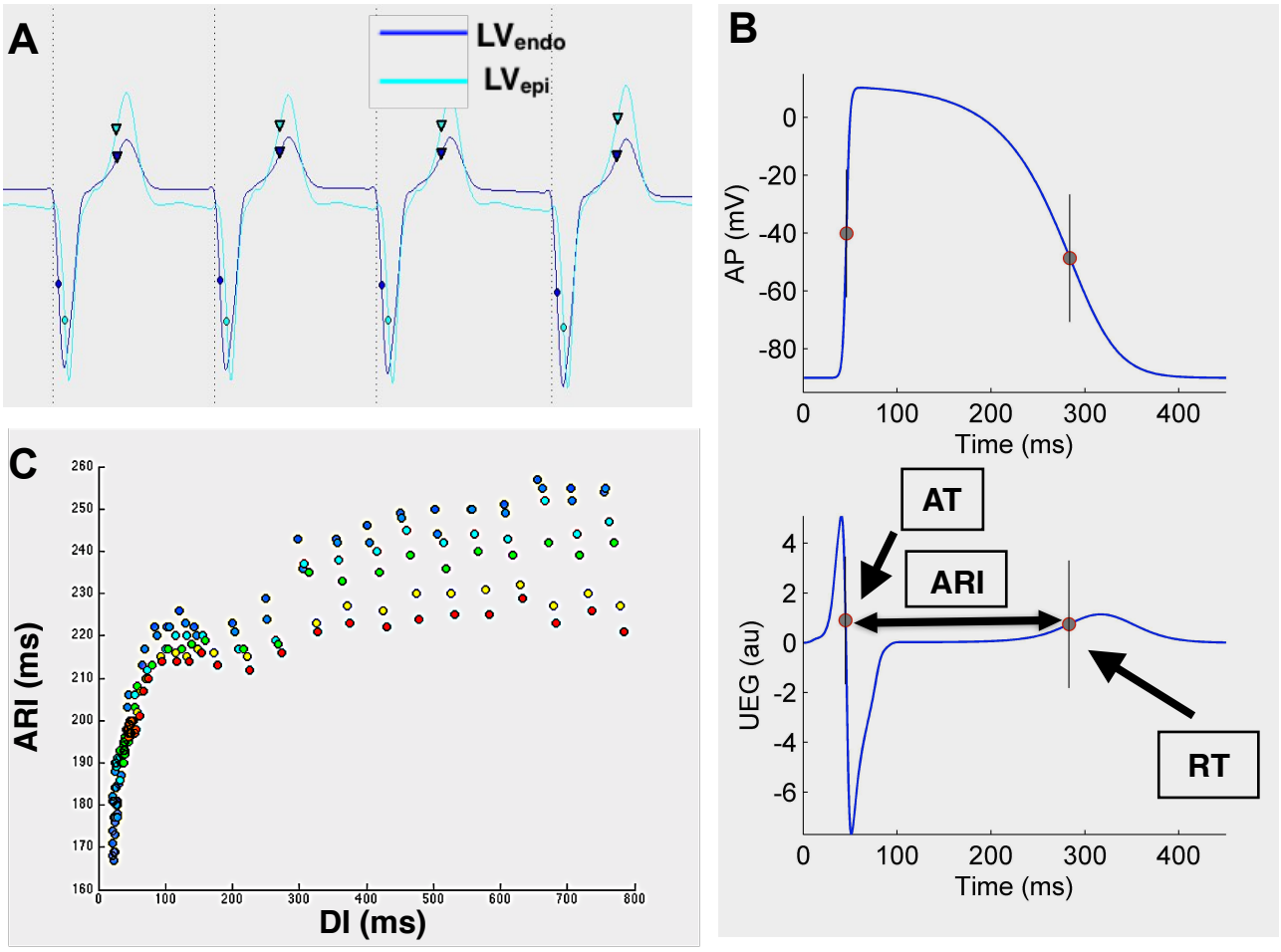

Figure 14. Analysis of cardiac restitution studies. (**A**) Example of simultaneous transmural unipolar electrogram recording at the LV_{endo} base and LV_{epi} base during LV endocardial restitution. Activation moments (circles) and repolarization moments (triangles) are shown. (**B**) The Wyatt method was used to determine activation time (AT) and repolarization time (RT), with activation recovery interval (ARI) taken as a surrogate marker of APD. (**C**) Example of an ARI restitution curve of one patient, from a series of catheter poles in the right ventricle, each pole is represented by a different colour.

the drive train to allow for any variation in adaptation. This was a better method as it enabled us to take a median ARI which was not biased by measurement error which can occur with automated dv/dt measurements of unipolar electrograms if only the final S1 beat were taken. Our preliminary analysis had demonstrated that most of the adaptation had occurred within the first 3 beats of the S1 drive train. Maximum slope of restitution was measured using piecewise liner regression segments of

sequential 40 ms diastolic interval windows in 10 ms steps as previously described by Taggart et al. (Taggart et al. 2003).

Drive trains that contained ectopic beats were excluded. Signals at the pacing site or where it was not possible to calculate local repolarization time due to abnormal T-wave morphology or ST segment elevation with no clear upstroke were excluded.

4.3.5. Siganal Processing and Statistical Analysis

Unipolar electrograms were processed off-line using MATLAB_R2014a (The MathWorks Inc., Natick, MA, 2014). AT, ARI and RT were calculated semi-automatically using a custom made MATLAB interface, as in previous studies (Orini et al. 2014; vanDuijvenboden etc al. 2015), and all markers were independently checked manually by two separate reviewers (NS & MO). Maximum slope of ARI restitution (S_{max}) was characterized by plotting ARI vs DI for each restitution curve, and defined as the steepest slope using piecewise linear regression on a moving 40ms window as previously described (Taggart et al. 2003).

For the analysis of regional differences within the heart, basal measurements were taken as the mean of the last four catheter poles located at the base of the RV and LV endocardium within each patient (Figure 13A&B.). Apical measurements were taken as the mean of the last 4 catheter poles located towards the apex of the heart in the RV and LV endocardium in each patient. Transmural comparisons could only be made across the base of the lateral LV comparing the mean of the four basal LV endocardial catheter poles and four catheter poles placed in the epicardium of the basal LV via the coronary sinus. This was because it was not possible to consistently record from the apex of the epicardium of the heart via the coronary veins due to variation in anatomy. Global AT, ARI, RT restitution curves across patients were obtained using lowes regression with 95% confidence intervals. This was because restitution did not follow a mono-exponential shape and was triphasic as described by Franz et al. (Franz et al. 2003) (Figure. 12D). Differences between different restitution curves were analyzed using quantile regression across the whole of the restitution curve, with statistical significance

inferred only if $p < 0.05$ across the entire restitution curve. To check that the results were independent from the chosen approach, data were also analyzed on a patient by patient basis. Results from Lowes regression and patient-by-patient analysis were highly consistent for each cardiac interval and pacing site.

The AT-ARI relationship was evaluated using the linear regression slope of the plot of AT vs ARI at a coupling interval of 600ms. Slopes were calculated for all three different pacing sites within each individual patient. Global AT-ARI coupling was assessed from the linear regression slope of all electrograms recorded within the heart. Regional coupling was assessed from the regression slope in the RV and LV endocardium of all electrograms recorded within the RV and LV respectively and transmurally from the electrograms recorded across the basal lateral wall of the LV (Figure 13B).

Statistical analysis was performed using R statistical software (R Core Team, 2013). Continuous parametric data are presented as mean ± standard deviation or, in the case of non-parametric data, median, unless otherwise specified. One sampled student's *t*-test was used to assess the statistical significance of Smax being >1 and AT/ARI slope being negative. Comparison between restitution slopes in the in the RV_{endo}, LV_{endo} and LV_{epi} performed using 1-way ANOVA with Tukey post hoc correction.

4.4. Relationship Between The Surface ECG T-Wave And Intracardiac Repolarization

4.4.1. Patient Demographics

Ten patients (mean age 35 +/- 15yrs 6 female) with structurally normal hearts who were due to undergo diagnostic electrophysiology study (EPS) for investigation of supraventricular tachycardia (SVT) were enrolled into the study. Studies were performed in the post-absorptive state under minimal conscious sedation. All patients had normal resting electrograms with no evidence of latent pre-excitation, normal echocardiograms and normal cardiac examination. All anti-arrhythmic drugs were stopped for 5 days prior to procedure. The study was approved by the local ethics committee and conformed to the declaration of Helsinki. All patients gave informed consent. The research protocol began after a 20-minute period of resting sinus rhythm at the end of clinical EPS

4.4.2. Intracardiac Recording And Surface T-wave Assessment

The methodology for our study is previously described in section 4.3 and elsewhere (Srinivasan et al. 2016). Briefly decapolar catheters (Response; St. Jude Medical, Minnetonka, MN) were placed in the right ventricle (RV) and lateral wall of the Left Ventricle (LV) for recording in an apico-basal orientation, and a steerable decapolar catheter (Inquiry; St. Jude Medical, Minnetonka, MN) was placed on the epicardium of the LV (LVepi) via the lateral cardiac vein of the coronary sinus (CS) for recording transmurally across the LV wall (Figure 15. A &B). For the research study, programmed electrical stimulation was performed at a pulse width of 2 ms and stimulus strength of twice the diastolic threshold. Restitution curves were performed by pacing in three separate regions within the heart: the RV apex, the LVendo at the base, and the LVepi at the base, with recording made apico-basally in the RV and LV and transmurally at the base of the LV. At each S2 interval for every pacing location (RV, LV and CS), SECGTW markers (Figure 15. C) were assessed and compared with simultaneously recorded unipolar intracardiac repolarization times (UEGMRT) in the LV and RV.

UEGMRT was defined using the Wyatt method (Wyatt et al. 1981), as the maximum the first derivative of the unipolar T-wave (dV/dtmax). The SECGTW was analysed for time of onset of the T-wave (Tiso), peak of the T-wave (Tpeak) and end of the Twave (Tend), in every ECG lead in every patient. Tend was measured from the point of dv/dt_{min} for the T-wave from which a tangent was drawn within our computational system until it met the baseline. T-end was measured as the timepoint of the intersect between the tangent and the baseline.. In total 23,946 SECGTW were analyzed and compared to regional UEGMRT. Markers were measured semi-automatically through our Matlab interface as previously described in section 4.3 and elsewhere (Srinivasan et al. 2016).

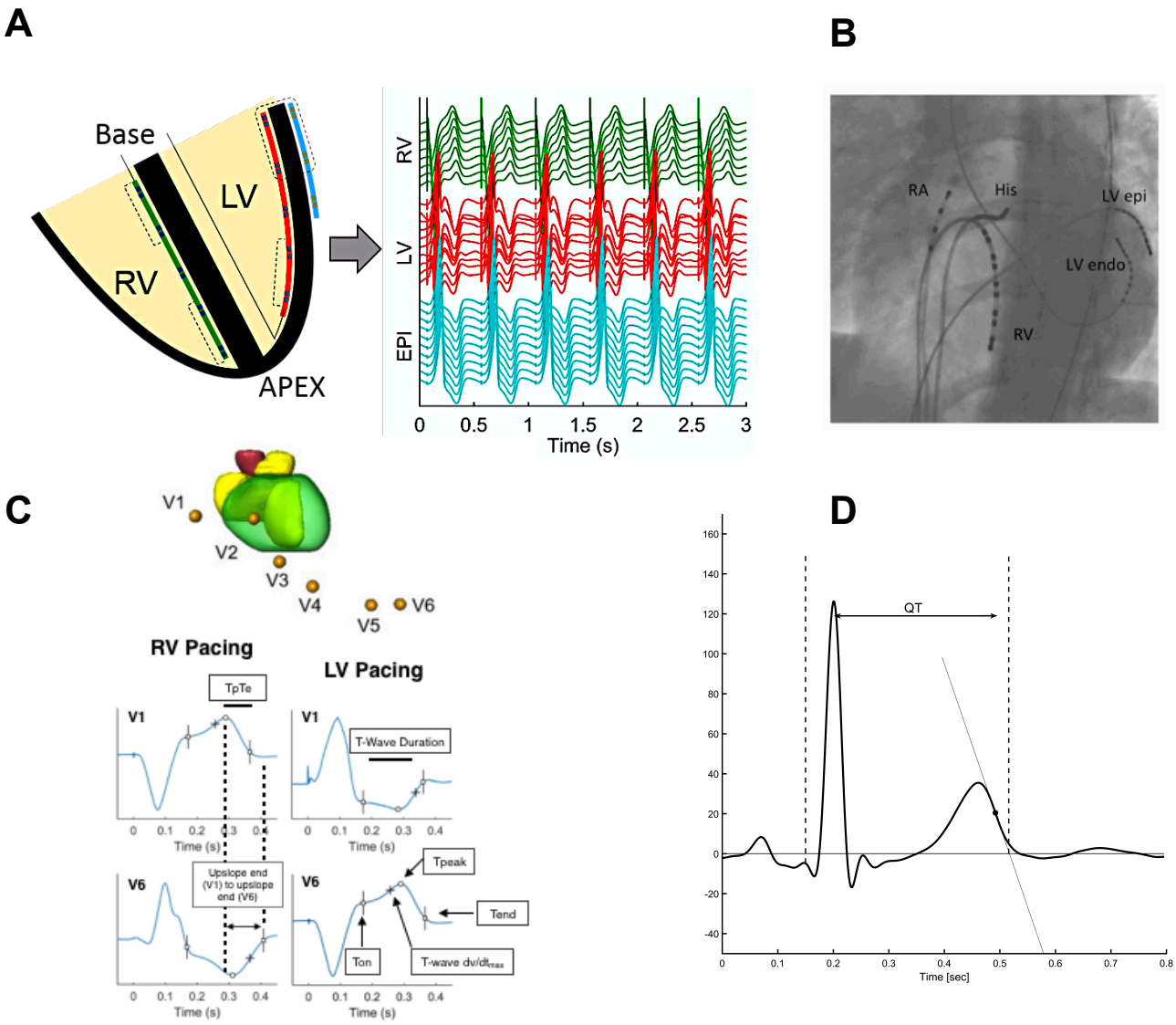

Figure 15. Orientation of catheters in the heart for recording. (**A**) Schematic showing positioning of catheters in an apicobasal orientation in the left-ventricle (LVendo) and right-ventricle (RV) endocardium, and transmurally across the lateral base of the LV epicardium (LVepi) via the CS, with corresponding unipolar electrograms recorded. Catheter positions were checked via fluoroscopy to ensure adequate apicobasal and transmural apposition(**B**). **C**, schematic of precordial ECG recorded in patient simultaneously, with change in ECG from different pacing sites. (**D**) Example of tangent method used to measure Tend. The point of dv/dt_{min} from which a tangent was drawn within our computational system until it met the baseline. T-end was measured as the intersect between the tangent and the baseline.

4.4.3. Statistics

Continuous variables are represented as mean +/-SD if normally distributed and median (25th-75th quantile) if not normally distributed. Assessment of normality was assessed through histogram plots, Q-Q plots and the correspondence of the mean and median. Comparisons between measured intracardiac repolarization time and SECG markers were assessed using a paired T-test. Measurement similarity between SECG T-wave markers and the intracardiac T-wave were assessed by calculating the intraclass correlation coefficient (ICC), using a two way mixed model of absolute agreement. The relationship between the upslope of the T-wave on the SECG, regardless of polarity, and regional intracardiac repolarization moments was assessed using sensitivity and specificity analysis. Relationship between the dispersion of repolarization and measures within the ECG T-wave were assessed using ICC, and R^2 of linear regression. A P value of ≤ 0.05 was considered statistically significant. Statistical analysis was performed using R statistical computing software (Version 3.2.2) (R Core Team, 2013).

4.5. Transmural Restitution Properties of The Structurally Abnormal Heart

4.5.1. Patient Population

Six patients (Median age 53 years, IQR 43-67 years), who were admitted acutely with VT resistant to medical therapy or recurrent ICD shocks, were referred for electrophysiology study and catheter ablation and were enrolled in a research study as part of their clinical ablation procedure. Clinical characteristics of the patients can be found in Table 1. All patients gave informed consent and the study was approved by our regional ethics board

Table 1. Patient Characteristics

Study Number	Age	LV Ejection Fraction	Pathology	Medications	Outcome
1	44	65	Myocarditis Elective case	Amiodarone stopped 6 weeks. Bisoprolol 5mg OD.	No further VT
2	64	14	Ischemic. Multiple MI's. PCI to 2002 and LAD. RCA Occluded Urgent case. BiV PPM	Bisoprolol 5bd. Amiodarone 200mg od	Further VT recurrence within 6 months
3	42	18	Ischemic cardiomyopathy /DCM. Recurrent VT shocks. Elective. Bi-V PPM	Amiodarone 200mg. Carvedilol 50mg BD.	Single shock within 6 months
4	68	52	Ischemic. CRT-D. Recurrent ICD shocks. CABG 1990.	Bisoprolol 10mg od.	No further shocks.
5	74	10	Ischemic.	Bisoprolol 5mg/ 2.5mg. Mexilitine 200mg od.	No further VT
6	34	55	ARVC. Single chamber icd. Recurrent VT	Bisoprolol 7.5mg od. Stopped 5 days before.	Further ICD Shocks and further ablation in different regions

4.5.2. Clinical Electrophysiological Study

4.5.2.1. Endocardial Mapping

Endocardial access to the LV was obtained via the retrograde and transseptal approaches in all patients. During LV mapping and ablation, heparin was administered to achieve an activated coagulation time of >300s. Detailed substrate maps were made during sinus rhythm, using the CARTO electroanatomic mapping system (Biosense Webster, Inc., Diamond Bar, CA, USA). Mapping was performed using a 7-French Navistar(Biosense Webster, Inc.) 4-mm deflectable tip catheter, a PentaRay high-density mapping catheter (PentaRay, Biosense Webster, Inc.) or a DecaNav mapping catheter (DecaNav, Biosense Webster, Inc.), depending on operator preference.

Initially detailed substrate maps were created in sinus rhythm. Normal myocardium was defined as a bipolar voltage >1.5mv, dense scar was defined as a bipolar voltage <0.5mv, and scar borderzone/ abnormal myocardium was defined as a bipolar voltage 0.5-1.5mv, consistent with previously published data (Reddy et al. 2003; Marchlinski et al. 2000; Stevenson 2009; Soejima et al. 2002; Verma et al. 2005). Bipolar electrograms were displayed on CARTO and on a real-time recording station (Bard Clearsign, CR Bard, NJ, USA, MN), filtered at 30-250Hz. Following this activation mapping was performed if hemodynamically tolerated, in order to identify sites of early activation which may have resented potential targets for ablation. Finally areas of low amplitude, mid-diastolic potentials were identified, if present, to further delineate areas of interest within the ventricle (Bogun et al. 2006).

4.5.2.2. Epicardial Mapping

Epicardial mapping was preformed in all 6 patients, as part of the clinical ablation study, either due to previous failed ablation, or a further clinical need to delineate the epicardial substrate. Pericardial puncture was performed in a manner consistent to previously described studies (Boyle & Shivkumar 2012), using a 17G Tuohy needle (Havel's Inc, Cincinnati, OH; BD Medical, Franklin lakes, NJ). The 7-French Navistar (Biosense Webster, Inc.) 4-mm deflectable tip catheter, a PentaRay high-density mapping catheter (PentaRay, Biosense Webster, Inc.) or a DecaNav mapping catheter (DecaNav,

Biosense Webster, Inc.) was used for epicardial mapping and ablation performed with the 7-French Navistar(Biosense Webster, Inc.) 4-mm deflectable tip catheter.

4.5.3. Research Protocol

4.5.3.1. Pacing Protocol

As the aim of this study was to delineate the transmural properties of scar and scar borderzone. Transmural restitution was performed after the endocardial and epicardial substrate maps were made and before initiation of VT or clinical ablation, which could potentially alter the substrate. Decapolar catheters, DecaNav (DecaNav, Biosense Webster, Inc.) placed epicardially, and a steerable decapolar catheter (Inquiry; St. Jude Medical) placed endocardially, were geometrically aligned to record across linear geometrically opposed transmural area, traversing, healthy tissue, scar-borderzone and dense scar, either on the endocardium or epicardium as selected by NS. The location of the transmural decapolar catheters was then logged on CARTO for offline analysis. The LV was then paced endocardially at a steady state of 600ms for 3 minutes, to enable APD adaptation, following which an S1-S2 restitution protocol was performed, beginning with an extra stimulus (S2) of 800ms, and decrementing in 50-ms steps until an S2 of 400ms, then by 20ms between 400ms and 300 ms and finally in 10ms intervals from an S2 of 300 until effective refractory period (ERP). This same protocol was then repeated pacing from the LV epicardium. We elected not to perform a dynamic restitution protocol in these patients due to the long pacing protocol involved and the risk of putting these patients into heart failure with long pacing periods at short cycle lengths.

4.5.4. Data Analysis

Transmural restitution studies were recorded using unipolar electrograms filtered at 0.05-500 Hz and recorded at a sampling rate of 2,000 Hz (Bard Clearsign, CR Bard, NJ). Local AT was calculated as the interval from pacing stimulus to the minimum of the first derivative of the unipolar QRS complex (dV/dt_{min})(Coronel et al. 2006). Local RT was defined using the Wyatt method, as the maximum the first

derivative of the unipolar T-wave (dV/dt_{max})(Coronel et al. 2006). ARI was used as a surrogate marker of APD and was calculated as ARI = RT − AT(Coronel et al. 2006). Diastolic interval (DI) was obtained by calculating the local cycle length as the interval from the AT after the last beat at basic cycle length S1 and AT after the premature beat S_2 ($AT_{S2} - AT_{S1}$) and then subtracting the median ARI for the preceding S_1 train after discarding the first three beats, as previously described(Srinivasan et al. 2016).

4.5.5. Statistical Analysis

Continuous variables are represented as mean +/-SD if normally distributed and median (25th-75th quantile) if not normally distributed. Discrete variables were compared with Fisher exact text or by chi-squared as appropriate. A p-value of <0.05 was considered statistically significant.

4.6. Non-Invasive ECG Imaging Of Arrhythmogenic Right Ventricular Cardiomyopathy Substrate

The work for this part of the thesis was performed in collaboration with the group of Dr Rudy in Washington University St Louis. For this I used the existing inverse solution validated by Dr Rudy's lab (Burnes et al. 1998; Jia et al. 2002). I collected the data in London with the aid of an engineer from the Rudy Lab, and the inverse electrogram analysis was provided by the engineer at thpage 72e Rudy lab, with joint collaboration for analysis of the data in relation to the disease. This study used the BioSemi (Amsterdam, Netherlands) multi electrode ECG strips to record the torso electrogram. The data was saved onto a Biosemi ECG platform and exported to the USA Rudy lab to perform the inverse solution coupled with the MRI segmentation. This study did not use the commercial CardioInsight™ (Medtronic Inc.) system that can be used clinically.

4.6.1. Patient Population

Twenty patients aged 24-75 years were selected from our inherited cardiomyopathy clinic. All patients were seen routinely due to a family history of arrhythmogenic cardiomyopathy or as a routine assessment due to abnormal clinical findings consistent with arrhythmogenic cardiomyopathy. All patients had genotyping performed for desmosomal; desmoplakin, plakoglobin, plakophilin-2, desmoglein-2 and desmocollin-2; mutations. Patient clinical characteristics are found in Table 2-4. Seventeen patients were known mutation carriers with a broad spectrum of structural and electrophysiological disease expression, representing the common spread of disease phenotype seen clinically. Three patients were negative for desmosomal genetic mutations but with extensive structural and electrophysiological abnormalities. The study was approved by the National Research Ethics Service Committee London (14/LO/0360) and the Human Research Protection Office at Washington University in St. Louis. All patients provided written informed consent.

Table 2. ARVC Patient Characteristics

Patient ID	Age	Gender	Mutation	Major Criteria	Minor Criteria
1	59	M	JUP	1	1
2	63	M	PKP2	1	3
3	54	F	PKP2	2	3
4	44	M	DSP	1	3
5	55	M	DSP	1	5
6	63	M	PKP2	3	3
7	59	M	DSP	1	3
8	69	F	PKP2	0	2
9	61	M	DSP	1	2
10	41	F	DSP*	1	1
11	49	F	PKP2	3	2
12	60	M	DSG	3	2
13	26	M	PKP2	0	3
14	66	M	PKP2	2	1
15	54	M	PKP2	2	0
16	74	M	DSG	1	3
17	24	M	DSP	1	0
18	54	M	Negative	2	2
19	39	M	Negative	2	2
20	75	M	Negative	2	3

Table 3. ARVC Patients CMRI Findings

Subject No	Tissue Wall Characterization (MRI)
1	
2	Basal RV free wall LGE
3	Fat in rv free wall and RV septum
4	
5	Fat in LV mid anterolateral wall. Circumfrential epicardial LGE in basal to mid segments including septum, sparing the infero lateral wall and apex
6	Extensive, pan-RV scarring
7	Extensive intramyocardial fat on T1. Extensive LV LGE circumfrentially basally.
8	RV insertion point LGE
9	Mid wall fat in LV basal infero-septum, with extensive LGE in that area
10	
11	LGE at mid RV free wall with fat.
12	Epicardial fat in LV mid inferior wall
13	
14	Moderate extensive LGE in RV and LV
15	LGE in basal to mid segs of RV free wall
16	
17	
18	Fatty infiltrate of rv free wall & basal septum. Several small patchy areas of RV LGE. Exensive LV LGE in the lateral wall.
19	Subepicardial LV LGE in basal to mid inferolateral wall and transmural in the apical inferior wall. RV LGE at the RVOT
20	Epicardial basal to mid lateral wall LGE. Patchy RV LGE in the inferior RV and free wall

Table 4. ARVC Patient Electrocardiographic Findings

Subject No	Repolarizatrion abnormalities	Depolarization/conduction abnormalities				Arrhythmias	
		Epsilon Waves	Positive SAECG	Terminal S wave duration >55ms	NSVT/SVT superior axis	NSVT/SVT inferior/indeterminate axis	>500 VE's per 24hours
1	-	-	-	-	-	-	-
2	-	-	+	-	-	-	+
3	T wave inversion V1-3	-	-	-	-	+	+
4	-	-	+	+	-	+	-
5	-	-	+	-	-	+	+
6	T wave inversion V1-4	-	-	+	-	-	+
7	T wave inversion V1-5	-	-	-	-	+	+
8	-	-	-	-	-	+	-
9	T wave inversion V5-6	-	-	-	-	+	+
10	Twave inverion V1-4	-	-	-	-	-	-
11	T wave inversion V1-4	-	+	-	-	-	+
12	T wave inversion V5-6	-	+	-	-	-	-
13	-	-	+	+	-	-	-
14	Twave inverion V1-3	-	-	+	-	-	-
15	T wave inversion V1-4	-	-	-	-	-	-
16	-	+	+	-	-	-	+
17	-	-	-	-	-	-	-
18	Twave inversion V1-6	-	-	-	-	-	+
19	T wave inversion V1-4	-	-	-	-	+	+
20	T wave inversion V1-5	-	-	-	+	-	+

Table 5. ARVC Patient Clinical Holter Findings

ID	Age	Gender	PVC Count	Monomorphic/Poloymorphic	Morphology
1	59	M	59	Monomorphic	LBBB
2	63	M	620	Polymorphic	LBBB+RBBB
3	54	F	1028	Monomorphic	LBBB
4	44	M	10	Monomorphic	LBBB
5	55	M	1000	Monomorphic	LBBB
6	63	M	2364	Monomorphic	LBBB
7	59	M	1111	Polymorphic	LBBB+RBBB
8	69	F	784	Monomorphic	LBBB
9	61	M	>3000	Monomorphic	LBBB
10	41	F	56	Monomorphic	LBBB
11	49	F	642	Monomorphic	LBBB
12	60	M	681	Polymorphic	LBBB+RBBB
13	26	M	52	Monomorphic	LBBB
14	66	M	26	Monomorphic	LBBB
15	54	M	38	Monomorphic	LBBB
16	74	M	1056	Monomorphic	LBBB
17	24	M	56	Monomorphic	LBBB
18	54	M	3496	Monomorphic	LBBB
19	39	M	890	Monomorphic	LBBB
20	75	M	>3000	Monomorphic	LBBB

Summary of 24-hour Holter findings from patient clinical records.

LBBB: Left bundle branch block morphology
RBBB: Right bundle branch block morphology

4.6.2. ECGI Methodology

Noninvasive, three-dimensional electroanatomic mapping has the potential to obviate the spatial and temporal limitations of the standard 12-lead ECG. One such system the ECGi (TM BioSemi Amsterdam, Netherlands) (Figure 16) combines body surface electrical potentials and heart-torso anatomical geometry to noninvasively determine the local electrical signals of the heart (electrograms) over the entire surface of both the left and the right ventricles. Using the relative timing of the constructed electrograms, activation sequences (isochrones) can be constructed in color-coded maps, and the propagation of activation wavefronts can be depicted in animated movies. ECGI images are constructed continuously and do not require the accumulation of data from multiple beats (Wang et al. 2011). A schematic of the ECGI procedure is presented in Figure 17. Two-hundred-and-fifty-six uniformly distributed body surface ECG potentials were recorded simultaneously from 250 electrodes, and were combined with the patients heart-torso geometry from cardiac MRI mathematically, to reconstruct epicardial potentials.

ECGI reconstructs epicardial potentials, electrograms, and isochrones from body surface potentials using mathematical reconstruction algorithms. The basis for ECGI methodology is the discretization of Laplace's equation, which computes the electrical potential field in the source-free volume between the heart and body surfaces. Application of Green's second theorem and the boundary element method results in a transfer matrix relating body surface potentials to epicardial potentials. Epicardial potentials are then computed from the body-surface potentials applying a constraint-based Tikhonov regularization and/or an iterative GMRes method (Ramanathan et al. 2006).

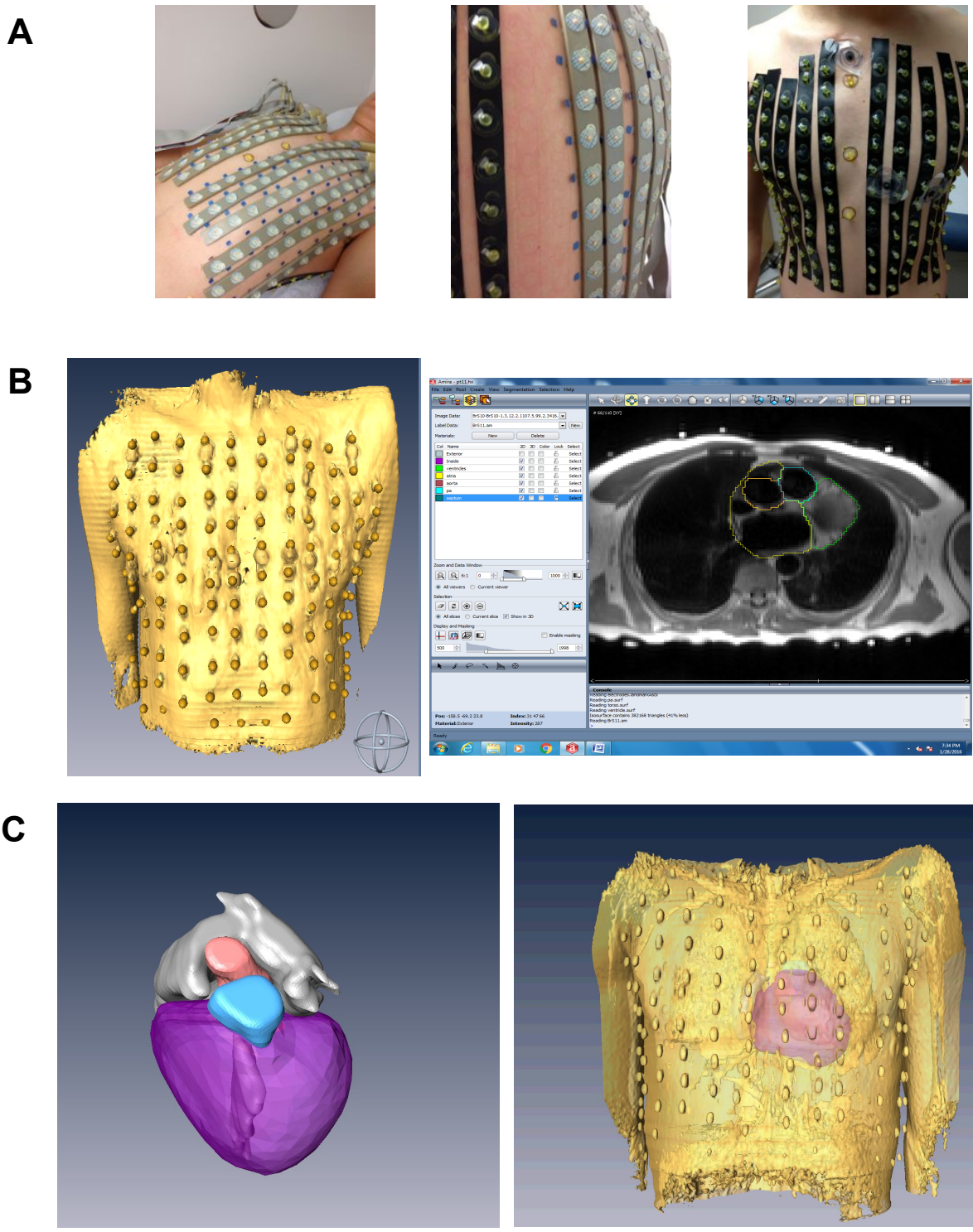

4.6.3.

Figure 16. ECGI cardiac segmentation. Two hundred and fifty six carbon electrodes mounted in strips are applied to the patient's torso before a pre-procedural thoracic MRI scan (**A**), which provides cardiac geometry and torso-electrode positions in the same reference frame. The electrodes are connected to a multichannel mapping system. These are then rendered in computer generated software, to delineate the location of the ECG electrodes (**B**), in relation to the segmented heart (**B**). The segmented individual patient cardiac model is shown in **C**, and its relation to the torso.

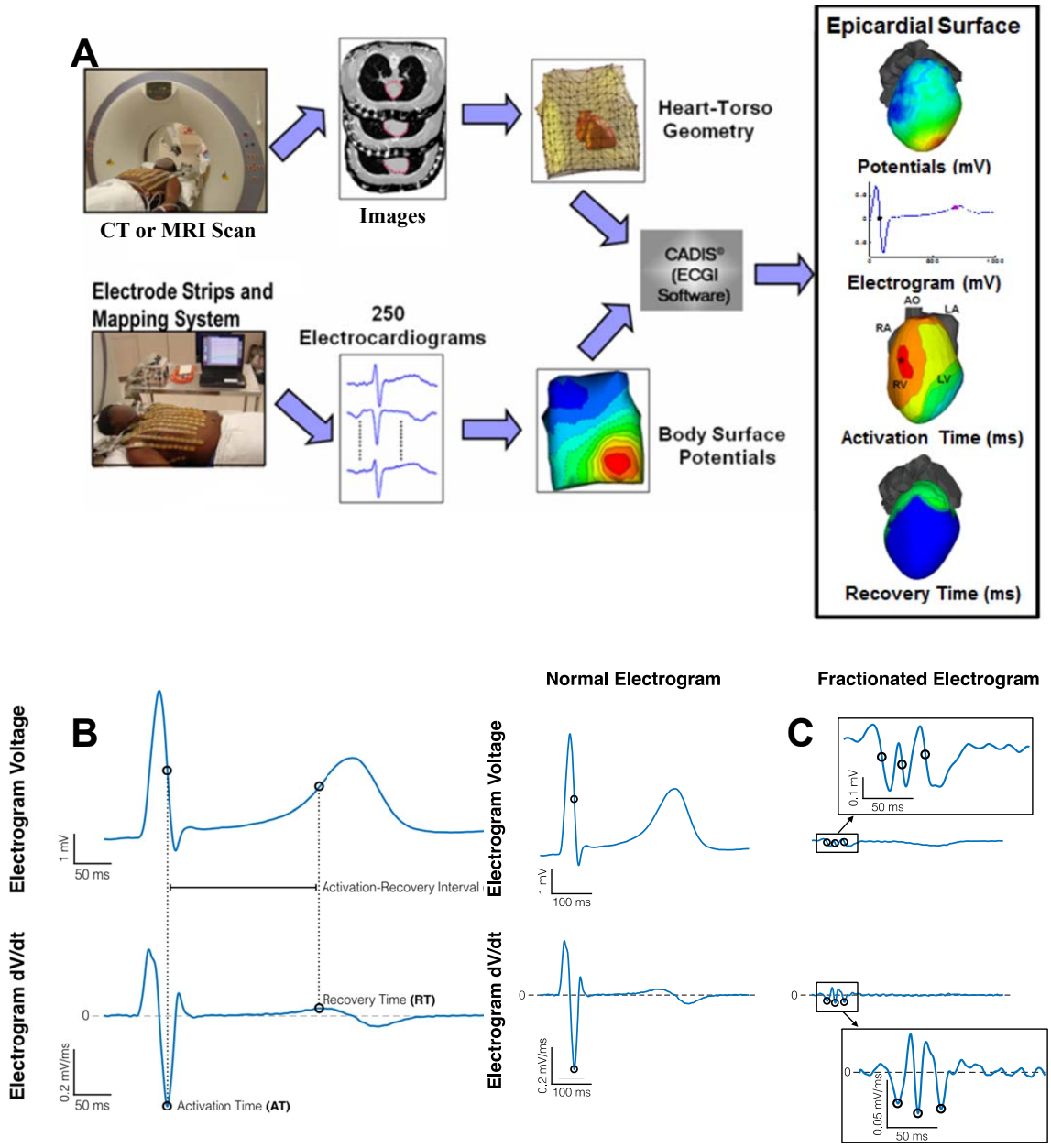

Figure 17. ECGI methodology. (**A**). Two-hundred and fifty carbon electrodes mounted in strips are applied to the patient's torso before a pre-procedural thoracic MRI scan, which provides cardiac geometry and torso-electrode positions in the same reference frame. The electrodes are connected to a multichannel mapping system. The electrical and anatomical data are processed mathematically to obtain noninvasive ECGI epicardial images that include potential maps, electrograms, isochronal activation sequences, and repolarization patterns. Although figure states that CT will be used, our study used cardiac MRI to avoid ionising radiation. Reproduced from Rudy (Rudy 2013). With permission from Wolters Kluwer Health, Inc. (**B**) Method for calculating AT and ARI. AT was calculated as the maximal negative derivative (-dV/dTmax) in the QRS complex. ARI was calculated using the Wyatt method as the maximal positive derivative (+dV/dTmax) of the upslope of the T-wave. (**C**) Assessment of fractionation. Fractionation was assessed as a count of the number of the number of steep downward deflections between the QRS and the T-wave. Steep downward deflections were defined as >10% the peak to peak voltage of the local electrogram and -dV/dTmax >70% of the max electrogram -dV/dTmax.

ECGI Protocol And MRI

Baseline recordings were performed in the supine position at rest. Following this patients were exercised on a supine ergometer, initially with unloaded exercise for 2 minutes, followed by a ramp protocol of 15-Watts/minute, to a maximum heart rate of 120 beats per minute. Recordings were made during exercise and recovery from exercise. Recordings were performed in the supine position at rest, during exercise, and immediately following exercise cessation.

CMR was then performed in a 1.5 T scanner (Magnetom Avanto, Siemens Medical Solutions, Germany). Prior to the scan, recording electrodes were replaced with MR-visible markers so the electrode positions could be obtained in the same coordinate system as the heart geometry (Figure 17). A navigated anatomical sequence was used so the ECGI electrical and anatomical data could be merged. Conventional cine imaging and advanced LGE imaging were conducted following the thorax scan. The contrast agent was 0.1mmol/Kg of Gadoterate meglumine (Dotarem, Guerbet S.A., Paris, France) with LGE images acquired 5-15 minutes post-contrast. The LGE sequence was a single shot steady state free precession (SSFP) phase sensitive inversion recovery sequence (PSIR) 19 with motion corrected averaging using gagetron and high resolution. Two patients declined contrast injection.

Unipolar epicardial electrograms (EGMs) were reconstructed using the solution to the inverse problem to compute epicardial EGMs from the recorded ECGs. Epicardial activation and repolarization maps were constructed. ECGI reconstructions of sinus rhythm were computed for each patient prior to exercise and immediately after exercise cessation at an elevated HR. Additionally, the epicardial activation sequence was computed for each unique premature ventricular contraction (PVC) morphology observed.

4.6.4. Analysis

4.6.4.1. Segmentation

ECGI maps and LGE images for each patient's ventricles were divided into basal, mid, and apical regions. Basal and mid regions were divided into anterior, anterolateral, inferolateral, and inferior regions. Apical regions were divided into anterior and inferior regions.

4.6.4.2. CMR

CMR analysis was performed using CVI42 software (Circle Cardiovascular Imaging Inc.,Version 5.1.2[303], Calgary, Canada), by two independent observers, Stefania Rosmini and Heerajnarain Bulluck, with checks performed by Professor James Moon. LGE in the LV, epicardial and endocardial borders were manually drawn on the short axis slices and the anterior RV insertion point was identified. The Otsu semi-automated technique was used to quantify LGE and was displayed on a bullseye plot as relative enhanced area (percentage) per segment on the 16-segment American Heart Association model.

An RV LGE, a segmentation model was created using the short axis stack. Basal, mid and apical segments were identified using the papillary muscles as markers and divided into anterior, anterolateral, inferolateral and inferior segments for the basal and mid RV segments and as apical anterior and apical inferior segments for the RV apical segments.

The amount of RV LGE was quantified visually as 0 (no LGE), 1 (some LGE), or 2 (high LGE) by 2 operators. In cases where the operators quantified the RV LGE differently, a third senior operator acted as adjudicator. Analyses of the ECGI and CMR data were conducted independently with investigators blinded to the results of the other modality.

4.6.4.3. Electrogram Analysis

Electrogram analysis was performed by Christopher Andrews and Neil Srinivasan as a joint collaborative project with the Rudy Lab, Cardiac Bioelectricity and Arrhythmia Center (CBAC), Washington University St Louis Missouri. Reconstructed unipolar epicardial electrograms were processed to compute electrical parameters of interest. Activation time (AT) was computed as the steepest negative time-derivative of voltage (-dV/dtmax) in the local QRS complex. Recovery time (RT) was computed as the time point of steepest positive time-derivative (dV/dtmax) during the T-wave (Coronel et al. 2006). Activation-recovery intervals (ARI, a surrogate for local action potential duration) were computed as the difference between RT and AT. Spatial gradient magnitudes of EGM parameters were computed for each EGM as the absolute value of the change between neighbouring EGMs divided by the distance between EGM locations, averaged across all neighbours. EGM amplitudes were computed as the peak-to-peak voltage during the QRS complex. Analysis of the electrogram was performed using the same method as described by Cuculich et al. (Cuculich et al. 2011). Fractionation was defined as the number of deflections in each EGM, computed as the number of steep downward deflections between QRS onset and the start of the T-wave. The criteria for steep deflections in an EGM were a minimum amplitude of 10% of its peak-to-peak magnitude and a -dV/dt greater in magnitude than 70% of its maximum -dV/dt. Additionally, both values were required to be greater than or equal to 5% of corresponding values for all EGMs to prevent the inclusion of noise effects in analysis of relatively flat EGMs. The earliest 10% of ATs were considered the epicardial initiation site of a PVC. PVC occurrence rates were computed as the number of times an EGM fell within a PVC initiation site divided by the total number of beats recorded. The data are presented as ARI mean to allow regional analysis in comparison to the MRI structural substrate. Maximum ARI is not resented because a single figure such as this is prone to outlier bias and measurement error., and may not be a true representation of the true ARI that region.

4.6.4.4. Statistical Analysis

Fractionation values within anatomical segments are presented as z-scores compared to a group of 20 healthy young adults. Electrical parameters in the ARVC study population were compared to the healthy controls using Wilcoxon rank-sum tests. Population data are presented as medians and interquartile ranges. Substrate and PVC rate comparisons were performed using Pearson correlation coefficients.

Chapter 5

Results: Normal Heart Human Restitution Study

5.1. Introduction

Cardiac restitution represents the dynamic interplay between activation time (AT), action potential duration (APD) and repolarization time (RT) in relation to a given extrastimulus coupling interval or diastolic interval. It is hypothesised that a steep APD restitution slope may be pro-arrhythmic (Garfinkel et al. 2000), although, steep restitution curves have not been directly linked to an increased cardiac risk (Franz 2003; Narayan et al. 2007; Dorenkamp et al. 2013). In the intact whole heart, dynamic ventricular restitution remains of great interest because it may modulate the spatial dispersion of RT during heart rate changes. The spatio-temporal organization of AT and RT in response to an extrastimulus may therefore play an important role in the development of arrhythmogenesis (Child et al. 2015). Spatial dispersion of RT is dependent on how APD varies along the pathway of activation and regionally throughout the ventricle. The AT-APD interaction is represented as a plot of AT and APD during the same beat at varying coupling intervals. The slope between AT and APD is referred to as AT-APD coupling (Hanson et al. 2009; Yue 2005). In a negative AT-APD slope, APD decreases along the pathway of activation limiting the dispersion of RT, while a positive AT-APD slope enhances the dispersion of RT due to increasing APD.

The spatial variation in restitution properties and AT-APD coupling in the intact human heart, has largely only been studied in situations where global activation time is relatively short, such as in sinus rhythm or right ventricular (RV) apical pacing, when early engagement of the Purkinje network occurs (Yue et al. 2005; Subramanian et al. 2011). This homogenizes total AT, while maintaining a normal endocardial to epicardial activation sequence. However, ventricular arrhythmias are frequently triggered by non-Purkinje related premature beats (Laurita et al. 1998) which may modulate repolarization gradients. Little is known about the role of varying the activation site in relation to the spatial restitution and AT-APD coupling properties of the RV and left ventricle (LV). In the intact human ventricle, negative coupling between AT-APD has been demonstrated during RV apical pacing (Subramanian et al. 2011; Hanson et al. 2009; Yue 2005) . In order to continually maintain negative AT-ARI coupling for varying stimulus sites, and therefore limit RT dispersion, regional APD would have to adapt to varying AT sequences. Regional variations in APD have been shown in animal studies using

ventricular wedge preparations, where transmural and apico-basal dispersion of APD and total RT have been demonstrated (Antzelevitch & Dumaine 2011; D. W. Liu & Antzelevitch 1995; Antzelevitch et al. 1991). Whether these regional variations in APD are present in the intact human myocardium and whether they adapt to varying stimulus site in order to maintain negative AT-APD coupling or are fixed in order to only homogenize total repolarization time in response to the normal activation sequence remains unclear.

5.2. Aim

I aimed to investigate the effect of varying stimulus site on the spatial apico-basal and transmural properties of AT, APD and RT, during restitution studies in patients with structurally normal hearts. I also sought to evaluate the effect of this on AT-APD coupling and the steepness of the APD-restitution slope.

5.3. Hypothesis Addressed

1. Transmural gradients of APD are present in the normal intact human heart.

2. Transmural and apico-basal gradients of APD play an important role in determining total repolarization time, depending on activation sequence.

5.4. Methods

Refer to section 4.3.

5.5. Results: Human Restitution Study

5.5.1. Shape of ARI restitution curve and maximum slope

The shape of the restitution curve across a series of 6 RV catheter poles during RV pacing a representative study patient is shown in Figure 14C. After excluding channels with signal to noise ratio <13dB and an R^2 <0.5 for the linear regression fit a total of 725 individual restitution slopes were analysed; 290 slopes from the RV, 290 slopes from the LV and 145 slopes from the Epi.; 74% of slopes had a gradient >1 ($p < 0.001$), with a mean S_{max}= 1.76 and median S_{max}= 1.54. Figure 18 displays the distribution of S_{max} grouped by recording and pacing sites. $S_{max}$was significantly >1 ($p<0.05$) for all regions except in the LVepi when performing restitution from the RV apex ($p=0.26$) and LV basal endocardium ($p=0.13$). Regional analysis irrespective of pacing site showed greater S_{max}(Figure. 18A) in the LVendo (mean S_{max}= 2.2) compared to the RV (mean S_{max}= 1.4, $p<0.01$) and LVepi (mean S_{max}= 1.5, $p<0.01$) and no significant difference in the mean slope between the RV and LVepi. The same pattern was noted with RV apical and LV basal pacing with steeper S_{max}throughout the LVendo when compared to the RV and LVepi (Figure 18. B&C). During CS pacing S_{max} was steepest in the LVepi and LVendo with no significant difference between the regions on ANOVA ($p=0.26$, mean Smax 2.9 vs 2.2 respectively), but significantly greater $S_{max}$for both regions when compared to the RV (mean S_{max}1.3, $p<0.01$ for both regions), as shown in Figure 18D.

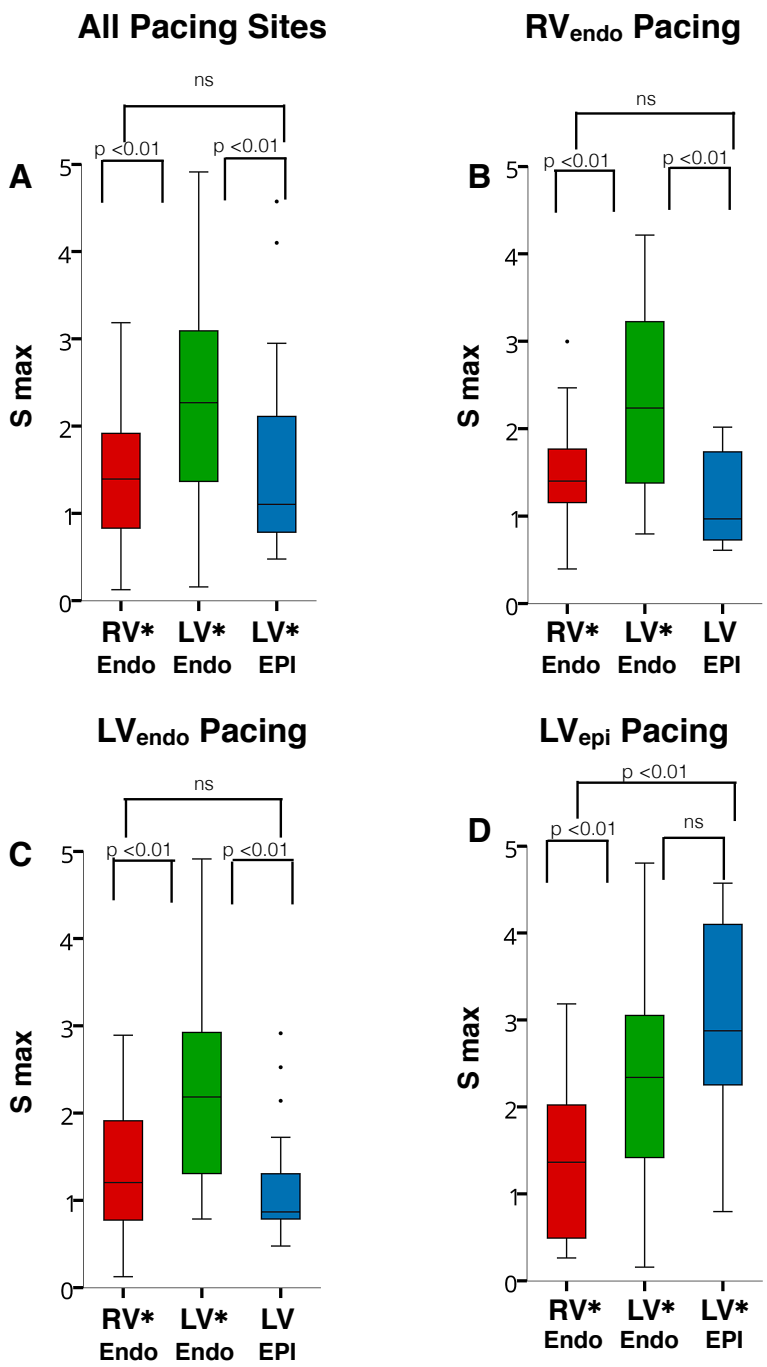

Figure 18. Boxplots of Smax for all patients. Smax on y-axis and recording region on the x-axis. **A**. All recorded values in the right ventricle (RV), left ventricle (LV) and epicardium (Epi), regardless of pacing site. **B, C&D**. Smax for RV, LV and coronary sinus (CS) Epi pacing. Then median Smax was >1 in all instances. Bars above the graph represent Anova comparisons of statistical difference between region Smax, based on pacing site. Asterix next to recorded region on x-axis signifies $p<0.05$ for regional Smax >1, based on one sampled T-test.

5.5.2. AT Restitution And Activation Pattern

Lowes regression with 95% confidence intervals of AT restitution when pacing from the RV apex (Figure. 19A-C) the following pattern of activation : RVendo(apex) → RVendo(base) → [LVendo(base)=LVendo(base)] → LVepi(base). When pacing from the base of the LV, the pattern of activation was: LVendo(base) → [LVendo(apex)=LVepi(base)] → LVepi(base) → [RVendo(apex)=RVendo(base)](Figure. 19D-F.). Finally, when pacing from the CS, the pattern of activation was: LVepi(base) → LVendo(base) → LVendo(apex) → RVendo(base) → RVendo(apex) (Figure. 19G-I.). All slopes displayed the expected finding of AT restitution with lengthening of AT at shorter CLs close to the refractory period of the ventricle (Figure. 19). Significant differences in apico-basal and transmural activation time are shown in Figure 19.

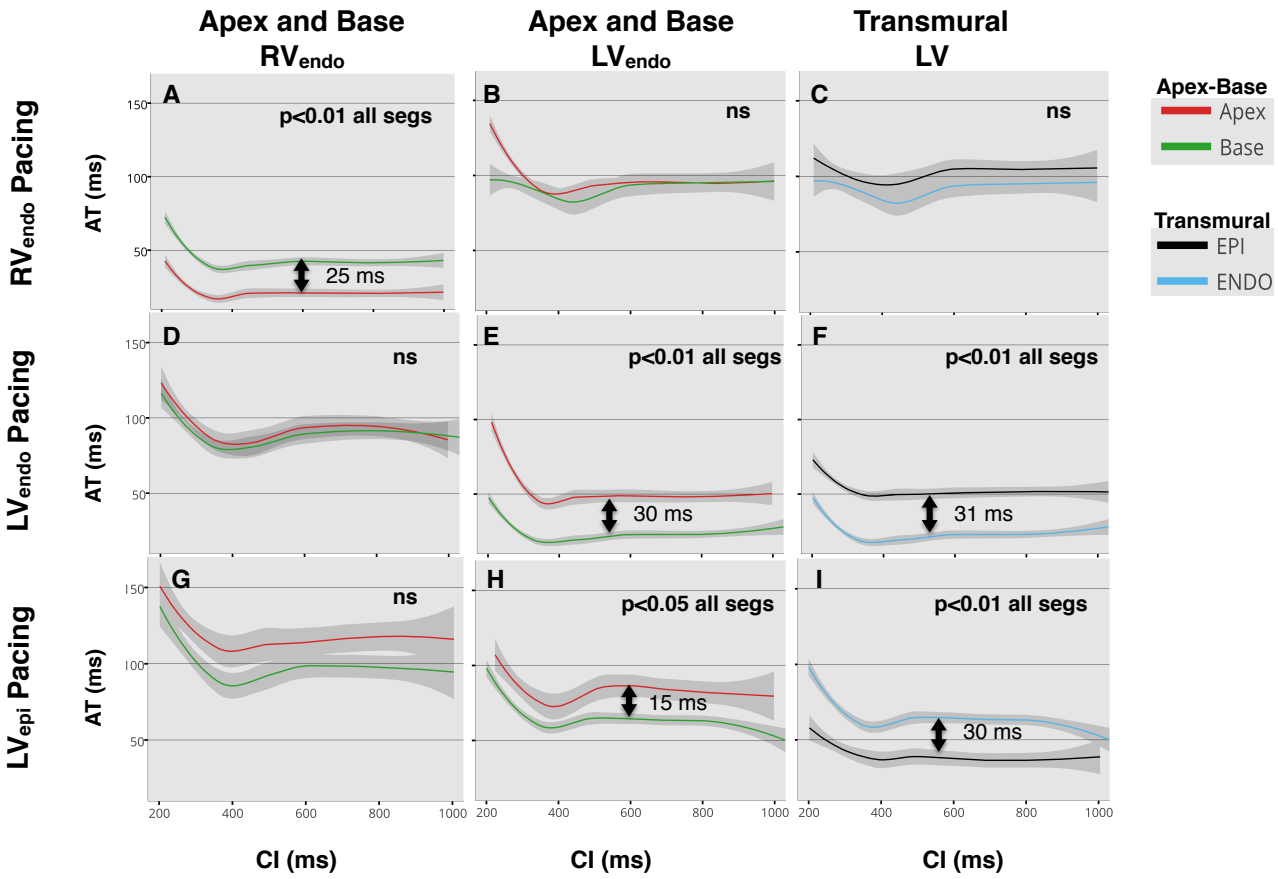

Figure 19. Lowes regression curves of Activation Time (AT) restitution. Pacing site for each row is shown in the far left, with comparisons made from apex to base made in the right ventricle (RV), left ventricle (LV) and transmurally across the LV base, represented by each column (top). Significant differences were assumed if quantile regression was <0.05 across the whole of the restitution curve and statistical significance shown inset within the graphs. Arrows with time in miliseconds (ms) represent difference at the 50th quantile where curves were significantly different. ns=no significance. CL = Cycle Length. AT = Activation time

5.5.3. Dispersion Of ARI Restitution Curves

Lowes regression with 95% confidence intervals of ARI restitution from all patients is shown in Figure 20. Transmurally (Figure. 20C, F & I) there was a significant difference in ARI throughout the entire restitution curves for all pacing modalities ($p<0.01$ for all curves) with shorter ARI epicardially than endocardially. At the 50th quantile there was a 30ms difference when pacing from the RV apex, 25ms difference when pacing from the LV base and 48ms difference when pacing at the LV base epicardially.

Restitution curves in the RV showed a trend towards shorter ARI at the base than the apex (Figure. 20A, D & G).but no significant apico-basal differences were observed regardless of the site at which restitution was conducted. Restitution curves in the LV endocardium (Figure. 20B, E & H) again showed a trend towards shorter ARI at the base than the apex, but this was only significant when restitution was conducted by pacing the LV base endocardially, where the local basal site ARI was 29ms shorter than the apex at the 50th quantile ($p<0.05$, Figure. 20E).

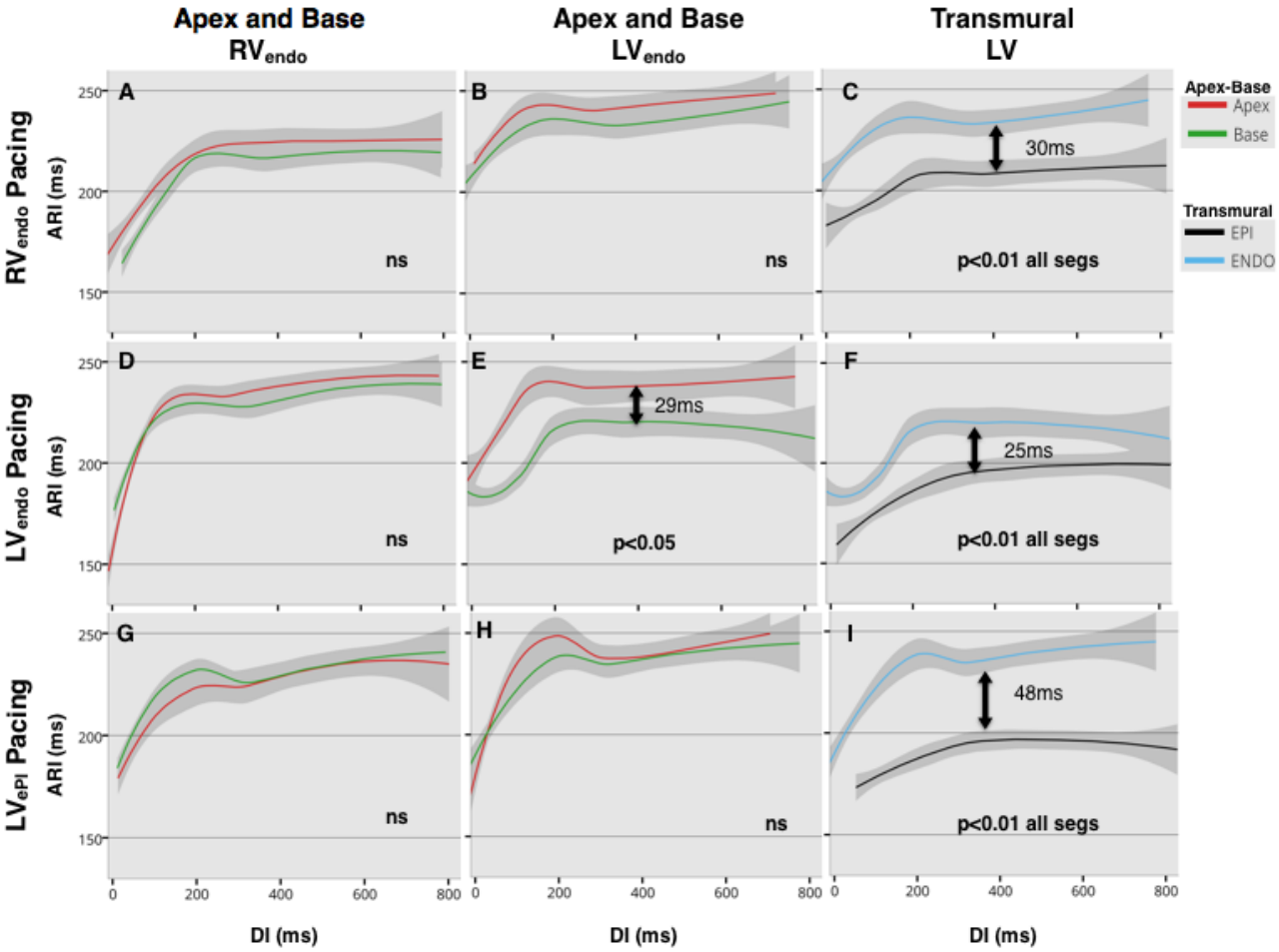

Figure 20. Lowes regression curves of Activation Recovery Index (ARI) restitution. Pacing site for each row is shown in the far left, with comparisons made from apex to base made in the right ventricle (RV), left ventricle (LV) and transmurally across the LV base, represented by each column (top). Significant differences were assumed if quantile regression was <0.05 across the whole of the restitution curve and statistical significance shown inset within the graphs. Arrows with time in miliseconds (ms) represent difference at the 50th quantile where curves were significantly different. ns=no significance. There is a consistent transmural difference in ARI regardless of pacing site(**C,F &I**), with an LV apicobasal difference in ARI on LV pacing only(**E**).

5.5.4. Dispersion of RT Restitution Curves

In the RV, RT restitution showed a small difference in quantile regression across the entire curve when pacing from the RV apex ($p < 0.01$); with a 19ms difference in RT at the apex compared to the base at the 50th quantile (Figure. 21A.). In the LV, significant apico-basal differences in RT were seen when pacing at the LV base both endocardially and epicardially (Figure. 21E&H), At the 50th quantile the basal RT was 56ms shorter than the apex in the LV on LV endocardial pacing (Figure. 21E) and 29ms shorter than the apex when pacing was conducted at the LV epicardial base. During endocardial pacing from the RV apex and LV base there was no significant transmural difference in RT (Figure. 21C&F). Performing restitution at the basal epicardium of the LV, however, produced a significant transmural difference of RT across the whole regression curve; $p < 0.01$; (Figure 21. I). At the 50th quantile the epicardial RT was 77ms shorter than the endocardium at the base of the LV.

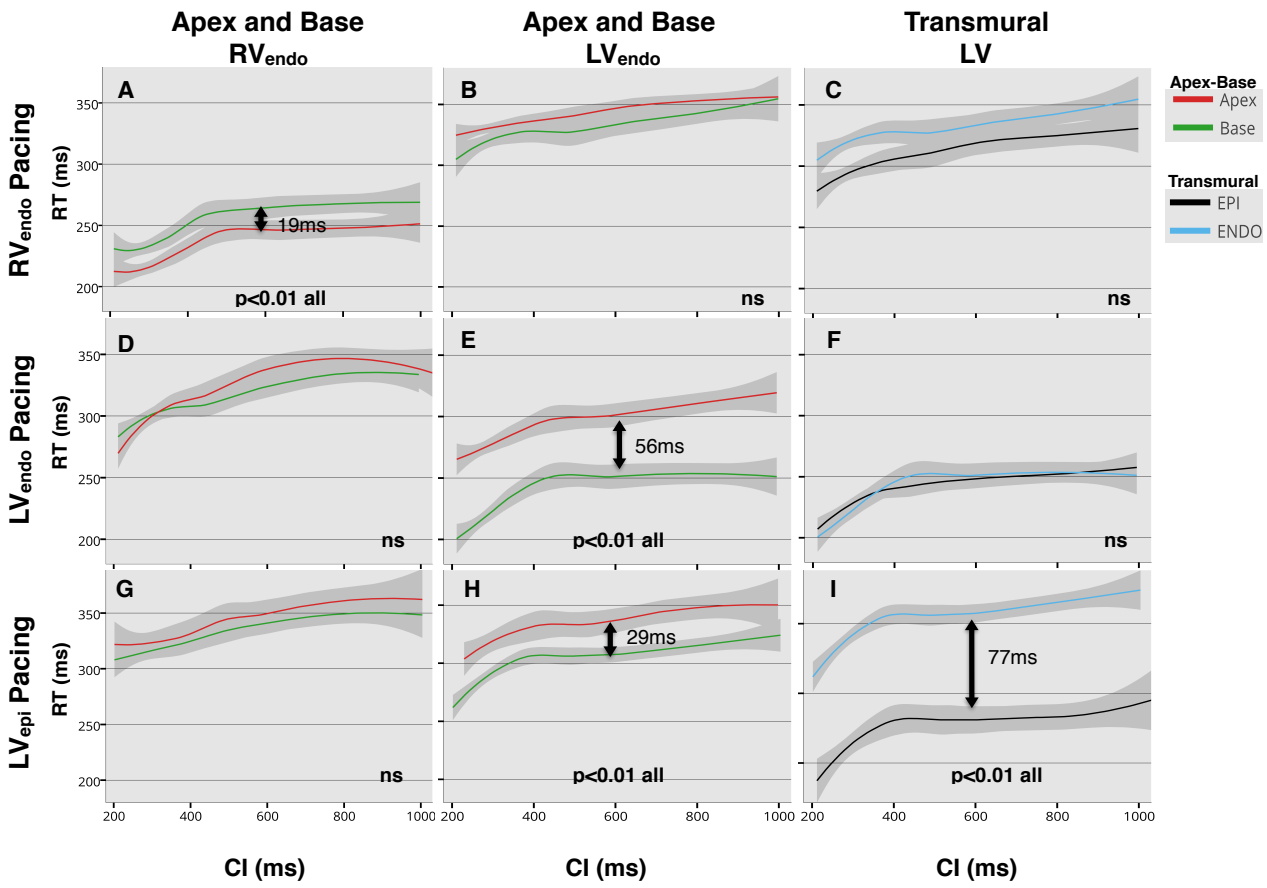

Figure 21. Lowes regression curves of Repolarization Time (RT) restitution. Pacing site for each row is shown in the far left, with comparisons made from apex to base made in the right ventricle (RV), left ventricle (LV) and transmurally across the LV base, represented by each column (top). Significant differences were assumed if quantile regression was <0.05 across the whole of the restitution curve and statistical significance shown inset within the graphs. Arrows with time in miliseconds (ms) represent difference at the 50th quantile where curves were significantly different. ns=no significance. There is an apicobasal difference in RT on RV and LV pacing (A&E), while CS pacing creates a significant transmural difference in RT (**I**), as well as an LV apicobasal difference in RT (**H**). CL=Cycle Length.

5.5.5. AT-ARI Coupling

Figure 22 demonstrates AT-ARI coupling during RV, LV endocardial and LV epicardial pacing. . During RV pacing at BCL 600ms, negative global and regional AT-ARI coupling was also demonstrated (Figure. 22A, $p<0.05$). However, pacing at BCL 600ms at the basal LV endocardium and LV epicardium, the global negative coupling and regional coupling in the RV and LV was lost (Figure. 22B&C), with only the epicardial poles maintaining negative coupling ($p<0.05$). Figure 22D demonstrates an example of negative regional AT-ARI coupling in the RV, LV and CS. Sites that activate early have a longer ARI than sites that activate later.

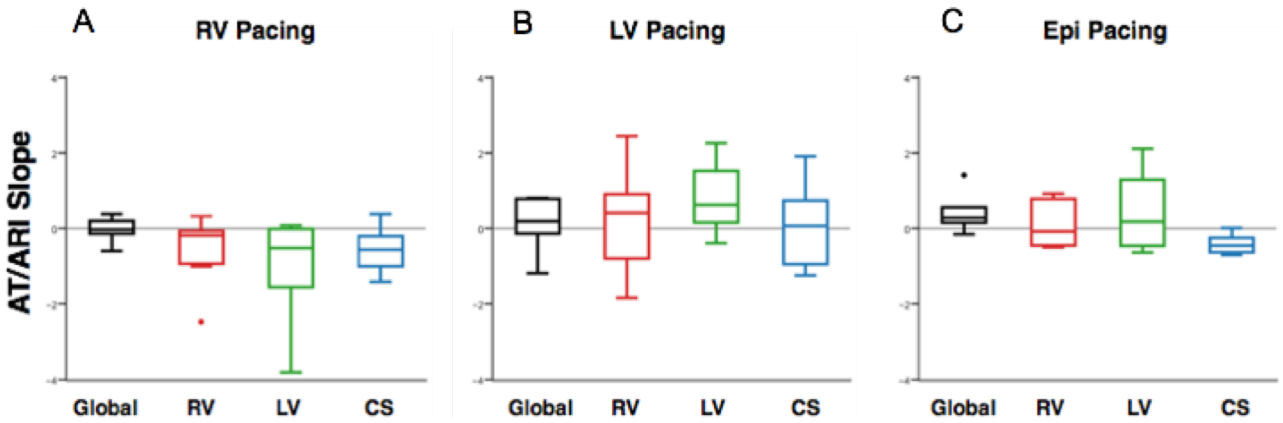

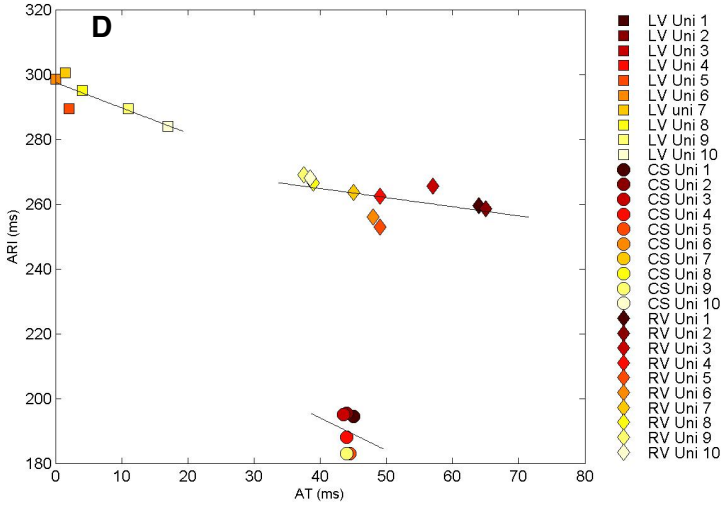

Figure 22. AT/ARI coupling. During right ventricular pacing (RV), the median global AT/ARI slope of all catheter poles recorded, as well as regional slopes of catheter poles in the right ventricle (RV), left ventricle (LV) and epicardium of the heart via the coronary sinus (CS) are all negative (**A**). During LV pacing this global as well as regional negative coupling between AT/ART is lost, as shown by a median slope >0 globally and regionally in the RV, LV and CS (**B**). During epicardial pacing (**C**), again negative global and regional RV and LV coupling is lost. (**D**) Example of negative regional AT-ARI coupling during a single beat in an individual patient in the right ventricle (RV), left ventricule (LV) and coronary sinus (CS).

5.6. Discussion

This is the first study to systematically examine the effects of stimulation site on RV, LV endocardial and epicardial conduction-repolarization dynamics in the intact human heart. The major finding of this study is that intrinsic heterogeneity of ARI/APD within the ventricle promotes a significant dispersion of repolarization depending on the stimulus site, which may play an important role in arrhythmogenicity. Secondly it shows that a significant proportion of restitution slopes measured in patients with structurally normal hearts and low risk of ventricular arrhythmia have an Smax >1. Finally though often studied and modelled in a monotonic exponential our data confirms that the human restitution curve is triphasic in nature as previously described (Franz et al. 1983; Franz et al. 1988), consisting of a steep early phase, followed by a 'hump' or 'dip' and lastly a plateau.

5.6.1. Intrinsic ARI Heterogeneity Synchronizes Ventricular Repolarization During Normal Activation But Fails To Adapt To Ectopic Stimulation Due To Escape From Negative AT/ARI Coupling

The presence of intrinsic APD heterogeneity within the ventricle has been shown in studies demonstrating electrical heterogeneity of channel expression (Antzelevitch 2000; Liu & Antzelevitch 1995; Di Diego et al. 1996; Antzelevitch & Dumaine 2011; Antzelevitch et al. 1991; Sicouri et al. 2010; Antzelevitch et al. 2009). A greater density of Iks channels are thought to be present at the base of the left ventricle compared to the apex resulting in shorter APD at the base (Akar 2002). In addition greater Ito channel density in the epicardium of the heart may cause a shorter APD in the epicardium than the endocardium (Li et al. 1998; Boukens et al. 2015). These apicobasal and transmural fs of APD have also been demonstrated in human studies(Cowan et al. 1988; Fish et al. 2005; Taggart 2001) and the findings are consistent with both in-vitro and in-vivo observations in showing a small apicobasal gradient in ARI in the RV and LV and a larger (30ms) LV transmural ARI gradient on RV apical pacing (Figure. 20A-C) is evident. The function of this heterogeneity in ARI may be to compensate for the normal apicobasal and endocardial to epicardial activation sequence within the ventricle in order to

homogenise total repolarization time(Figure. 21A-C.), as has as previously demonstrated in human and animal studies (Boukens et al. 2015; Cowan et al. 1988; Franz et al. 1987; Janse et al. 2005; Marrus et al. 2012; Ozgen & Rosen 2009; Patberg et al. 2005; M. B. Rosenbaum et al. 1982; M. B. Rosenbaum et al. 1983; Taggart 2001) . This homogenisation of total repolarization within localised regions of the heart, occurs over a range of coupling intervals and may be protective against localised re-entry during normal physiological working parameters of the ventricle, particularly sinus tachycardia.

By varying the stimulus site, however, the data shows that local ARI within the normal heart is governed not only by regional location but also the activation sequence, which determines the presence or absence of electronic modulation via negative AT-ARI coupling. When basal LV endocardium and epicardium are paced, there is escape from global negative AT-ARI coupling(Figure. 22). The resultant effect of this loss of coupling is a shorter local ARI at the early activating stimulus site; with 29ms apico-basal dispersion in ARI(Figure. 20E) during LVendo pacing and a 48ms transmural ARI dispersion during LVepi pacing(Figure. 20I). The failure of AT-ARI coupling to adapt to varying stimulus site by continuing to be negative, brings into question whether it is a true electronic phenomenon, or a function of differential channel expression due to the effect of cardiac memory based on the normal expectant activation sequence (Janse et al. 2005; Patberg et al. 2005; M. B. Rosenbaum et al. 1982; M. B. Rosenbaum et al. 1983) . It is well known for instance, that short and long-term pacing can modulate regional APD within the heart particularly in the epicardium and change APD dependant on the new expectant activation pattern (Rosen & Cohen 2006; M. B. Rosenbaum et al. 1982), potentially to prevent dangerous localised repolarization gradients from occurring. However ectopic beats that alter the normal activation sequence may have a greater effect on ARI and therefore RT dispersion, because initial adaptation does not occur.

5.6.2. Activation Sequence Influences Transmural And Apico-basal Dispersion Of Repolarization

Dispersion of ventricular repolarization is associated with a increased risk in the development of ventricular arrhythmia (Glukhov et al. 2010; Laurita et al. 1998; Olsson et al. 1995; Laurita et al. 1996) . It has previously been demonstrated that during sinus rhythm and RV apical pacing mean global repolarization dispersion ranges from 30-80ms (Kongstad et al. 2002; Yuan et al. 1995; Morgan et al. 1992) while localized regional endocardial dispersion between latest activating sites or between apicobasal regions, ranges from 5-30ms (Kongstad et al. 2002; Morgan et al. 1992). This protective minimization of spatial dispersion of repolarization is mediated by electronic forces within the ventricle, which create a negative coupling between AT and ARI (Yue 2005; Franz et al. 1987). Negative coupling between AT and ARI results in repolarization completing earliest at sites of latest activation, with the resultant repolarization wave moving in an opposite direction the depolarization wave, thus preventing localized reentry. The presence of protective negative coupling has only been demonstrated during sinus rhythm and RV apical pacing where global activation time is short (Yue 2005; Franz et al. 1987; Hanson et al. 2009; Subramanian et al. 2011) . The effect of disruption and prolongation of the activation sequence particularly via epicardial stimulation has not been well studied. Yue et al. (Yue 2005) suggested a trend towards less negative coupling during ventricular ectopy, though they did not account for the location of the ectopy and its effect on global activation and activation dispersion. Our study has shown that altering the stimulus site to the LVepi causes a significant (77ms) local transmural dispersion of repolarizarion (Figure. 21I), while stimulating the basal LV endocardium at the base causes a significant (56ms) local apicobasal repolarization dispersion (Figure. 21E) due to disruption of the normal transmural and intra-ventricular activation sequence. This dispersion of repolarization occurs as a result of loss of the regular negative coupling that occurs by stimulation at these sites (Figure 22) Thus the location of ectopic or pacing beats within the heart may play as important a factor in arrhythmogenicity as its timing, by creating regional windows of dispersed repolarization. This has important implications both with regard to determining whether ventricular ectopy is benign and in relation to where VT stimulation protocols are currently performed.

5.6.3. Findings In Relation To The Potential Arrhythmogenic Nature Of Epicardial Ectopy/ Pacing

Global ventricular dispersion in the range of 80-190ms (Yuan et al. 1995; Morgan et al. 1992) have been described in mapping studies of patients with sustained monomorphic ventricular tachycardia of a variety of aetiologies. Importantly premature stimulation may augment this dispersion, and increase susceptibility to inducibility of sustained VT during programmed electrophysiology studies(Yuan et al. 1995). Additionally localised dispersion of repolarization between adjacent regions of the ventricle with similar activation times may be in the range of 5-20ms in patients with structurally normal hearts and 20-85ms in patients with previous structurally abnormal hearts and sustained monomorphic VT (Morgan et al. 1992). In their seminal study Allessie et al.(Allessie et al. 1976) showed that dispersion of the refractory period of 11-16ms was sufficient to produce reentry around a 5mm line of conduction block. Our finding of a significant localised transmural dispersion of repolarization on epicardial stimulation (Figure. 21I), may therefore be within the arrhythmogenic range seen in patients with sustained VT, and explain why epicardial ectopy or pacing may be arrhythmogenic in certain groups of patients (Fish et al. 2005; Shukla et al. 2005; Tayeh et al. 2013; Nademanee et al. 2011; Kaltenbrunner et al. 1991; Pogwizd et al. 1998). It should be remembered, however, that dispersion of repolarization is just one factor in the in the development of such functional reentry, and critical timing of the impulse for the encroachment of the wavefront into relative refractory period is also a prerequisite. Thus our patients did not develop VT during epicardial pacing and the majority of CRT patients do not develop arrhythmia due to epicardial pacing. Our study would only be relevant to patients with relatively narrow QRS, non-specific-interventricular conduction block or RBBB where the LV has previously been exposed a normal activation sequence and would be expected to have a similar RT response to epicardial pacing, however, this group of patients have adverse outcomes to CRT (Moss et al. 2009; Tang et al. 2010) and our findings may explain why. Additionally one would expect either critically timed epicardial ectopics or the initial epicardial pacing phase to be pro-arrhythmic as has previously been described clinically (Shukla et al. 2005), because prolonged pacing would all invoke protective repolarization adaptations via cardiac memory (Rosenbaum et al. 1982; Rosenbaum et al. 1983).

5.6.4. Steepness And Shape Of The Restitution Slope In Relation To Arrhythmogenesis

Although restitution slopes with $S_{max}>1$ have been theoretically implicated in an increased risk of ventricular arrhythmia (Karma 1994; Nolasco & Dahlen 1968; Pastore et al. 1999; Qu et al. 1999); Smax >1 has been demonstrated in normal human ventricles (Franz et al. 1983; Franz et al. 1988; Nash et al. 2006; Taggart et al. 2003). Additionally in patients at high risk of ventricular arrhythmia $S_{max}>1$ has not been shown to be associated with long term prognostic outcome or risk of T-wave alternans (Dorenkamp et al. 2013; Narayan et al. 2007; Zabel et al. 2013) . This study is the first to document that ARI restitution curves with $S_{max}>1$ predominate in the normal intact human myocardium and shows the importance of preforming a restitution curve until ERP in order to measure restitution at short DI's that invoke AT restitution. This calls into question the theoretical basis of an $S_{max}>1$ being associated with arrhythmic risk. Due to the rapid adaptive shortening of APD (Franz et al. 1988) which results in reciprocal lengthening in DI for a given coupling interval (Franz 2003) steeper slopes may actually be protective in the normal ventricle during sinus tachycardia and closely coupled ventricular ectopy, as subsequent beats at a similar coupling interval could therefore "run-off" to a flatter portion portion of the restitution curve. This may explain this finding in our study of normal ventricles. Thus steep restitution curves with Smax >1 may not be a major contributor to vulnerability to VF. It may be that at shorter DI's heterogeneity in ventricular conduction velocity restitution and repolarization play a more important role in arrhythmogenicity.

Our restitution slopes were also triphasic in morphology as has previously been demonstrated(Franz et al. 1983; Franz et al. 1988). Given that there may be important cellular mechanisms governing this triphasic nature(Franz 2003), flatter restitution curves would be a more likely finding in diseased ventricles where impaired sodium channel kinetics would be expected to flatten the restitution curve as have been shown experimentally in the rabbit ventricle(Kurz et al. 1994). Additionally, the 'hump' or second phase of the ventricular restitution curve may be governed by the kinetics of the L-type calcium channel and the delayed rectifier potassium channels (Franz 2003), the expression of this is known to be heterogeneous throughout the heart (Akar 2002). Thus, the behaviour of this phase of

the restitution curve, close to the steep portion of the curve and the refractory period may play an important role in dispersion of repolarization and arrhythmogenesis.

It should be noted that some studies have suggested that the dynamic restitution protocol results in steeper restitution curves than the standard restitution protocol (Koller et al. 1998) and that VF restitution kinetics at short coupling intervals are similar to those of the dynamic restitution protocol but not the standard protocol, thus the dynamic protocol may be a better indicator of VF APD dynamics. Additionally the steepness of the restitution curve varies by species (Tolkacheva et al. 2006) and along with the behaviour of the dynamic restitution curve and therefore animal study data may not be applicable to human VF.

5.6.5. Scientific And Clinical Implications

The finding of a significant transmural localised gradient in repolarization on basal LV epicardial stimulation has implications for cardiac resynchronisation pacing (CRT). In a subset of patients epicardial pacing during CRT has been shown to be arrhythmogenic (Cori et al. 2005; Fish et al. 2005; Medina-Ravell 2003; Shukla et al. 2005; Tayeh et al. 2013). This may potentially be explained by the fact that LV epicardial pacing promotes a significant transmural repolarization gradient when the ventricle was previously exposed to a relatively normal LV activation sequence. This transmural repolarization gradient was not seen in LV endocardial pacing and provides further support for the development of LV endocardial pacing systems (Scheffer et al. 2014; Gamble et al. 2013).

This study also has important implications with regard to the nature of the restitution curve. Firstly given that a significant proportion of our restitution curves had a steepest slope gradient >1 this calls into question the true clinical relevance of theoretical concept that steeper slopes are associated with a risk of **alternans** and VF (Weiss et al. 1999). Additionally we show that in humans, the restitution curve is triphasic in nature, and thus the majority of modelling studies are too simplistic to truly relate

restitution properties to arrhythmia generation (O'Hara et al. 2011). The finding of negative AT-ARI coupling only in sinus rhythm and RV apical pacing, suggests that ectopics that disrupt the normal coupling may have greater arrhythmic propensity by causing a greater global dispersion of repolarization (Figure 22. C.). It calls into question whether negative AT-ARI coupling is a true phenomenon or merely a function of a normal activation sequence and ARI memory in structurally normal hearts, especially given that negative coupling is not seen in pathology, such as hypertrophy secondary to aortic stenosis (Cowan et al. 1988).

5.7. Limitations And Conclusion

Data were confined to multi-electrode unipolar contact catheter recordings in the RV endocardium, LV endocardium and LV epicardium in patients admitted for EPS as opposed to global mapping. However, it should be noted that significant assumptions, limitations and inaccuracies may occur with both contact and non-contact global mapping methods (Earley et al. 2006; Benharash et al. 2015). Additionally due to the anatomy of the CS we were unable to measure the apical LV epicardium and therefore our finding of a transmural gradient in ARI may be related to sampling in this region where Ito may be more prominent(Li et al. 1998; Volders et al. 1999). Although great care was taken to ensure fluoroscopic transmural apposition of the catheters, it should be noted that true fiber orientated transmural measurements, akin to wedge preparations (Yan & Antzelevitch 1998) or plunge electrode recordings (Taggart 2001) were not possible However, we did consistently record shorter ARI's epicardially in our patients and the finding of no significant difference in RT transmurally during endocardial activation sequences would support the accuracy of our catheter positioning (Boukens et al. 2015). Finally the stimulus protocol where S1 and S2 occur at the same site, do not account for the fact that ectopy may occur from different sites hence altering the ventricular activation sequence.

In conclusion, the work so far shows that steep ARI restitution slopes predominate in the normal ventricle & dynamic ARI, RT gradients exist in the normal ventricle which are modulated by the site of activation. Epicardial stimulation of ventricular activation may promote significant transmural gradients in repolarization which may be pro-arrhythmic.

Chapter 6

Results: Relationship Between The Surface ECG T-Wave And Intracardiac Repolarization

6.1. Introduction

The relationship between the intracardiac repolarization of the heart and the surface electrogram Twave ($SECG_{TW}$), is poorly understood and subject to much debate. Several markers of repolarization including QT interval (Chugh et al. 2009; Kinoshita et al. 2012; Zhang et al. 2011), JT interval (Crow et al. 2003) and Tpeak-Tend(TpTe) (Panikkath et al. 2011; Letsas et al. 2010; M. Shimizu et al. 2002), have been associated with an increased risk of cardiac events. However, these markers have limitations in their predictive accuracy in large scale cohorts, perhaps because their specificity to local intracardiac repolarization time is poor. Although T-waves recorded directly on the intracardiac surface can accurately determine local repolarization time (Coronel et al. 2006; Haws & Lux 1990), the $SECG_{TW}$ is thought to represent a far-field recording, displaying a summary of repolarization of the entire heart (Noble & Cohen 1978). Hence there is uncertainty as to what these $SECG_{TW}$ markers represent within the heart, particularly with regard to TpTe (Patel et al. 2009; Opthof et al. 2009; Janse et al. 2012; Opthof et al. 2007) .

The normal $SECG_{TW}$ is upright in almost all SECG leads, and concordant to the QRS complex. Yet at a cellular level depolarization and repolarization reflect current flow in opposite directions. It has therefore been hypothesized that in order for the $SECG_{TW}$ to be concordant, the wave of repolarization must travel in the opposite direction to the wave of depolarization (Brink & Goodwin 1952; Franz et al. 1987). Previous studies have focused on single dominant repolarization gradients to explain the morphology of the T-wave. Opposing depolarization and repolarization apico-basal wavefronts within the heart have been shown in several studies(Burgess et al. 1972; Cohen et al. 1976; Watanabe et al. 1985; Autenrieth et al. 1975; Franz et al. 1987) and are thought to form the morphology of the SECG T-wave. Others studies have demonstrated a predominantly transmural gradient, of earlier epicardial repolarization to endocardial repolarization opposing the normal depolarization sequence (Spach & Barr 1975; Antzelevitch et al. 1998; Yan & Antzelevitch 1998; Franz et al. 1987) , and have suggested that T-peak and T-end of the surface ECG represents this transmural dispersion of repolarization (Yan & Antzelevitch 1998). However, the repolarization sequence of the intact human ventricle is complex,

and is also related to the sequence of activation (Durrer et al. 1970; Srinivasan et al. 2016) and this may be reflected by changes in the $SECG_{TW}$.

6.2. Aim

This study aimed to examine the association between intracardiac ventricular repolarization in the intact human heart and the $SECG_{TW}$ morphology, in order to better understand the genesis of the $SECG_{TW}$ and examine the extent to which it represents local intracardiac repolarization.

6.3. Hypothesis Adressed

Localized disruption of transmural and apico-basal gradients of APD affects the morphology of the surface ECG T-wave manifest as changes in Tpeak-Tend.

6.4. Methods

Refer to section 4.4

6.5. Results: Relationship Between The Surface ECG T-Wave And Intracardiac Repolarization

6.5.1. Polarity Of The Surface ECG T-wave In Relation to the Intracardiac Electrogram

Figure 23 shows the relationship between the $SECG_{TW}$ amplitude of the precordial and limb leads (Figure 23. A,C&E), to the intracardiac unipolar electrogram T-wave (EGM_{TW}) amplitude/polarity and repolarization time regionally within the heart (Figure 23. B,D&F), during restitution pacing at the RV apex (Figure 23. A&B), LV basal endocardium (Figure 23. C&D) and LV basal epicardium (E&F). Dots represent the mean amplitude or repolarization time throughout restitution studies, along with 95% confidence intervals.

RV Pacing

During RV pacing (Figure 23. A&B) it can be seen that there is trend towards more a positive $SECG_{TW}$ in leads V1-V4, while V5-6 have a more negative amplitude(Figure 23. A). This matches the distribution within the myocardium (Figure 23. B), where early repolarizing sites; RV base and apex; have a positive EGM_{TW}, while late repolarizing sites; LV basal epicardium, basal endocardium and apex; have electrograms that become progressively negative as repolarization time increases.

Effect of LV Pacing

During LV pacing at the basal endocardium (Figure 23. C&D) and basal epicardium (Figure 23.E&F), however, the opposite pattern in the precordial lead $SECG_{TW}$ polarity is observed (Figure 23. C&E, respectively), with a negative amplitude in the RV leads (V1-2) and a positive amplitude in the LV leads (V5-6). This again corresponds to the pattern of regional intracardiac repolarization(Figure 23. D&F), with early repolarizing sites in the left ventricular base having more positive T waves, and late repolarizing sites in the right ventricle having more negative T-waves.

Limb Leads

The limb leads on the $SECG_{TW}$ (Figure 23. A, C&E), however, showed no consistent pattern in $SECG_{TW}$ polarity, despite the change in repolarization dispersion, in the apicobasal, transmural LV and RV to LV orientation(Figure 23. B,D&F). Leads, II, III and AvF were always positive in all three pacing scenarios, despite a large RV to LV dispersion during RV pacing (Figure 23. B), a large LV apicobasal dispersion during LV basal endocardial pacing (Figure 23. D), and a large LV transmural and apicobasal repolarization dispersion during LV basal epicardial pacing (Figure 23. F). Lead I was of neutral or low positive amplitude throughout, while aVR was negative during LV pacing and RV pacing (Figure 23. C&E), while aVL was negative during RV pacing, and neutral or low positive amplitude during LV pacing.

Table 6. shows the intraclass correlation (ICC) between regional EGM_{TW} and $SECG_{TW}$ amplitude/ polarity, including all pacing sites, through the whole of the restitution protocol in all patients. Strong agreement is demonstrated between V1 and V2 and the amplitude of EGM_{TW} at the RV base (ICC 0.78 % 0.61 respectively; p-value <0.001). Moderate agreement was demonstrated between V4 and V5, and the RV base (ICC 0.54 & 0.6 respectively; $p<0.001$), as well as V1 to V4 and the RV apex (ICC 0.59, 0.48, 0.43 & 0.41 respectively; $p<0.001$). Fair agreement was demonstrated between V6, Lead I and Lead aVL and the LV base endocardially (ICC 0.3, 0.26 & 0.26 respectively; $p<0.001$), as well as V6, Lead I and aVL and the LV base epicardially (ICC 0.28, 0.4 & 0.4 respectively; $P<0.001$). Weak agreement was noted between V5 and the LV base (ICC 0.12, $p=0.022$); V4 and the LV apex (ICC 0.12, $p=0.002$); and Lead II, Lead III and aVR (ICC 0.11, 0.15 & 0.134 respectively; $p<0.001$).

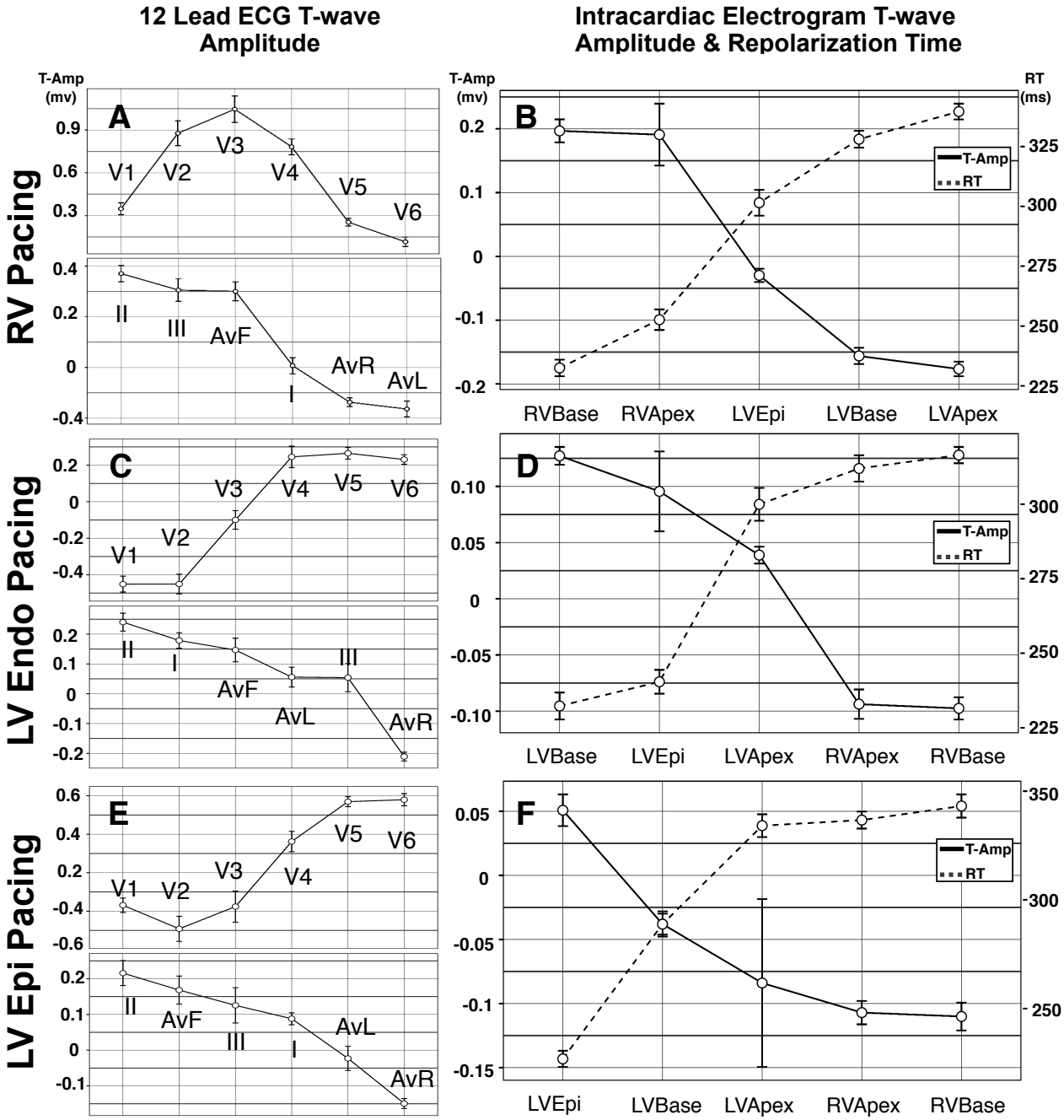

Figure 23. T-wave amplitude in the precordial and limb leads (**A,C** & **E**), compared with unipolar T-wave amplitude regionally within the heart, in relation to local repolarization time (**B,D** & **F**). Rows depict mean and 95% confidence interval data for restitution pacing during right ventricular apical pacing (**A** & **B**), left ventricular basal endocardial pacing (**C** & **D**) and left ventricular basal epicardium (**E** & **F**). LV=Left Ventricle. RV = Right ventricle. Epi = Epicardium. Amp = Amplitude

Table 6. Relationship Between The Amplitude of the T-wave on the SECG to the Regional Intracardiac T-wave Amplitude.

		LV Base Tamp	LV Epi Tamp	LV Apex Tamp	RV Apex Tamp	RV Base Tamp
V1	**ICC**	-0.87	-0.80	-0.06	**0.59**	**0.78**
	P-value	ns	ns	0.92	**<0.001**	**<0.001**
V2	**ICC**	-0.54	-0.36	-0.11	**0.48**	**0.61**
	P-value	ns	ns	0.99	**<0.001**	**<0.001**
V3	**ICC**	-0.44	-0.29	-0.04	**0.43**	**0.54**
	P-value	ns	ns	0.83	**<0.001**	**<0.001**
V4	**ICC**	-0.37	-0.37	**0.12**	**0.41**	**0.6**
	P-value	ns	ns	**0.002**	**<0.001**	**<0.001**
V5	**ICC**	**0.12**	-0.25	0.043	0.058	0.03
	P-value	**0.022**	ns	0.15	0.07	0.28
V6	**ICC**	**0.30**	**0.28**	0.04	-0.38	-0.59
	P-value	**<0.001**	**<0.001**	0.17	ns	ns
I	**ICC**	**0.26**	**0.40**	0.068	-0.51	-0.25
	P-value	**<0.001**	**<0.001**	0.06	ns	ns
II	**ICC**	-0.23	-0.55	-0.05	**0.11**	0.21
	P-value	ns	ns	0.84	**0.003**	<0.001
III	**ICC**	-0.19	-0.40	-0.03	**0.15**	0.08
	P-value	ns	ns	0.77	**<0.001**	0.07
aVF	**ICC**	-0.18	-0.35	-0.02	0.10	-0.004
	P-value	ns	ns	0.72	0.005	0.53
aVR	**ICC**	-0.16	-0.25	-0.003	**0.134**	0.26
	P-value	ns	ns	0.53	**<0.001**	<0.001
aVL	**ICC**	**0.26**	**0.4**	0.028	-0.28	-0.17
	P-value	**<0.001**	**<0.001**	0.26	ns	ns

6.5.2. Relationship of Intracardiac Repolarization To Markers On The SECG

Analysing all three pacing sites, the earliest measured start of the SECGTW always occurred before repolarization time measured simultaneously at any individual intracardiac catheter pole (-177.2 +/-54 ms, $p<0.001$), and before the minimum measured RT at each individual cycle length (-85 +/-45ms, $p<0.001$). The latest measured T-end in the SECGTW always occurred after, the latest measured RT in any individual intracardiac catheter pole (110 +/- 57ms, $p<0.001$), and after the maximal measured RT (43 +/- 25ms, $p<0.001$). Table 7 shows the percentage of all recorded sites RV and LV that repolarized before T-peak on the SECG leads, during restitution pacing in the RV apex, LV endocardial base and LV epicardial base. The proportion of sites that repolarized before T-peak on the SECG showed significant heterogeneity between the LV and RV, based on the location of pacing site. During RV pacing a greater proportion of RV sites repolarized before T-peak, while LV sites repolarized after T-peak. During LV pacing both endocardially and epicardially a greater proportion of LV sites repolarized before Tpeak.

Table 7. Percentage of all recorded sites RV and LV that repolarized before T-peak on the SECG

Pacing Site	Repolarized sites	V1	V2	V3	V4	V5	V6	I	II	III	aVL	aVR	aVF
RV apex	RV (%)	93	97	92	91	95	94	85	92	93	92	94	93
	LV (%)	13	1	10	15	28	44	24	20	15	11	31	16
LV endo	RV (%)	13	18	27	21	19	13	14	28	13	7	16	18
	LV (%)	70	71	72	76	76	70	76	72	68	92	71	67
LV epi	RV (%)	18	16	12	33	19	19	20	21	20	11	18	16
	LV (%)	54	55	53	59	56	56	55	58	57	46	54	58

6.5.3. Relationship Between Regional Intracardiac Repolarization to $SECG_{TW}$ Upslope

Figure 24. demonstrates the relationship between the regional unipolar electrograms recorded in the RV and LV, to the simultaneously recorded SECGTW in Leads V1 and V6, in a single S2 interval in one patient during pacing from the RV, LV endocardium and LV epicardium. Panels A-C demonstrate the consistency between regional EGMTW polarity and the polarity of the SECGTW. During RV pacing (Figure 24. A), repolarization occurred earlier in the RV, resulting in an upright EGMTW, with repolarization markers (inset panel) all falling within the upslope of the positive T-wave in V1. LV repolarization occurred later resulting in an inverted EGMTW and SECGTW in V6. Although there was evidence of a small transmural gradient with earlier repolarization of the epicardium and that the endocardium, all recorded repolarization times occurred within the duration of the the upslope of the inverted V6 electrogram.

During LV endocardial pacing (Figure 24. B), RV repolarization occurred later, resulting in an inverted EGMTW and SECGTW in V1, with again all repolarization times occurring within the duration of the upslope of the inverted V1 SECG electrogram. In the LV there was a significant apicobasal repolarization gradient (inset), with the basal endocardial, epicardial and mid endocardial EGMTW being upright in polarity, consistent with the V6 electrogram, while the apical EGMTW was inverted or bifid. Thus the basal endocardial and epicardial, as well as mid endocardial repolarization times occurred along the upslope of the V6 electrogram, while LV apical repolarization occurred at the peak and into the downslope of the V6 T-wave.

Finally LV epicardial pacing (Figure 24. C) resulted in a similar RV endocardial and V1 SECGTW morphology to LV basal endocardial pacing, with repolarization times occurring along the upslope of the V1 electrogram. In the LV there was a transmural difference in repolarization, this time with earlier repolarization of the epicardium to the endocardium, however, repolarization times of the basal epicardium and endocardium, as well as the mid endocardium all occurred along the upslope of upright V6 SECGTW, which reflected the upright polarity of the EGMTW in these regions, while the apical repolarization times occurred along the downslope of V6, as a result of later apical repolarization.

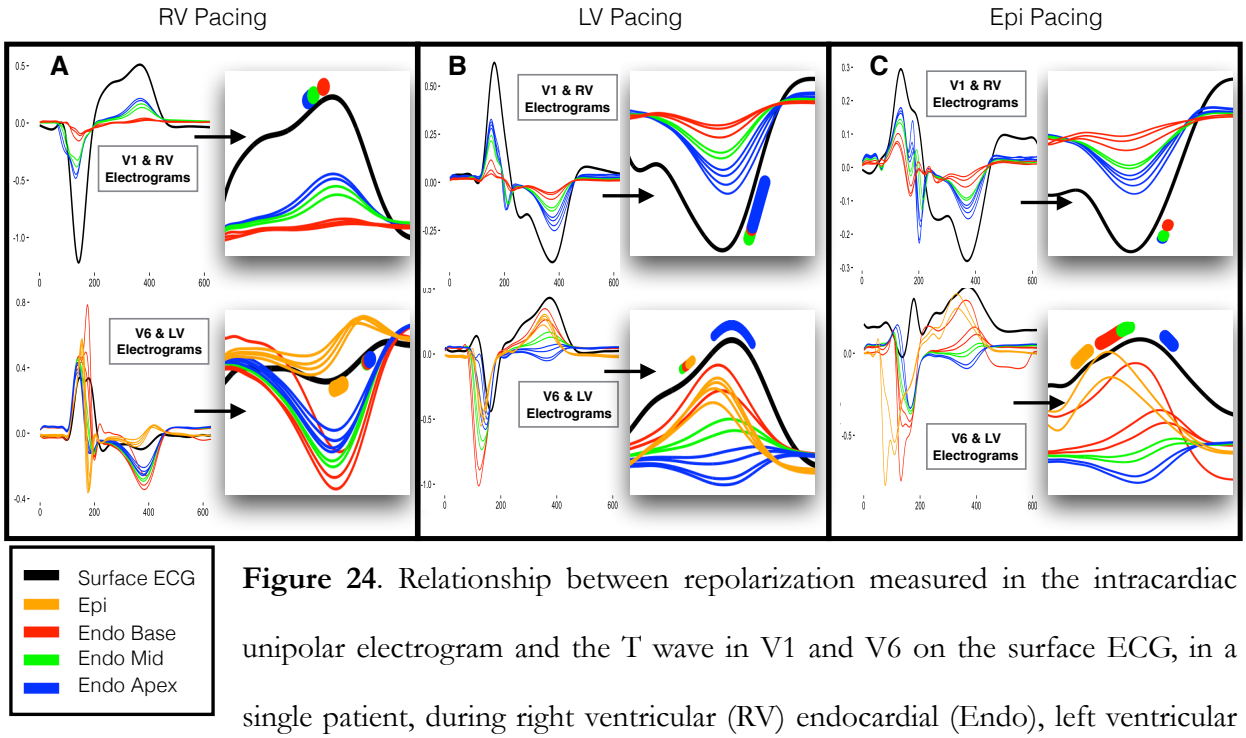

Figure 24. Relationship between repolarization measured in the intracardiac unipolar electrogram and the T wave in V1 and V6 on the surface ECG, in a single patient, during right ventricular (RV) endocardial (Endo), left ventricular (LV) endocardial and left ventricular epicardial (Epi) pacing. Each panel **A,B** and **C** represents the simultaneously recorded unipolar electrograms from the RV and LV during a single pacing beat with the colours representing the electrograms in the base (red), mid (green), apex (blue) and epicardium (orange), along with the body surface ECG (black). Inset within each panel, is focused view of the T-wave, with range of measured regional repolarization moments overlaid on the body surface ECG T-wave.

The relationship between the upslope of the SECGTW regardless of polarity, pacing site or cycle length for all patients; and the regional repolarization times within the ventricle are demonstrated in Table 8. RV endocardial repolarization times, including all measured regions from apex to base, occurred on the upslope of the V1-V3 SECG electrogram with a sensitivity of 0.89, 0.91 and 0.84, and a specificity of 0.67, 0.68 and 0.65 respectively. As the precordial SECG markers moved further away from the RV anatomically (V4-V6), sensitivity and specificity decreased, while the limb leads showed a general poor sensitivity and specificity for repolarization moments in the RV. LV basal endocardial, epicardial and mid endocardial regions displayed the opposite phenomenon, with a sensitivity of 0.79

and 0.8, and specificity of 0.66 and 0.67 in V6 and Lead I respectively, but with decreasing sensitivity and specificity from leads V5-V1, and a poor sensitivity and specificity in the rest of the limb leads. Finally LV apical repolarization times showed a poor sensitivity and specificity to the upslope of the SECG, with only aVR showing a sensitivity of 0.76, but with a poor specificity of 0.52.

Table 8. Sensitivity and Specificity Of The Upslope Of The SECG To Regional Repolarization Within The Heart

Surface ECG Lead Upslope	RV Apex to Base (endo)		LV-Base to Mid (endo & epi)		LV-Apex (endo)	
	Sensitivity	Specificity	Sensitivity	Specificity	Sensitivity	Specificity
V1	**0.89 (0.88-0.90)**	0.67 (0.66-0.68)	0.20 (0.19-0.21)	0.22 (0.21-0.23)	0.52 (0.50-0.54)	0.29 (0.28-0.30)
V2	**0.91 (0.91-0.92)**	0.68 (0.66-0.69)	0.22 (0.20-0.23)	0.21 (0.20-0.22)	0.48 (0.46-0.50)	0.35 (0.34-0.36)
V3	**0.84 (0.83-0.85)**	0.65 (0.64-0.67)	0.28 (0.26-0.29)	0.28 (0.27-0.29)	0.44 (0.43-0.47)	0.37 (0.36-0.38)
V4	0.59 (0.57-0.60)	0.52 (0.51-0.53)	0.56 (0.54-0.57)	0.48 (0.46-0.49)	0.37 (0.35-0.39)	0.42 (0.41-0.43)
V5	0.38 (0.37-0.40)	0.46 (0.45-0.47)	0.73 (0.71-0.74)	0.65 (0.64-0.66)	0.27 (0.25-0.29)	0.49 (0.48-0.50)
V6	0.36 (0.34-0.37)	0.42 (0.41-0.43)	**0.79 (0.77-0.80)**	0.66 (0.65-0.67)	0.29 (0.27-0.31)	0.49 (0.48-0.50)
I	0.29 (0.27-0.30)	0.34 (0.33-0.36)	**0.80 (0.78-0.81)**	0.67 (0.66-0.68)	0.45 (0.43-0.47)	0.53 (0.51-0.54)
II	0.47 (0.46-0.48)	0.50 (0.49-0.52)	0.67 (0.65-0.68)	0.59 (0.58-0.61)	0.25 (0.23-0.27)	0.49 (0.48-0.50)
III	0.58 (0.57-0.59)	0.61 (0.60-0.62)	0.45 (0.43-0.47)	0.50 (0.49-0.51)	0.31 (0.29-0.33)	0.47 (0.46-0.48)
aVF	0.53 (0.52-0.55)	0.54 (0.53-0.56)	0.54 (0.53-0.56)	0.53 (0.52-0.54)	0.33 (0.31-0.35)	0.46 (0.45-0.47)
aVL	0.37 (0.36-0.38)	0.35 (0.34-0.36)	0.62 (0.60-0.63)	0.53 (0.52-0.55)	0.70 (0.68-0.72)	0.54 (0.53-0.55)
aVR	0.61 (0.60-0.62)	0.53 (0.52-0.55)	0.26 (0.25-0.28)	0.35 (0.34-0.36)	**0.76 (0.74-0.77)**	0.52 (0.51-0.53)

Numbers highlighted in bold indicate a sensitivity >75%

6.5.4. Relationship Of The $SECG_{TW}$ To Dispersion of Repolarization In The Major Anatomical Axes

TpTe, has previously been reported as a marker of dispersion of repolarization, transmurally in the wedge preparation (Yan & Antzelevitch 1998) or globally within the whole heart in animal studies (Opthof et al. 2007). I studied the relationship between the TpTe, the time difference between the end of the SECGTW upslope across all leads, and the difference between the start and end of the SECGTW in all leads to dispersion of repolarization in the major anatomical axes.

A strong correlation was seen between right to left dispersion of repolarization and the difference between the end of the SECGTW upslope in lead V1-V6 (ICC 0.81, R 0.45 $p<0.001$), lead V2-V6 (ICC 0.83, R 0.5 $p<0.001$), lead V3-V6 (ICC 0.85, R 0.55 $p<0.001$), V1-aVL (ICC 0.82, R 0.5 $p<0.001$), V2-aVL (ICC 0.81, R 0.42 $p<0.001$) and V3-aVL (ICC 0.83, R 0.55 $p<0.001$)(Figure 25.A), regardless of T-wave polarity, pacing site or cycle length. No strong correlations existed between the difference in the end of the SECGTW upslopes in any other lead and right to left dispersion (best ICC <0.5 for all other variables). No strong correlations existed between the difference between the end SECGTW upslopes and apicobasal (best ICC <0.5 for all measures) or transmural dispersion of repolarization (best ICC <0.5 for all measures).

I was not able to demonstrate any strong correlation between TpTe measured in leads V4, V5, V6 or lead II on the SECG and dispersion of repolarization in the transmural (best ICC <0.2 for all measures), apicobasal (best ICC <0.12 for all measures), or right to left orientations(best ICC <0.22 for all measures) (Figure 25. B). Additionally, differences between the start and the end of the T-wave, and the start and the end of the T-wave upslope did not demonstrate any strong correlation with dispersion of repolarization (Fig.ure 25. C) in the right to left axis (best ICC <0.47 for all measures), apicobasal axis (best ICC <0.48 for all measures) and transmural dispersion of repolarization (best ICC <0.23 for all measures).

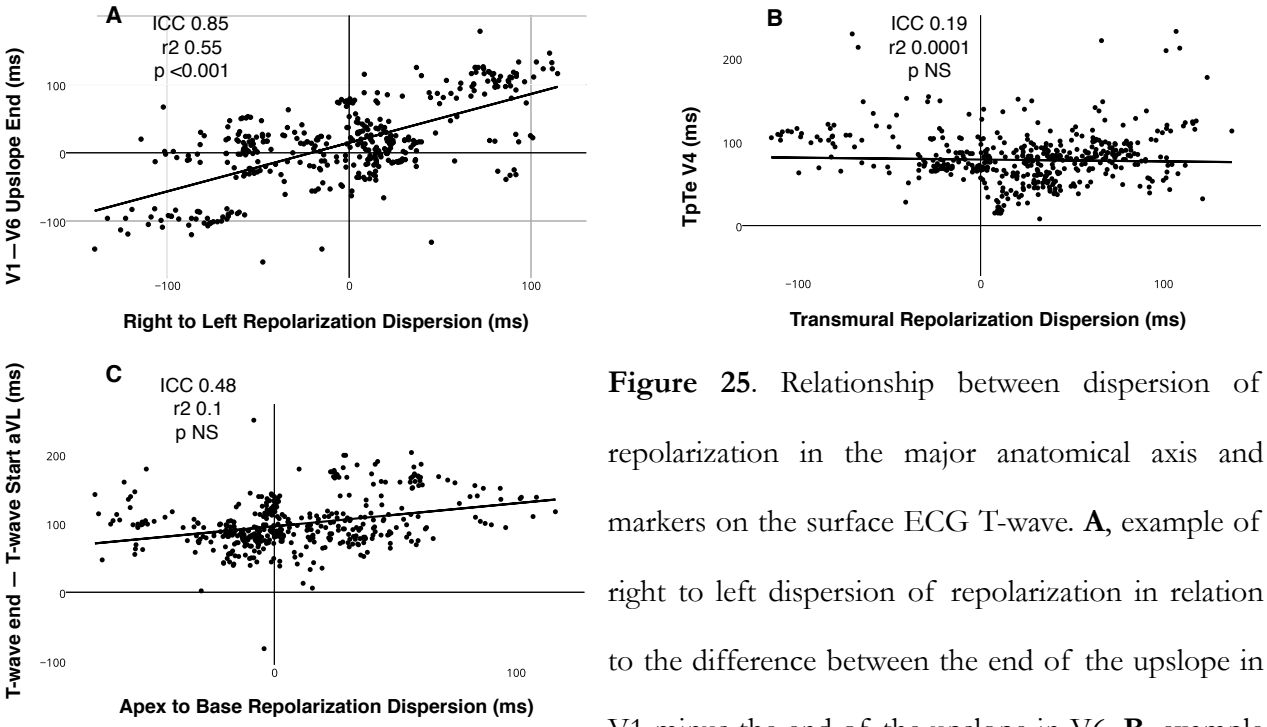

Figure 25. Relationship between dispersion of repolarization in the major anatomical axis and markers on the surface ECG T-wave. **A**, example of right to left dispersion of repolarization in relation to the difference between the end of the upslope in V1 minus the end of the upslope in V6. **B**, example of the best correlation of TpTe and transmural dispersion of repolarization; seen in V4. **C**, example of the best correlation between apicobasal dispersion of repolarization and surface ECG markers; seen by measuring the difference between the end and the start of the T-wave in lead aVL.

6.6. Discussion

This is the first study to provide correlation between local repolarization in the major anatomical axis and SECGTW, in the intact human heart. I have shown that although often thought of as a representation of global repolarization with the heart, the SECGTW actually reflects a balance between local and global repolarization components. The main findings are that (1) the amplitude/polarity of the T-wave on the precordial leads reflects the polarity of the underlying nearby myocardium in the precordial leads; (2) local repolarization times in the RV and LV occur along the upslope of the SECGTW in leads V1-V3 and V5,V6 & Lead-I respectively; (3) the difference between the end of the upslope in V1 and V6 provides a good representation of right to left dispersion of repolarization; (4) no strong markers for apico-basal or transmural repolarization differences were seen on the SECG; and (5) TpTe did not correlate with dispersion of repolarization in the right to left, apico-basal or transmural axis.

6.6.1. Polarity Of The Precordial Lead $SECG_{TW}$ Mirrors The EGM_{TW} Of The Underlying Myocardium

Extensive experimental and modelling evidence suggests that the polarity and upslope of the contact EGMTW, is related the local repolarization component of the underlying myocardium (Coronel et al. 2006; Haws & Lux 1990; Potse et al. 2009). The EGMTW is more positive when the repolarization of local tissue is early, biphasic in intermediate repolarization times and negative in late depolarising sites where the rest of the heart has repolarized (Potse et al. 2009). The far-field or whole heart component is represented by the downslope of the T-wave. Thus the contact EGMTW is essentially a rescaled and inverted action potential, with local activation moments representing the steepest QRS downslope and local repolarization moments representing the steepest T-wave upslope. Our data using the well validated Wyatt method (Wyatt et al. 1981; Chinushi et al. 2001; Coronel et al. 2006; Haws & Lux 1990; Millar et al. 1985) confirms this (Figure 23. B,D,F) in that early repolarizing sites have an upright T-wave, while late repolarizing sites had a negative T-wave. The precordial lead SECGTW, mirrored the

polarity of the T-wave in underlying myocardium, with V5-V6 matching the polarity of sites measured in the LV, while V1-V3 matched the polarity of sites measured in the RV (Figure 23. A,C,E). The T-wave in the limb leads, displayed no pattern in relation to local repolarization, despite changes in both the right to left, apicobasal and transmural intracardiac repolarization axis. This is reflected in Table 6, where moderate to substantial agreement (ICC 0.43-0.78) was seen between the intracardiac T-wave amplitude in throughout the RV and leads V1-V3 on the SECG, while fair agreement was demonstrated between the T-wave amplitude in the LV base and V5-6, I and aVL on the SECG. The weaker agreement between the LV markers and V5-6, I and aVL, may be a reflection of amplitude attenuation across the lateral wall of the chest, as these leads lie further away from the heart than the RV SECG. The poor amplitude correlation of the limb leads to the intracardiac unipolar electrograms, is likely a reflection of their substantial distance from the myocardium and they are therefore likely to represent a far field electrogram of the entire heart repolarization, with little in the way of local component. Additionally, the lack of correlation between SECGTW polarity and the apex of the LV, may highlight that the planar precordial ECG fails to extend inferiorly enough to cover the local repolarization component of the LV apex and that repolarization times in the LV apex may have been similar to the RV apex, causing some degree of overlap.

6.6.2. Right And Left Heart Intracardiac Repolarization Times Lie Along The Upslope Of The Precordial $SECG_{TW}$ Regardless of Polarity

As demonstrated in Figure 24, RV repolarization consistently occurred along the upslope of V1 electrogram, despite alterations in the right to left and apicobasal repolarization axis, while LV basal and mid repolarization, consistently occurred along the upslope of the V6 electrogram, regardless of the pacing induced variations in right to left or apicobasal repolarization gradients. These findings were independent of Twave polarity. It has previously been suggested that variations in the transmural gradient across the ventricular wall (Yan & Antzelevitch 1998; Antzelevitch 2001; Shipsey et al. 1997) may inscribe the morphology of the $SECG_{TW}$. Although we have previously demonstrated transmural heterogeneity of APD within the intact human ventricle (Srinivasan et al. 2016) confirming previous

experimental studies (Antzelevitch et al. 1991) our data does not support the idea that this is reflected in the $SECG_{TW}$. Regardless of the transmural gradient (Figure 24. B&C), the repolarization of the base of the LV occurred along the upslope of the V6 and this did not alter its polarity. This is perhaps due to the differences between experimental studies (Yan & Antzelevitch 1998) and our intact whole human heart studies, where the influence of the far-field or global myocardial muscle mass has a greater effect on the $SECG_{TW}$, with local components being represented by an upslope, and far field components being represented by a downslope on the precordial $SECG_{TW}$. The LV apex, displayed a poor correlation to the upslope of the precordial ECG. Where significant apico-basal LV repolarization dispersion was induced (Figure 24. B&C), repolarization occurred after the upslope of the V6 electrogram. This is reflected in Table 3 where the upslope of V1-3 showed good sensitivity to all measured RV repolarization, while the upslope of V5-V6 and I showed good sensitivity to transmural LV basal and LV mid myocardial repolarization. LV apical repolarization showed good sensitivity to the upslope of aVR, but poor specificity, reflecting the overlap of this region to repolarization times at the RV apex (Figure 24. B&C), as well as the possible lack of a specific near-field $SECG_{TW}$ electrogram that represents this region.

6.6.3. The $SECG_{TW}$and Dispersion Of Repolarization In The Major Anatomical Axis

In view of the regional relationship between the SECG and intracardiac repolarization moments, we sought to assess the relationship between the SECG and dispersion of repolarization within the heart. Our data shows that differences between the end of the upslope in V1-3 vs V6/aVL provides an excellent correlation to right to left dispersion of repolarization (Figure 25. A) regardless of the polarity of the T-wave. Poor correlations existed between TpTe and dispersion of repolarization in the transmural, apicobasal and right to left axis. Indeed the best correlation between TpTe and transmural dispersion of repolarization occurred in V4 (Figure 25. B). This is in contrast to previous studies(Antzelevitch 2001) and may again reflect differences between local and far field electrogram components in experimental studies compared to whole heart studies. This highlights the limitation of TpTe in a single SECGTW as a measure of dispersion of repolarization (Xia et al. 2005). Our data

suggests that the upslope in the precordial lead SECGTW represents local regional repolarization of the nearby underlying myocardium. Thus if the SECG T-wave is negative, TpTe may reflect a local repolarization component, however, where the T-wave is positive, it may represent a difference between the end of a regional repolarization component and the far field or late repolarization regions within the heart. This may explain the flat regression curve in Figure 25.B, as TpTe is a constant measure of the balance between the local and global components of repolarization which do not change.

The strongest relationship to apicobasal dispersion of repolarization and SECG markers was seen by measuring the difference between the end and start of the entire T-wave in aVL (Figure 25. C), but this relationship was weaker than that seen with right to left dispersion of repolarization. Previous work has suggested that the T-wave morphology may be inscribed by predominant apicobasal differences in repolarization(Janse et al. 2005; Opthof et al. 2009). Mijborg et al. (Meijborg et al. 2014) have therefore suggested that differences in the earliest peak to the latest end of the SECGTW, reflects global dispersion of repolarization within the porcine heart, which is largely governed by apicobasal differences. In the intact human heart, however, differences in repolarization between the thin right ventricle and the large muscle mass of the left ventricle may predominate(Bueno-Orovio et al. 2012), reflecting differences between species. Thus our finding that differences in the latest upslope in V1-3 vs V6/aVL reflect dispersion of repolarization in the right to left axis would be consistent with the findings on Mijborg et al. (Meijborg et al. 2014), in that largest measured dispersion of repolarization was reflected in differences in the upslope of the early repolarizing SECGTW regions against the end of the upslope in the late repolarizing SECGTW regions.

6.7. Limitations And Conclusion

As mentioned in section 5.7, we were unable to perform whole heart recordings. Other limitations have previously been mentioned in section 5.7.

The upslope of the precordial leads on the SECG represents regional repolarization within the RV and LV. Differences between the end of the upslope in V1-3 vs V6/aVL represent right to left dispersion of repolarization. Further assessment of the consistency of this marker in human hearts with pathological changes is required, and its role in risk prediction is needed. There is no direct correlation between TpTe and transmural or apico-basal dispersion of repolarization in the intact human heart.

Chapter 7

Results: Transmural Restitution Properties of The Structurally Abnormal Heart

7.1. Introduction

I have previously described the transmural APD and RT response to varying stimulus site in response to S1-S2 restitution protocols from varying stimulus sites within the healthy normal ventricle (Srinivasan et al. 2016). These properties are less clearly defined in patients with structurally abnormal hearts, who are at risk of sustained ventricular tachycardia (VT).

Sustained VT is an important cause of the estimated 150,000-300,000 sudden cardiac deaths in the US (Chugh et al. 2008; Adabag et al. 2010). VT can be either polymorphic; with a continually changing QRS morphology, indicating a beat to beat change in ventricular activation, with irregular activation waves spiralling through the ventricles; or monomorphic; where the QRS complexes are similar beat-to-beat, often in association with a fixed arrhythmia substrate (Stevenson 2009). This arrhythmic substrate may be a region of enhanced automaticity, but most commonly in the context of a structurally abnormal heat, is manifest as a region of scar that provides the substrate for reentry (Stevenson & Soejima 2007).

Myocardial scar is most commonly associated with ischemia to the ventricle but can also be present in diseases where replacement fibrosis occurs. Numerous cellular changes occur within these regions of scar including a reduction in the content of connexion43 (Cx 43) gap junctions (Peters et al. 1993) and the transformation of myofibroblasts within the region (Sun & Weber 2000), which affect the conduction properties of the tissue. In addition to the structural changes, cellular properties are altered through heterogeneously abnormal sodium, calcium and potassium handling (Baba et al. 2005; Wilson & D. S. Rosenbaum 2007; Ebinger et al. 2005; Dun & Boyden 2005; Jiang et al. 2000; Dun et al. 2004; Litwin & Bridge 1997; Pinto et al. 1997; Aimond et al. 1999).

Within regions of dense scar there are areas of surviving tissue, which together serve as sites of slow conduction and conduction block creating the necessary conditions for reentry (Soejima et al. 2002; Nayyar et al. 2014). Additionally the scar border zone serves as an important substrate for VT (Verma et al. 2005). Surgical case series studies using open chest mapping and encircling endocardial ventriculotomy (Ostermeyer et al. 1984; Moran et al. 1982) or encircling endocardial cryoablation

(Guiraudon et al. 1994), showed treatment encircling the scar border zone or the earliest activating site within the scar border zone was successful in preventing arrhythmic recurrence in 73-92% of patients. More recently Marchlinski et al. (Marchlinski et al. 2000)and Reddy et al. (Reddy et al. 2003) have had similar success using catheter ablation of the border zone, again highlighting this region as an important electrophysiological substrate for maintenance of VT.

However, arrhythmias within heart do not traverse a one dimensional course on a planar wave across the endocardium. It is highly likely that the wavefront is heterogeneous, involving epicardial loops (Kaltenbrunner et al. 1991; Reddy et al. 2003) or isthmuses(Harris et al. 1987), as well as taking a complex path, involving the endocardium, mid-myocardium and the epicardium (Delacretaz & Stevenson 2001), and may even be ablated in regions outside the scar and scar borderzone in healthy normal myocardium representing a distant exit site (Verma et al. 2005). There are also limitations to conventional catheter based activation mapping of VT, in that it uses sequential methods to map a wavefront that may not always be stable or consistent, it fails to provide a global picture of the transmural propagation and many patients are unable to haemodynamically tolerate sustained arrhythmia well enough for it to be adequately mapped.

Importantly, the fundamental transmural electrophysiological properties of APD, and thus RT and RT dispersion across scar and scar borderline are poorly defined. RT dispersion is known to play an important role in sustaining arrhythmia, and its heterogeneity across scar and scar borzerzone is poorly defined. In canine hearts, infarct borderzone myocytes demonstrated a reduced resting membrane potential, decreased action potential upslope and shortened APD 4-5 days post infarct (Gardner et al. 1985). Porcine models of tetralogy of Fallot have demonstrated transmural APD heterogeneity and APD gradients, again highlighting this as a possible arrhythmic mechanism (Benoist et al. 2017). Optical mapping studies in failing human hearts show prolonged APD's and reduced transmural gradients (Glukhov et al. 2010), with cellular studies of late infarcts confirming a prolongation of APD (Myerburg et al. 1982; Li et al. 2004). Restitution studies in canines have suggested that regions of scar borderline has an Smax >1 over a longer range of diastolic intervals(Ohara et al. 2001). Intact human

data on the subject is limited. Taggart et al. (Taggart et al. 2000) have demonstrated inhomogeneous transmural conduction during early ischemia and a lack of transmural APD gradients over a range of coupling intervals (Taggart 2001). These properties have not been dynamically studied in the intact human heart in conditions of chronic scar that is capable of sustaining VT.

7.2. Aim

The aim of this study was to investigate the planar and transmural properties of AT, APD and RT across the borderzone of defined scar and viable tissue in patients undergoing VT ablation.

7.3. Hypothesis Addressed

1. Transmural gradients of APD are present in the structurally abnormal human heart.

2. Transmural and regional planar gradients of APD play an important role in determining regional total repolarization time dependent on the activation wavefront.

3. Disruption of transmural and planar dispersion of APD occurs in disease and results in dispersion of localised total repolarization time which may facilitate reentry.

7.4. Methods

Refer to section 4.5

7.5. Results: Transmural Restitution Properties of The Structurally Abnormal Heart

7.5.1. Baseline Characteristics

Baseline clinical characteristics of the patients can be seen in Table1 (Section 4.5.1). Five Male (Median Age 53 years, IQR 43-67 years). All patients had an ICD in situ, two patients the VT ablation was preformed acutely for incessant VT with recurrent ICD shocks, the remaining patients were elective procedures for multiple ICD shocks. The underlying myocardial pathology was ischemic heart disease (ICM) in 4 patients, 1 patient had diagnosis of previous myocarditis based on clinical history and epicardial scar distribution on cardiac MRI and one patient had a clinical diagnosis of arrhythmogenic cardiomyopathy (ARVC) based on task force criteria for ARVC (Marcus et al. 2010). Median LV ejection fraction was 35% (IQR 15-54%). Antiarrhythmic medications are documented in Table 1. (Section 4.5.1) along with clinical outcome.

7.5.2. Patterns Of Endocardial And Epicardial Scar And Their Association With ARI and RT

7.5.2.1. Predominant Epicardial Scar

Figure 26 shows an example of a paired endocardial and epicardial voltage map in a patient with predominant epicardial scar, from previous myocarditis (Patient 1). Decapolar catheters are placed across the epicardial scar region traversing regions of dense scar, scar borderzone and healthy tissue and are paired for comparison with a transmurally opposed decapolar catheter in the endocardium which displays normal bipolar voltage (Figure 26.).

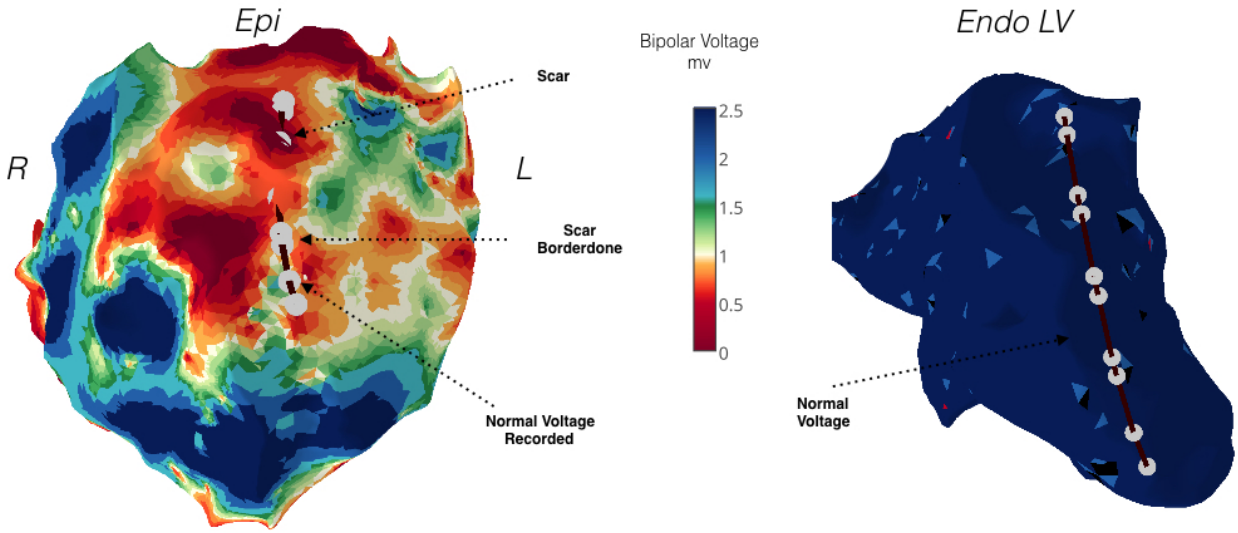

Figure 26. Schematic depicting the epicardial and endocardial Carto voltage maps in a patient (patient 1) with predominant epicardial scar and healthy endocardial tissue. Decapolar catheters are placed transmurally to measure APD differences across the scar borderzone (black line with grey dots). highlighting a large region of epicardial scar anteriorly. Position of catheters simultaneously placed endocardially and epicardially for transmural recording is shown.

During endocardial pacing restitution curves recorded over a region of healthy transmural tissue (Figure 27. A(i)), demonstrate early endocardial activation with a transmural activation delay to the epicardium (36ms difference at 50th quantile, $p<0.05$), with shorter epicardial ARI (median ARI 173ms vs 209ms in endocardium), across all coupling intervals (38ms difference at the 50th quantile, $p<0.05$ across all coupling intervals), resulting in no significant transmural differences in total repolarization (median epiccardium vs endocardium RT, 251ms vs 248ms) during across all coupling intervals (2ms difference at 50th quantile, $p=0.66$ and ns across all coupling intervals). Recording in a region of epicardial scar borderzone and normal endocardium (Figure 27. A(ii)), again showed early endocardial activation (25ms difference at 50th quantile, p=ns across all coupling interval), with smaller transmural ARI differences (median epicardial ARI 187ms vs 207ms in endocardium, 22ms difference at 50th quantile p=ns across all coupling interval), and no significant differences in transmural total repolarization time (epicardium vs endocardium median 232ms vs 233ms, 4ms difference at the 50th quantile, $p=0.5$ and ns across all coupling intervals). Finally recording in a region of dense epicardial scar and normal endocardial tissue(Figure 27. A(iii)), again showed early endocardial activation (26ms difference at the 50th quantile, $p<0.05$), but with further prolongation of epicardial ARI (median epicardial ARI 190ms, vs 203ms, 11 ms difference at 50th quantile $p=0.58$) and no significant differences in transmural repolarization time (median epicardial RT 220ms vs endocardium 217ms, 4ms difference at the 50th quantile $p=0.45$ and ns across all coupling intervals). Thus although transmural ARI differences were diminished in epicardial scar and scar borderzone due to lengthening of epicardial ARI , there were no recorded differences in total RT, due to a reduction in transmural AT.

During epicardial pacing, since pacing was performed from a region of epicardial scar remote to the normal transmural tissue(Figure 27. B(i)), there was conduction delay due to block across the epicardial layer with earlier endocardial activation in the region of transmural normal tissue (32 ms at 50th quantile $p=<0.05$ across all coupling intervals), however ARI showed a similar pattern of shorter epicardial ARI (median ARI 185ms vs 210ms endocardium, 32ms difference at 50th quantile, $p=<0.05$ for all coupling intervals), with no significant difference in repolarization time (median epicardial RT 279ms vs 275ms endocardium, 5ms difference at 50th quantile, $p=<0.52$ and ns for all coupling

intervals). In the scar borderzone (Figure 27. B(ii)), a similar activation pattern was observed (26ms difference at the 50th quintile, p=<0.05 all segments), ARI was again shorter epicardially (median 187ms vs 195ms endocardium, 24ms difference at the 50th quantile, p=0.06 and ns for all segments), while total repolarization time showed no significant difference (median epicardial RT 264 vs 260 endocardial, 2ms difference at the 50th quantile and ns across all coupling intervals). Finally across the region of dense scar(Figure 27. B(iii)), earlier epicardial activation was seen (15ms difference at 50th quantile, p<0.05 all segments), with again prolongation of epicardial ARI and no significant transmural ARI difference (median epicardial ARI 205 vs 202ms endocardium, 2ms difference at 50th quantile, p=ns all coupling intervals), resulting in earlier epicardial repolarization (18ms at 50th quantile p<0.05 all segments, median epicardial RT 236ms vs 254ms endocardium). Thus in regions of scar and scar borderzone, the transmural ARI differences were again diminished because of ARI prolongation in the epicardial scar region, but this resulted in no significant transmural differences of repolarization during epicardial pacing due to earlier epicardial activation in the dense scar region but not in the normal or borderzone tissue due to activation delay.

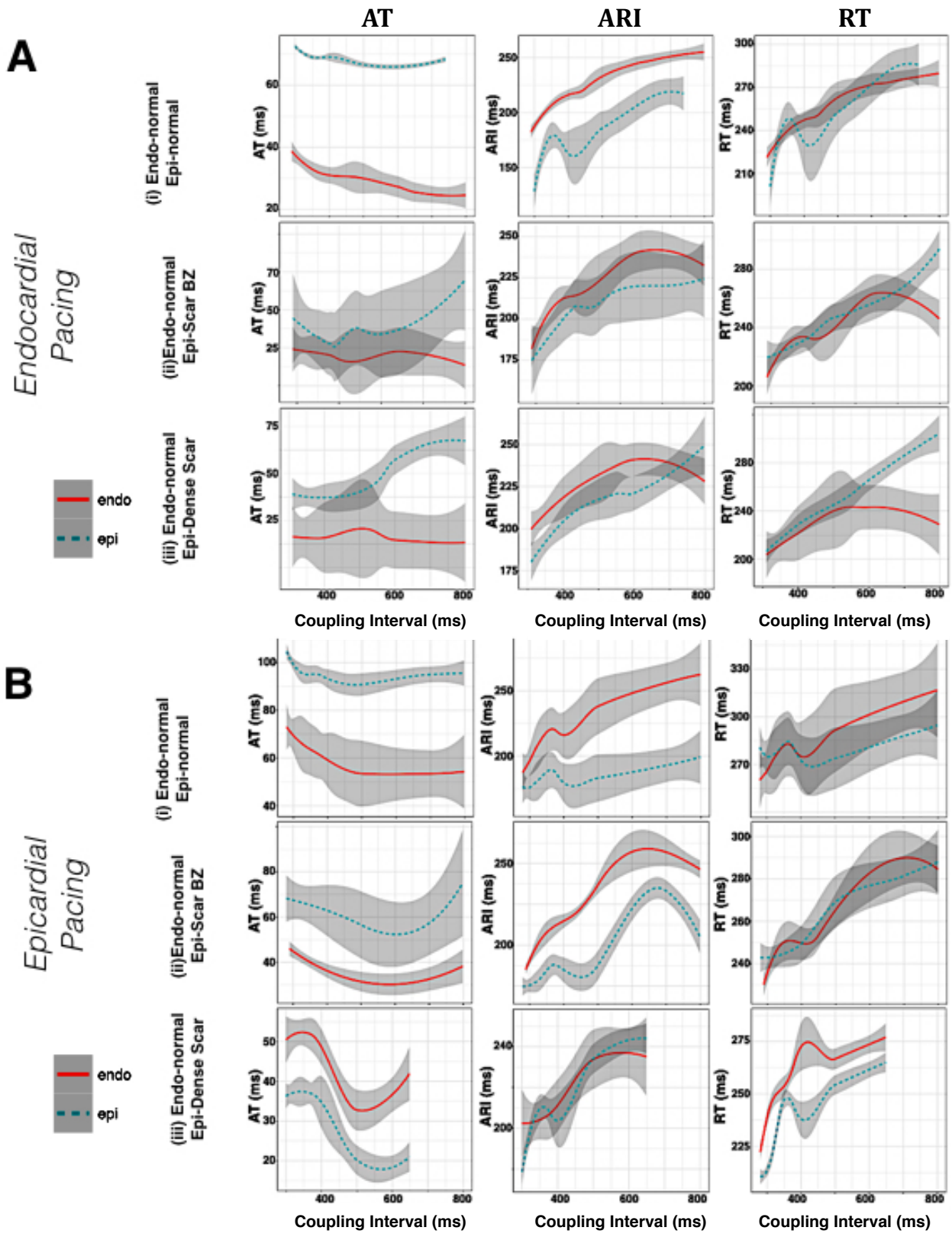

Figure 27. **A**, restitution studies during basal endocardial pacing in normal endocardial voltage, with transmural recording in region of epicardial normal voltage tissue (i), epicardial scar borderzone (ii) and epicardial scar (iii). **B**, restitution studies in same regions as A but with epicardial basal pacing. AT =activation time, ARI = activation recovery interval, RT = repolarizaiton time.

7.5.2.2. Predominant Endocardial Scar

Figure 28 shows an example of restitution studies performed across a region of endocardial scar in the apex of the LV in a patient with ischemic cardiomyopathy (patient 3), with previous anterior myocardial infarction. There is extensive low voltage in the anterior wall and apical cap, with some preservation of the posterior wall voltage endocardially, with minimal epicardial scar. Catheters are opposed transmurally for comparison recording over the apex (Figure 28).

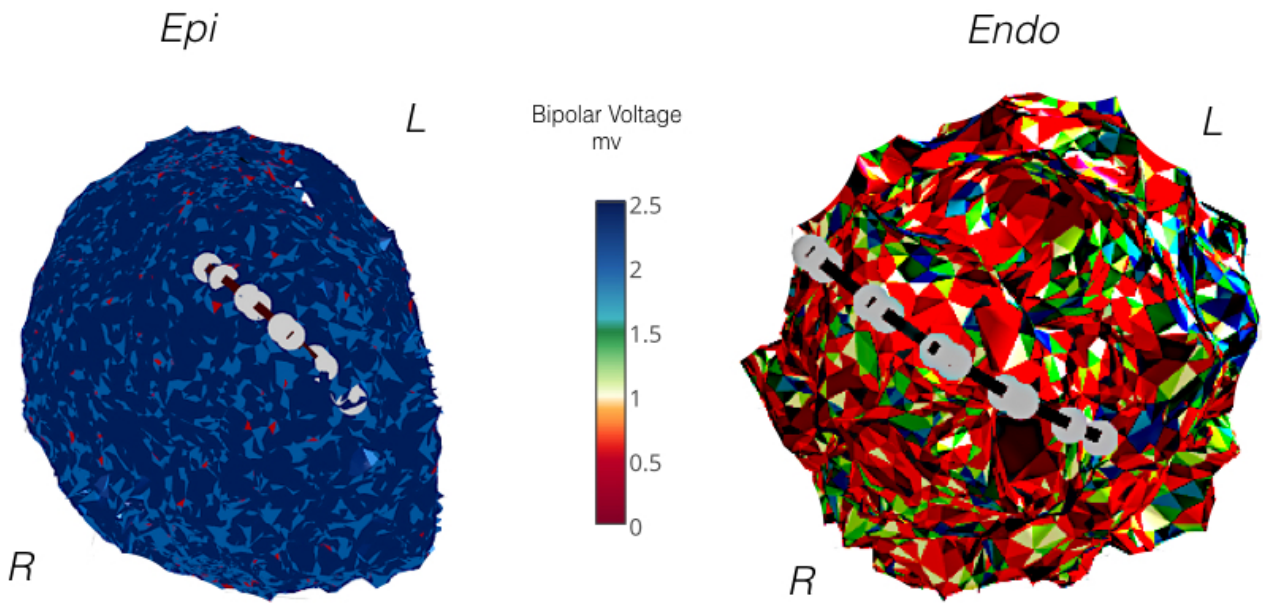

Figure 28. Restitution studies in a patient with ischemic cardiomyopathy and predominant endocardial scar from the anterior wall and along the apex left ventricle due to previous anterior myocardial infarction (patient 3). Catheters are positioned across the apical scar in the endocardium and epicardium for transmural pole comparison during restitution studies while pacing the endocardium and epicardium.

Restitution studies during endocardial (Figure 29. A) and epicardial (Figure 29. B) RV pacing are shown as the regression of all recorded catheter poles in the region because of the homogeneity of the transmural scar pattern. During endocardial pacing, (Figure 29. A) there is earlier activation of the endocardium (10ms difference at the 50th quantile, p=ns all segments), ARI was longer in the endocardium where there was dense scar (median endocardial ARI 226ms vs 200ms epicardial, 10ms difference in the 50th quantile, $p<0.05$), while RT was also prolonged endocardially (median endocardial RT 320 vs 303ms epicardial, 18ms difference at 50th quantile $p<0.05$ all coupling intervals). Thus despite the earlier endocardial activation, endocardial repolarization was delayed due to prolonged ARI in this region.

During epicardial pacing, (Figure 29. B) there was earlier epicardial activation (15ms difference at the 50th quantile, $p<0.05$ all coupling intervals), ARI was longer in the endocardium than the epicardium (median endocardial ARI 291ms vs 231ms epicardially, 33ms at 50th quantile, $p<0.05$, but ns across all coupling intervals), and repolarization longer in the endocardium than the endocardium (median endocardial RT 336, vs 270 in epicardium, 42ms transmural difference at 50th quartile $p<0.05$ all coupling intervals). Thus again the longer ARI in the scar region of the endocardium resulted in longer RT.

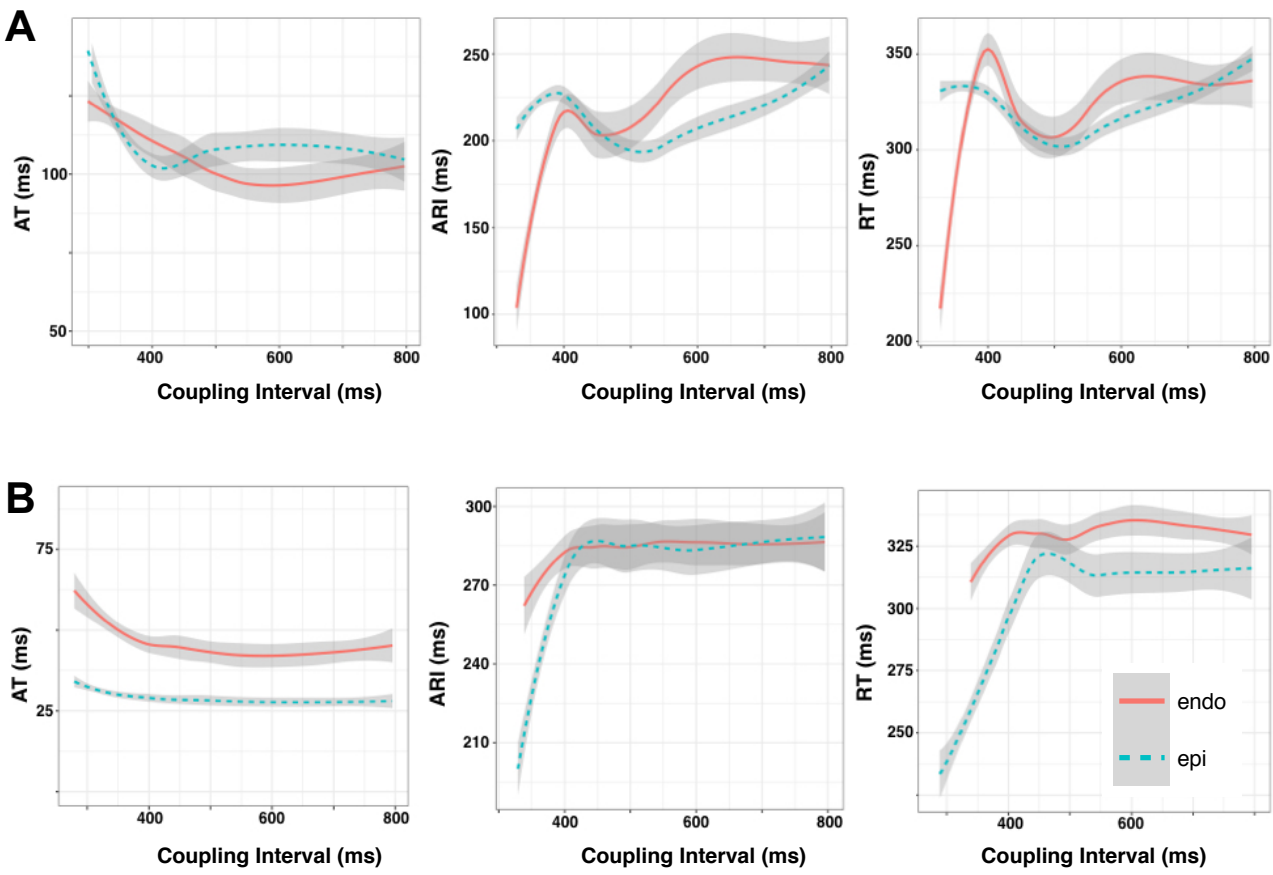

Figure 29. Restitution studies while pacing the endocardium (**A**) and epicardium (**B**) in patient 3, where there was predominant endocardial scar in the anterior wall and the LV apex secondary to previous myocardial infarction. AT =activation time, ARI = activation recovery interval, RT = repolarization time.

7.5.2.3. Transmural Scar

Figure 30 shows an example of restitution studies in a patient with ARVC and transmural dense scar across the RVOT. Patchy dense scar is seen throughout the RV with some relative sparing of the lateral LV on the epicardial voltage map.

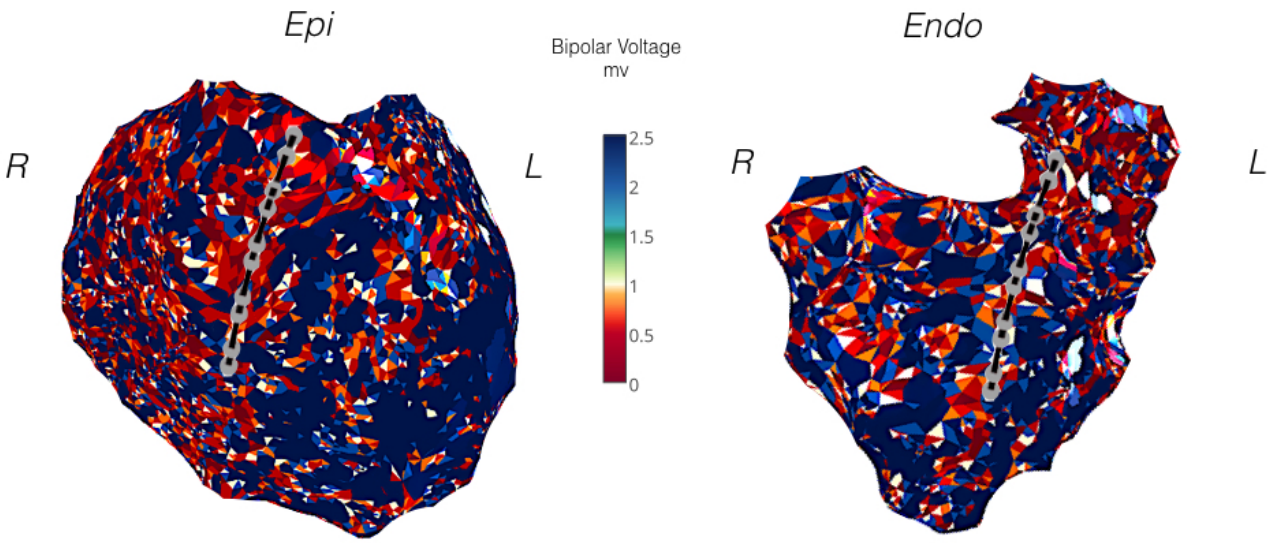

Figure 30. Restitution studies in a patient with ARVC across a region of transmural scar in the RVOT (patient 6). Catheters are positioned across the anterior RVOT in the endocardium and epicardium for transmural pole comparison during restitution studies while pacing the endocardium and epicardium.

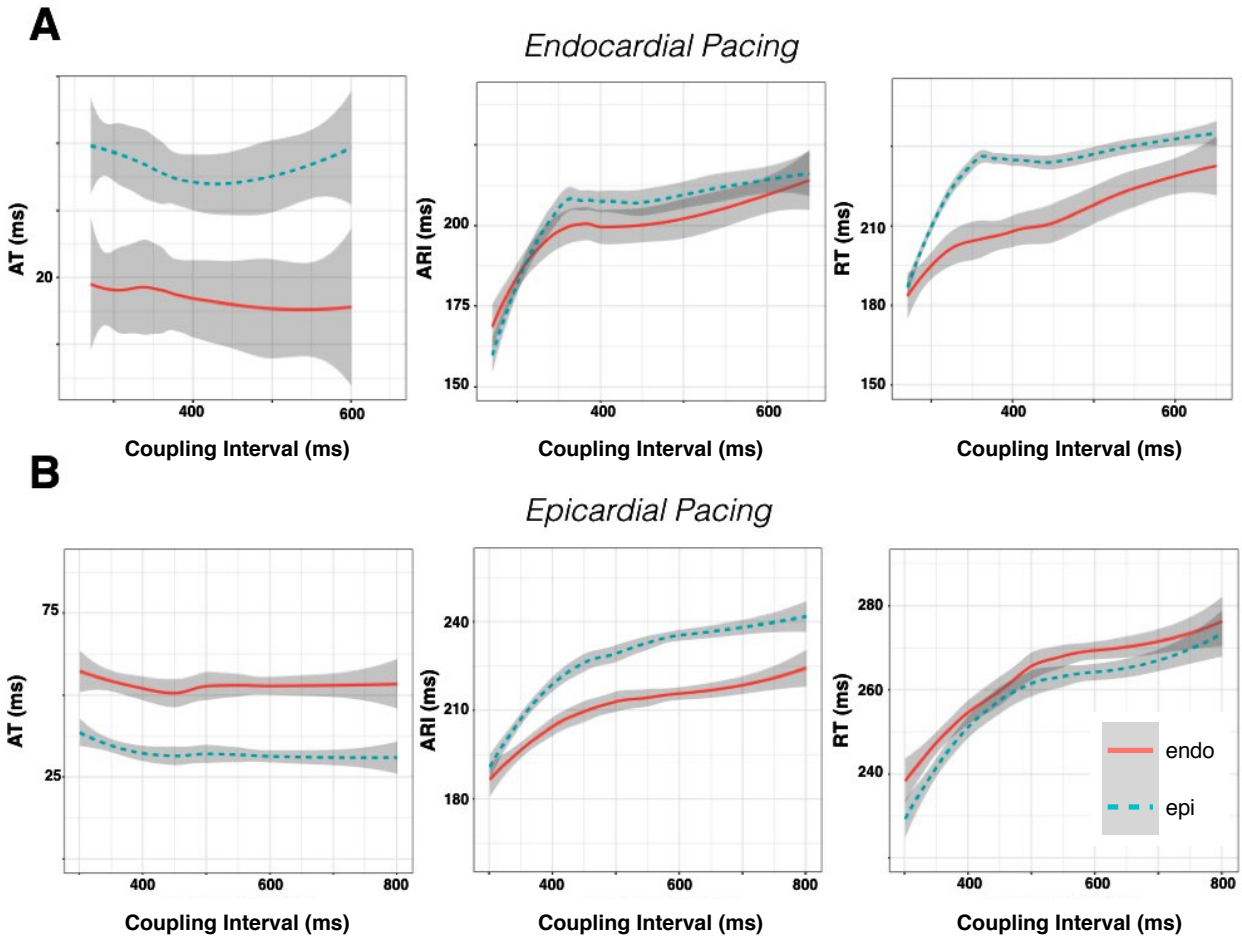

Figure 31. Restitution studies while pacing the endocardium (**A**) and epicardium (**B**) in patient 6, where there was where there was transmural scar across the RVOT secondary to ARVC AT =activation time, ARI = activation recovery interval, RT = repolarization time.

Restitution studies during endocardial (Figure 31. A) and epicardial (Figure 31. B) RV pacing are shown as the regression of all recorded catheter poles in RVOT in a region where endocardial and epicardial poles were in contact with dense scar consistent with a transmural scar pattern. During endocardial pacing (Figure 31. A) there is earlier activation of the endocardium (7ms difference at the 50th quantile, $p<0.05$ all coupling intervals), however epicardial ARI was longer than in the endocardium(median epicardial ARI 209ms vs 199ms endocardial, 9ms at 50th quantile, p=ns all coupling intervals), and transmural repolarization time was longer in the epicardium compared to endocardium (median

epicardial RT 229ms vs 218ms endocardium, transmural RT difference 50ms at 50th quantile p=0.06 and ns for all coupling intervals).

During epicardial pacing (Figure 31. B), there was earlier activation of the epicardium (20ms difference at 50th quantile, $p<0.05$ all coupling intervals), ARI was again prolonged in the epicardium (median epicardial ARI 230ms vs 208 in epicardium, 20ms difference at the 50th quantile $p<0.05$ for all segments), with no significant transmural repolarization time difference (median epicardial RT 260ms vs 265ms in endocardium, 6ms difference in the 50th quantile p=ns all coupling intervals). Thus ARI in this patient with transmural scar was prolonged in the endocardium and epicardium, with a greater prolongation in the epicardium. Significant differences in transmural repolarization time were therefore seen only during endocardial pacing, due to the additional transmural conduction delay, while epicardial pacing reduced this.

7.5.3. ARI Differences in Endocardial and Epicardial Scar

Figure 32 shows the ARI characteristics of endocardium and epicardium with normal voltage, scar borderzone and dense scar. Dense epicardial scar and epicardial scar borderzone result in a significant prolongation of ARI compared to normal epicardial ARI (Figure 32. A). Endocardial scar resulted in an increase in endocardial ARI compared to normal tissue but the difference compared to normal was less significant than in epicardial scar (Figure 32. B)

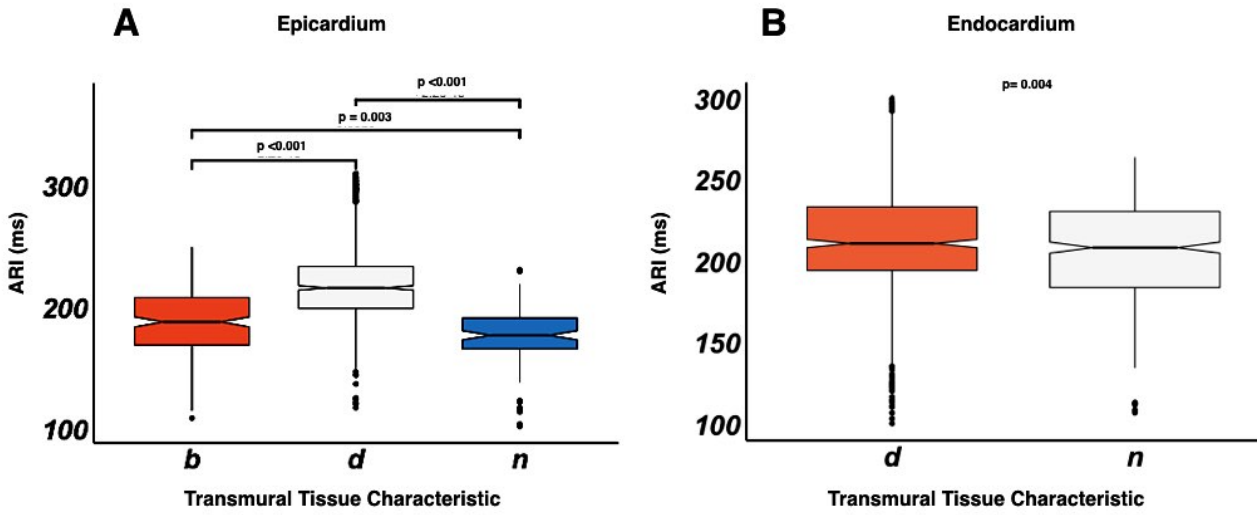

Figure 32. Boxplot of epicardial (**A**) and endocardial (**B**) ARI in relation to the tissue voltage characteristic. Tissue characteristic is denoted on the x-axis, d= dense scar, n = normal tissue and b= scar borderzone. Statistical significance between box plots is shown above the plots.

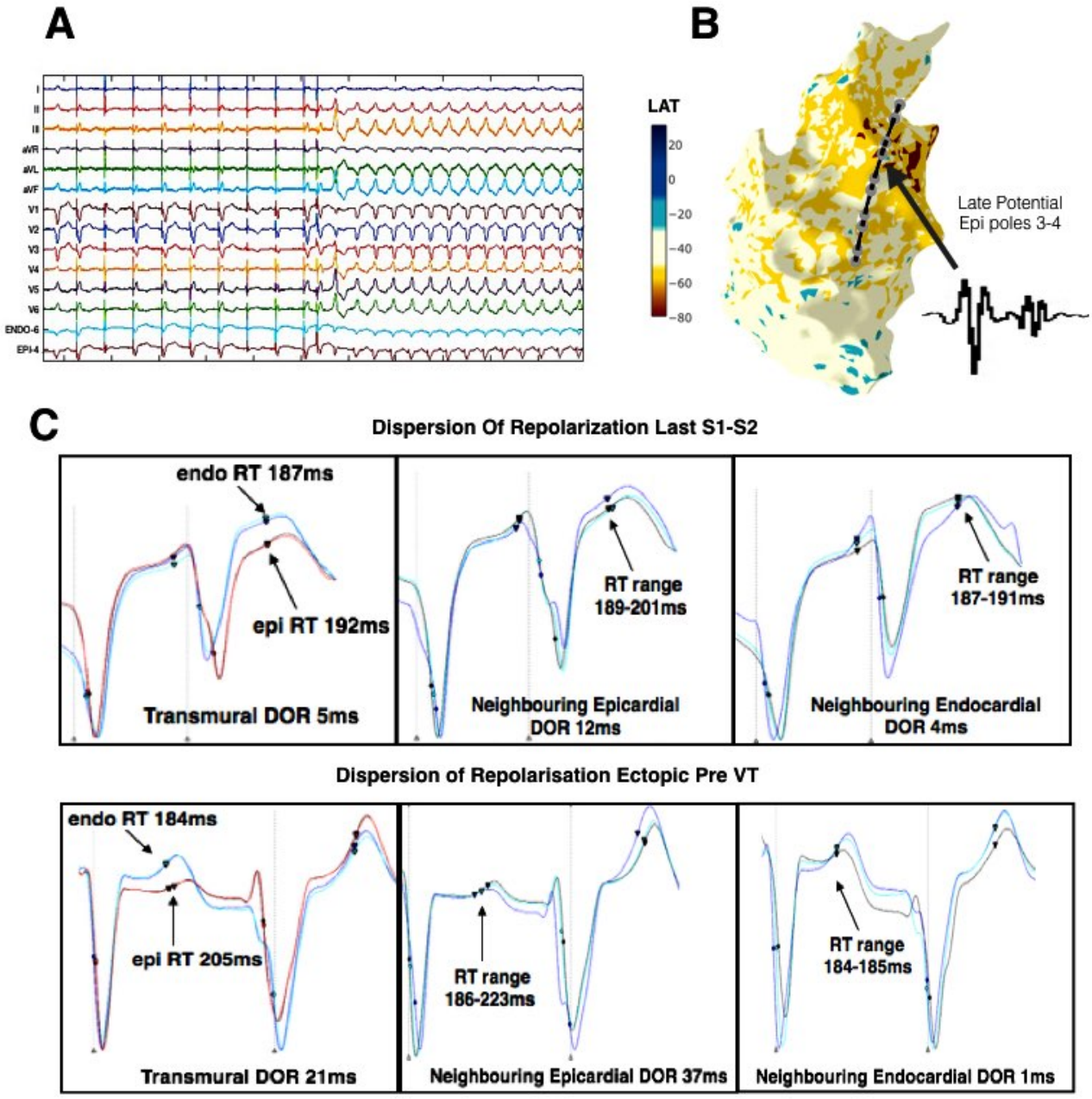

Figure 34. Dispersion of repolarization and initiation of VT in example patient. (**A**) S1-S2 restitution protocol, showing 12-lead ECG and sample unipolar electrograms from the right ventricular endocardium and right ventricular (RV) epicardium. Following a train of S1 pacing, an S2 beat is delivered, following this an RV ectopic beat is initiated which triggers sustained ventricular tachycardia (VT). (**B**) RV endocardial geometry and activation mapping of the sustained VT showing earliest activation (red area), in the right ventricular outflow tract, along with location of transmurally opposed endocardial and epicardial decapolar catheters from the restitution study. Poles 3 and 4 of epicardial catheter were located over a region of late potentials in sinus rhythm (inset). (**C**) Dispersion of repolarization transmurally (DOR) at epicardial catheter pole location 3-4 (where fractionation was recorded), in the neighbouring epicardial poles to 3-4, and in the neighbouring adjacent endocardial poles. DOR is shown for the last S2 beat (above panel) and for the ectopic beat subsequent to this which initiates sustained VT.

7.5.4. All Patient Analysis Of Endocardial/Epicardial Scar Pattern And Its Association With ARI and RT

Figure 33 shows the association of endocardial and epicardial scar pattern to ARI and RT of all the combined patients in the study. Transmural catheter poles that were geometrically opposed were paired and their endocardial ARI (Figure 33. A) or RT (Figure 33. B&C) subtracted from the epicardial ARI or RT respectively, to give the transmural difference for each coupling interval of restitution. Data were then analysed based on their endocardial and epicardial scar pattern as described in the figure, and assessed for statistical differences against regions where normal endocardial and epicardial voltage was recorded (n_n in Figure 33). RT is separated for endocardial and epicardial pacing because activation pattern influences total repolarization time.

Figure 33. A shows that in regions of dense endocardial and epicardial scar (d_d), there is a significant reduction of the transmural ARI difference due to preferential lengthening of epicardial ARI as described above. In regions of endocardial scar but normal epicardial tissue (d_n) and dense epicardial scar but normal endocardial tissue (n_d) again there was a reduction in ARI difference compared to normal, while where there was normal endocardial tissue and scar borderzone epicardially again a significant reduction in transmural ARI differences were observed due to an increase in epicardial ARI by less than in other scar patterns. Thus regions of scar reduce transmural ARI differences, due to a lengthening of local ARI.

Thus during endocardial pacing regions of dense scar (d_d) and regions of normal endocardial tissue with dense scar epicardially (n_d) display a significantly negative transmural endocardial to epicardial RT gradient compared to normal tissue, due to the effect of conduction delay and prolonged epicardial ARI increasing epicardial RT.(Figure 33. B). While during epicardial pacing the endocardial to epicardial RT difference is increased compared to normal tissue in d_d tissue and d_n tissue due to activation delay and prolonged ARI in the endocardial scar tissue, but also in n_d tissue and to a lesser extent n_b (Figure 33. C).

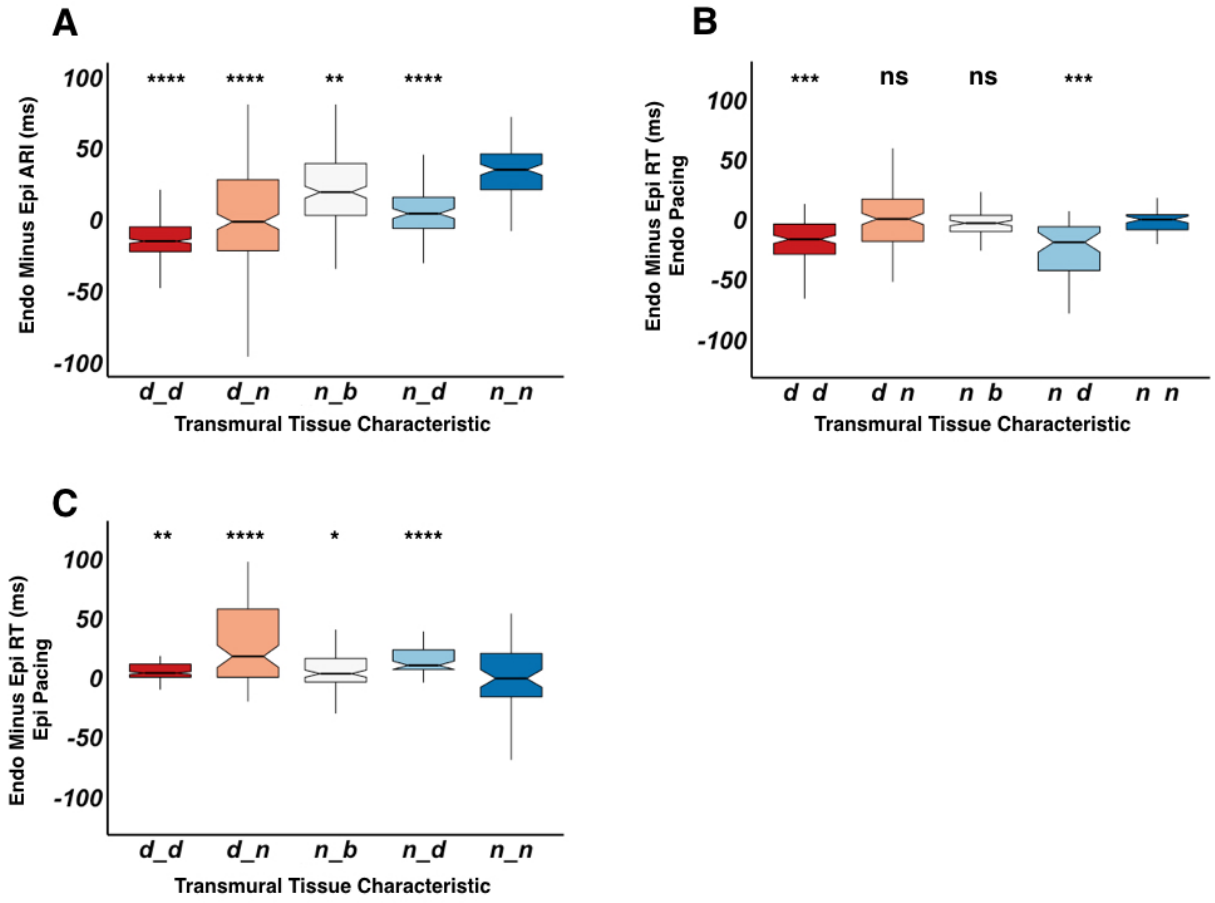

Figure 33. Boxplot of endocardial to epicardial scar pattern, and its association to endocardial subtracted by epicardial ARI (**A**), endocardial subtracted by epicardial RT during endocardial pacing (**B**) and endocardial subtracted by epicardial RT during epicardial pacing(**C**). Scar tissue characteristic is denoted on the x-axis, the first letter is the characteristic of the endocardium and the second letter is the characteristic of the epicardium. d= dense scar, n = normal tissue and b= scar borderzone. Statistical significance is assessed as a comparison against normal endocardial and epicardial tissue (n_n), with statistical significance denoted above the boxplot. ns= not significant, ***** = $p<0.05$, ****** = $p<0.01$, ******* = $p<0.001$, ******** <0.0001.

7.5.5. Dispersion Of Repolarization And Arrhythmogenesis

Figure 34 shows an example where VT was induced in patient 6 during the S1-S2 restitution protocol. Catheters were placed across the RVOT in a geometrically opposed region across scar endocardially and epicardially as in Figure 30. Figure 34.A shows the surface ECG and sample intracardiac electrograms recorded during an S1-S2 restitution protocol. At an S2 interval of 280ms, the last paced beat is followed by an RV ectopic which initiates VT. The VT was mapped endocardially (Figure 34.B) and earliest activation was recorded to a site in the anterior RVOT. Position of the epicardial decapolar catheter is shown in relation to this, and the superior poles (Poles 1-4), displayed late potentials during resting sinus rhythm in this region (inset electrograms).

Figure 34.C shows the transmural electrograms from geometrically opposed catheters in this regions, as well as the neighbouring electrograms from neighbouring electrodes away from this region in the epicardium and in the endocardium, at the last S1-S2 beat and on the ectopic beat that follows this and initiates VT. It can be seen that transmural dispersion of repolarization (DOR) is only 5ms at the S2 beat, while neighbouring epicardial DOR is 12ms in the region where fractionation was recorded, while negligible DOR is seen in the opposite endocardial tissue to this region (DOR = 4ms). The effect of the ectopic beat is to increase transmural DOR to 21ms in this same region, and neighbouring epicardial catheter pole DOR to 37ms, with negligible endocardial DOR, this initiates VT, which was mapped to this region of repolarization dispersion and ablation to this region rendered VT non-inducable. This may provide the substrate for transient functional block and initiation of VT.

7.6. Discussion

The main findings of this study are (1) that areas of myocardial scar, regardless of pathology, have prolonged ARI compared to normal healthy tissue. While we have previously demonstrated (Srinivasan et al. 2016) that in normal tissue there is a transmural ARI gradient with longer ARI in the endocardium then the epicardium, (2) we show here that where the presence of scar decreases that transmural gradient of APD, the extent to which is dependent on the endocardial and epicardial scar characteristics. Finally, (3) alterations in transmural APD gradient, result in localised transmural dispersion of repolarization, dependent on the scar pattern and the activation sequence, which may play a role in arrhythmogenesis.

7.6.1. Myocardial Scar Results In Prolongation Of APD

Studies of myocardial infarction in dogs (Gardner et al. 1985), have demonstrated shorter APD acutely, which lengthened as the infarct became chronic. Additionally, numerous studies of chronic heart failure remodelling, scar, and ischemia have demonstrated prolongation of regional APD in these disease states (Glukhov et al. 2010; Myerburg et al. 1982; Li et al. 2004). Our findings are consistent with these previous studies showing a prolongation of APD both in the epicardium and the endocardium in a series of intact human ventricles with a variety of pathologies (Figures 27,28,31 &32). Uniquely we show that the process of APD prolongation occurs in both the endocardium and the epicardium in regions of scar and scar borderzone, contrary to previous work (Glukhov et al. 2010). We also demonstrate that this property is unique to myocardial scar and not a globalised phenomenon as previously reported (Glukhov et al. 2010), because within patients with diseased ventricles, regions of normal myocardial voltage display shorter APD that is in a range consistent to what we have previously demonstrated (Srinivasan et al. 2016) in normal tissue (Figures 26, 27 &32). The mechanism for this is unclear, but may involve structural changes, such as down regulation of Cx43 (Glukhov et al. 2010; Peters et al. 1993), or more likely ionic changes such as up regulation of Ica (Baba et al. 2005; Dun et al. 2004; Litwin & Bridge 1997; Pinto et al. 1997; Aimond et al. 1999) which may primarily be an adaptive mechanism to cause calcium overloading of the cell in order to improve contractility, and down

regulation of Iks and an increase in the KCNQ1(Ikr)-to-KCNE1(Iks) mRNA ratio (Dun & Boyden 2005; Jiang et al. 2000), which may help counteract the down regulation of Ito. (Dun et al. 2004). Additionally a fundamental part of the myocardial remodelling in structurally abnormal or failing hearts involves the development of myocyte hypertrophy (Anversa & Nadal-Ginrad 2002). APD prolongation in the failing heart is seen in both animal and human models, as a result of an increase in the amplitude of the intracellular calcium transient, which is an adaptive feature that causes positive inotropy (Wickenden et al. 1998). The mechanism for this is similar to that described above but there may also be an increase in INa/Ca in the hypertrophies heart which results in intracellular overload (Wickenden et al. 1998).

7.6.2. Myocardial Scar Reduces Transmural APD Gradients

My previous studies in the intact normal human ventricle have demonstrated the presence of a transmural gradient in APD, with longer endocardial APD compared to epicardial APD (Srinivasan et al. 2016), consistent with experimental studies (Boukens et al. 2015). This transmural gradient of APD was still present in regions of normal endocardial and epicardial voltage, however, where there was either endocardial, epicardial or transmural scar/scar-borderzone, this gradient was diminished(Figure 32.A). This is consistent with experimental work in heart failure (Glukhov et al. 2010) and in intact human hearts (Taggart et al. 2000; Taggart 2001), but again we show the phenomenon is not global. Additionally the reduction in transmural gradients of APD, are related to the scar characteristics, with regions of dense scar both endocardially and epicardially displaying zero to negative transmural APD gradients (Figure 33.A), due to the greater proportional lengthening of APD in the epicardium (Figure 32). Regions of dense scar in either endocardium or epicardium with normal tissue opposite showed the next lowest reduction in APD; followed by regions where there was scar borderzone opposite normal tissue, where the transmural APD gradient similar to that of normal voltage tissue. This demonstrates that the process of both APD lengthening and also reduction in APD gradients is a spectrum, dependent on the level of scar and adaptive processes within the scar. This finding would not be unexpected from a mechanistic perspective as progressively less diseased tissue would be

expected to have more normal ionic properties and less channel adaptation (Dun & Boyden 2005; Jiang et al. 2000). Additionally, the reduction in transmural APD gradients may be an important adaptive process that negates the changes in conduction velocity within the tissue to prevent dispersion of repolarization.

7.6.3. Alterations In Transmural APD Alter Repolarizaiton Characteristics And May Contribute To Arrhythmogenesis

The interplay between activation and APD to influence transmural dispersion of repolarization is demonstrated in Figure 33.B&C demonstrating the transmural gradient of RT (endocardial RT - epicardial RT). Where there were regions of dense scar on the endocardium and epicardium, epicardial ARI was prolonged to a greater extent, resulting in a negative transmural repolarization gradient of RT during endocardial pacing, due to conduction delay and the prolonged ARI epicardially (Figure 33.B), and a positive transmural gradient during epicardial pacing (Figure 31). Where predominant endocardial or epicardial scar was demonstrated, due to prolongation of APD in the scar region transmural dispersion of repolarization occurred when pacing on the side opposite the scar (Figure. 27.B, 29.A, 33.B&C) due to the addition of conduction delay and the prolonged APD.

Although dispersion of repolarization is only one factor in the initiation of reentrant arrhythmia, Figure 34, shows an example of VT initiation in a patient with scar present both endocardially, and epicardially across the RVOT (Figure 30). Due to the greater lengthening of epicardial APD, epicardial RT is longer during endocardial pacing (Figure 31), with the expected negative ARI and RT gradients (Figure 33. A&B). During restitution pacing the epicardial 3-4 bipoles are located over a region of fractionated late potentials (Figure 34.B), and VT is initiated by an ectopic that follows an S2 beat. It can be seen that there is both transmural and neighbouring epicardial dispersion of depolarization along the site of earlier activation of the VT, with relatively little endocardial dispersion of repolarization. The dispersion of repolarizaiton is further exacerbated by the ectopic beat, which then

triggers VT. Late potential mapping has become an important tool in performing substrate ablation for patients with VT (Sacher et al. 2015; Jaïs et al. 2012), however the underlying origin of these potentials is unclear. Canine studies have suggested that this occurs over regions of myocardial disarray and conduction slowing (Gardner et al. 1985), while isolated tissue studies have suggested that this may occur in regions of localised phase 2 reentry (Yan et al. 2004), or dispersion of repolarization (Szél & Antzelevitch 2014). Our findings are in keeping with the latter work of Antzelevitch and colleagues (Szél & Antzelevitch 2014), in demonstrating fractionation and VT initiation over regions of abnormal repolarization, and is the first demonstration of this in the intact human heart.

7.7. Limitations And Conclusions

Data were confined to multielectrode contact mapping, without dynamic global assessment of repolarization as may be provided by non-contact methods. Future advances in technology may permit this, using contact electrograms. Additionally traditional voltage cut-off's for scar threshold were applied based on published data (Reddy et al. 2003; Marchlinski et al. 2000; Stevenson 2009; Soejima et al. 2002; Verma et al. 2005), however debate exists as to what the correct optimal voltage cut-off's should be (Venlet et al. 2017). It is therefore possible that some of our recordings in regions of low voltage, were not in fact overlying tissue that would display scar in imaging modalities. Nevertheless, we were able to record APD differences in these regions based on their voltage characteristics.

This is the first human study to demonstrate that regions of electrical scar within the myocardium have prolonged APD. We demonstrate the interaction of this, in relation to scar pattern and transmural dispersion of repolarization, which represents the interplay between APD and activation sequence, and show an example of exaggerated dispersion of repolarization, both transmurally and with one plane at the site of earliest VT activation. This may provide further insights into the mechanisms of VT initiation, but also new methods to better delineate the pro-arrhythmic substrate if it becomes possible to rapidly map dynamic differences in APD and RT as part of routine global 3D mapping.

Chapter 8

Results: Non-invasive ECG Imaging Of Arrhythmogenic Right Ventricular Cardiomyopathy Substrate

8.1. Introduction

Arrhythmogenic right ventricular cardiomyopathy (ARVC) is an inherited cardiac condition that is associated with sudden cardiac death (SCD) in young individuals. It has an estimated prevalence of 1:1000 (Marcus et al. 2010; Corrado et al. 2011). The disease is characterised by fibro-fatty replacement of the myocardium, with myocyte loss (Basso et al. 1996, Corrado et al. 2011). The fibro-fatty infiltration of the myocardium has an epicardial predominance, suggesting that the disease progresses from epicardium to endocardium (Basso et al. 1996). Disease expression is variable with classical presentation involving disease of the right ventricle (RV) along the "triangle of dysplasia" involving the RV inflow, outflow and apex. However, some patients display diffuse RV or bi-ventricular disease or predominant LV disease (Marcus et al. 2010). Though some patients may remain asymptomatic through their life classically patients display a progressive phenotype consisting of an early concealed phase where they are often asymptomatic but are still at risk of SCD, followed by an electrical phase consisting of overt arrhythmias predominantly VT and VF, and later a diffuse disease characterised predominantly by heart failure (HF) with a lower arrhythmia risk (Marcus et al. 2010). Exercise may increase disease progression and has been linked to episodes of SCD (Rojas & Calkins 2015). Thus diagnosis and clinical management of these patients remains a challenge because patients are at risk of SCD in the absence of clinical abnormalities or pathologically detectable changes.

Several desmosomal protein mutations have been shown to be associated with the disease(Delmar & McKenna 2010) resulting not only in reduced cell-to-cell adhesion, but also decreased expression of sodium channels and gap junctions in cardiomyocytes (Delmar & McKenna 2010). Common genes associated with ARVC include plakoglobin (JUP), desmoplakin (DSP), plakophilin-2 (PKP2), desmoglein-2 (DSG2), desmocollin-2 (DSC2), trans- forming growth factor beta-3 (TGF 3) and TMEM43. (Marcus et al. 2010)

Human and murine studies have demonstrated that electrophysiological changes precede the structural disease (Gomes et al. 2012). Patients with ARVC exhibit slow conduction within the right ventricle and low endocardial bipolar voltages, indicative of endocardial scar (Tandri et al. 2009; Corrado et al. 2008).

The concealed and variable progress of the disease presents a significant diagnostic challenge and despite task force criteria, definitive diagnosis requires histological demonstration of fibrofatty replacement of myocardium or the presence of a known disease causing ARVC mutation(Marcus et al. 2010). Fibro-fatty infiltration is patchy, making biopsy challenging, and known disease causing mutations are present in only 30-40% of cases (Marcus et al. 2010; Delmar & McKenna 2010). Therefore, current diagnosis utilises a combination of structural, functional, and electrophysiological (EP) criteria (Marcus et al. 2010). Additionally risk stratification and decision making regarding primary prevention with an implantable cardioverter defibrillator (ICD) remain a significant clinical challenge given the morbidity associated with ICD implantation (Corrado et al. 2015, Zorzi et al. 2016).

8.2. Aim

The aim of this study was to use cardiac MRI with advanced late gadolinium enhancement using motion correction and gagetron reconstruction: LGE-CMR (Kellman & Arai 2012)and electrophysiological function (electrocardiographic imaging: ECGI) (Ramanathan et al. 2004) to study the structural and electrical substrates,patients with ARVC.

8.3. Hypothesis Addressed

Body surface and non-invasive ECGi mapping is able to identify non-invasive pre-clinical markers of disease, before established imaging modalities such as cardiac MRI and CT.

8.4. Methods

Refer to section 4.6

8.5. Results: Non-invasive ECG Imaging Of Arrhythmogenic Right Ventricular Cardiomyopathy Substrate.

Patient characteristics are shown in Tables 2-5. A wide spectrum of clinical phenotypes and mutations were studied.

8.5.1. Spectrum of Electrical Substrate At Rest

The normal epicardial activation pattern is well described (Ramanathan et al. 2004). The earliest epicardial activation appears as a breakthrough, most commonly in the anterior RV and the basal lateral LV is usually the latest region to activate. A representative control is presented in Figure 35, showing an activation pattern consistent with previously described work**.** As expected the normal sinus activation of this healthy adult hearts does not have regions of discontinuous conduction or fractionated EGMs.

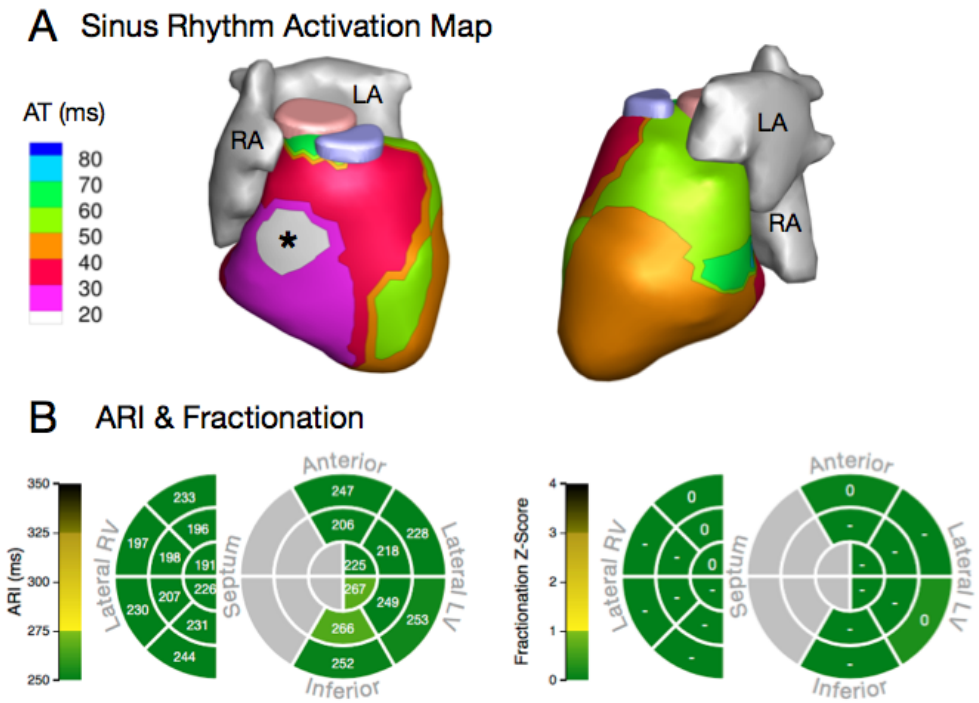

Figure 35. Control electrical substrate in a healthy young adult demonstrating (**A**) normal sinus activation with a typical RV epicardial breakthrough pattern marked by an asterisk and (**B**) normal ARI values and an absence of fractionated EGMs. Generally, the earliest epicardial activation appears as a breakthrough, most commonly in the anterior RV, and the basal lateral LV is usually the latest region to activate.

Figure 36 shows an example of ECGI reconstructions in a patient (patient 6) with advance disease and a high PVC rate. Abnormal epicardial breakthrough is seen (Figure 36. A) with earliest sinus rhythm breakthrough at the basal inferior LV. Compared to the control patient there is prolonged ARI (Figure 36. B), particularly in the RV where there is the presence of extensive late gadolinium enhancement(LGE) (Figure 36. C).

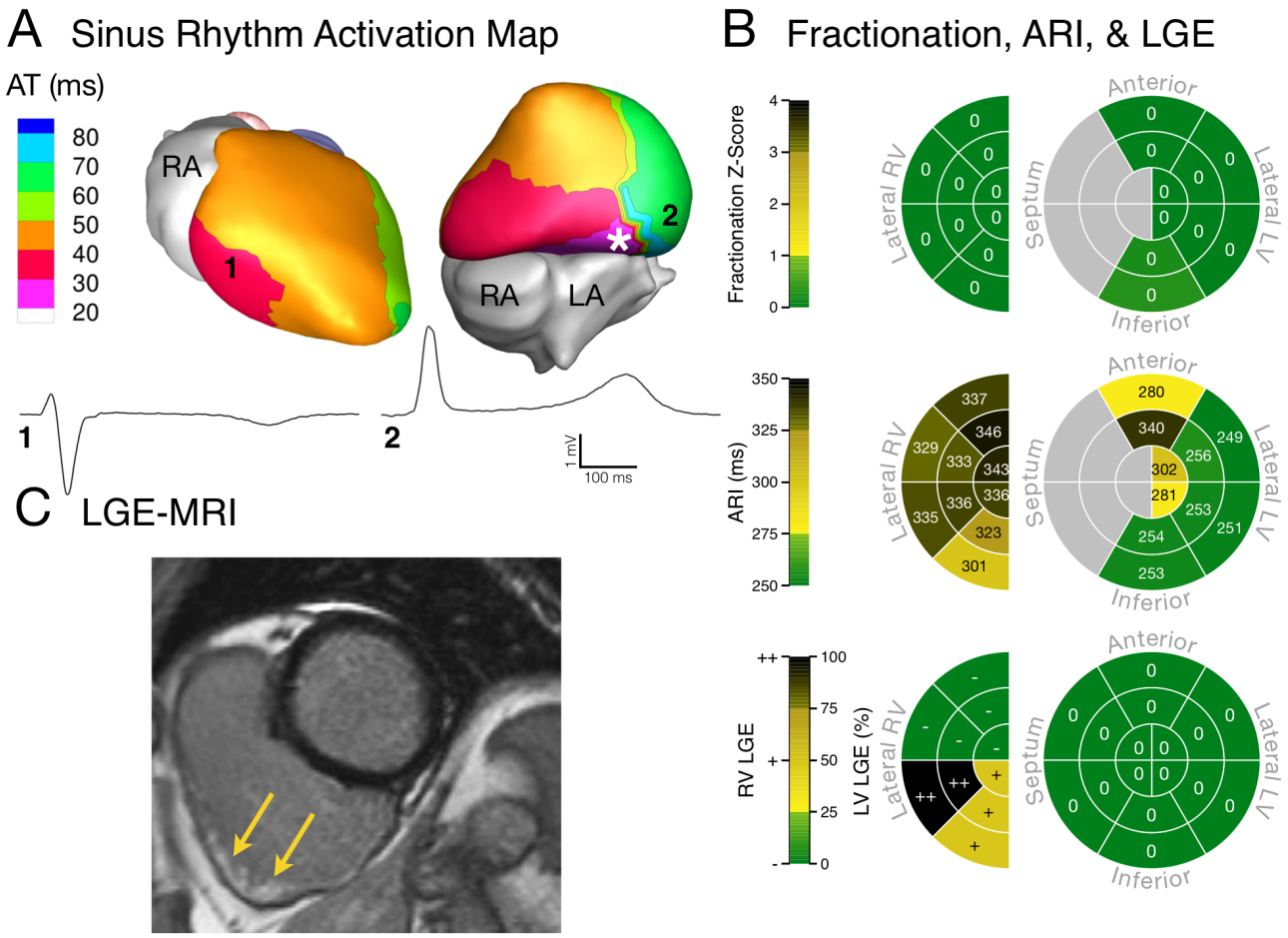

Figure 36. Electrical substrate of a patient (Pt 6) with advanced disease and a high PVC rate (18.69%). (**A**) abnormal epicardial breakthrough is seen, with earliest sinus rhythm ventricular epicardial activation originating from the basal inferior LV (marked by asterisk). (**B**) Substrate showed prolonged ARI, particularly in the RV, normal deflections, and a concentration of RV gad in the inferior RV. (**C**) MRI revealed extensive LGE, which was confined to the RV (indicated by yellow arrows), and RV. LGE values are presented as none (-), some (+), and high (++).

Figure 37 shows an example of ECGI reconstructions in a patient (patient 14) with biventricular disease and a PVC rate of 1.11%. Again abnormal epicardial breakthrough is seen from the basal lateral LV wall, with prolonged ARI's in both ventricles and the presence of fractionated electrograms and extensive LGE.

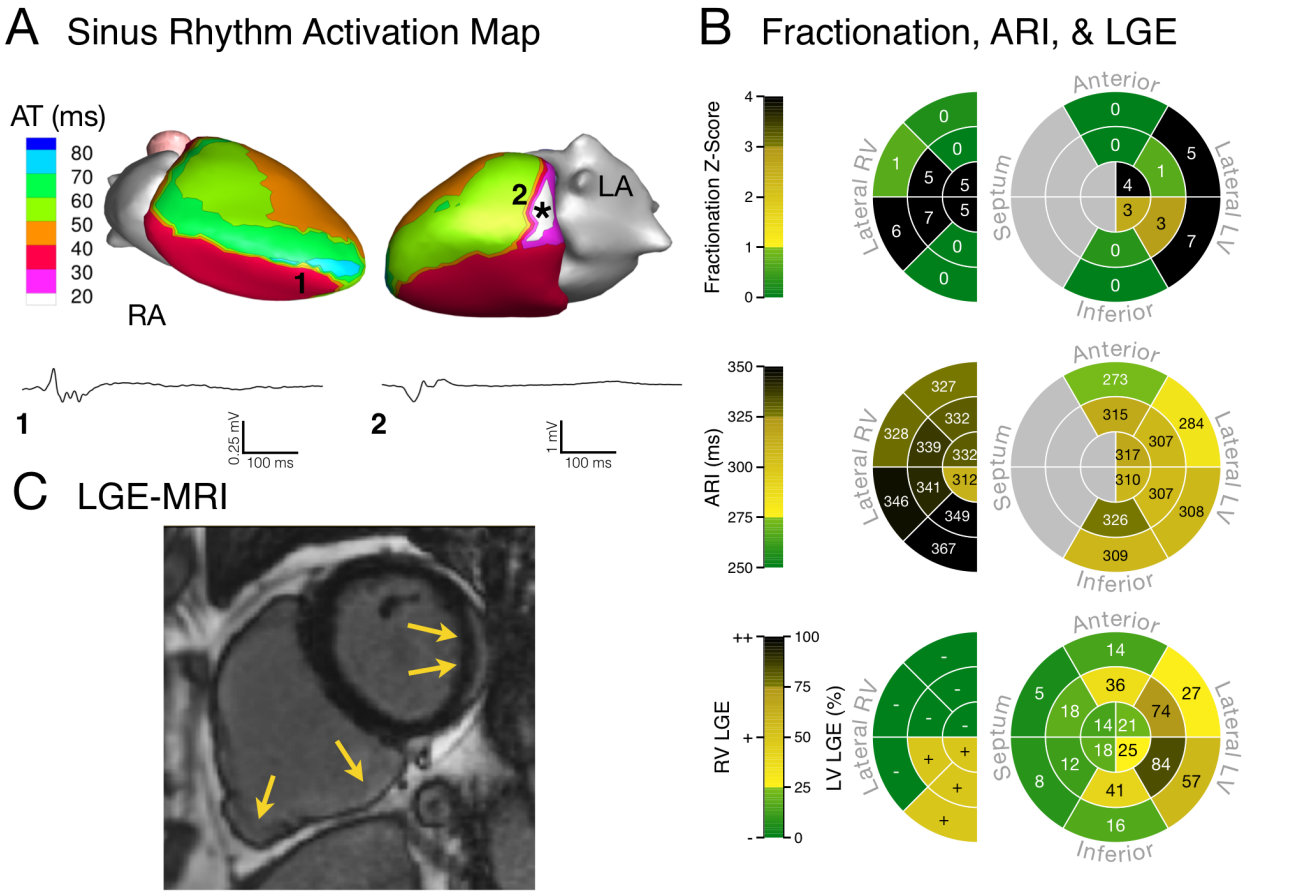

Figure 37. Electrical substrate of a patient (Pt 14) with biventricular disease and a moderate PVC rate (1.11%). (**A**) abnormal epicardial breakthrough, with earliest sinus activation originating from the basal lateral LV (marked by asterisk) is seen. (**B**) Substrate showed prolonged ARI in both ventricles, increased prevalence of fractionated electrograms, and extensive LGE. (**C**) MRI revealed extensive biventricular LGE (yellow arrows).

Figure 38. shows the ECGI reconstructions in a patient (patient 13), with early disease and no observed ectopy. Despite his pre-clinical manifestation, there is abnormal activation seen, with earliest breakthrough in the inferolateral RV with evidence of prolonged ARI on ECGI despite low amounts of LGE.

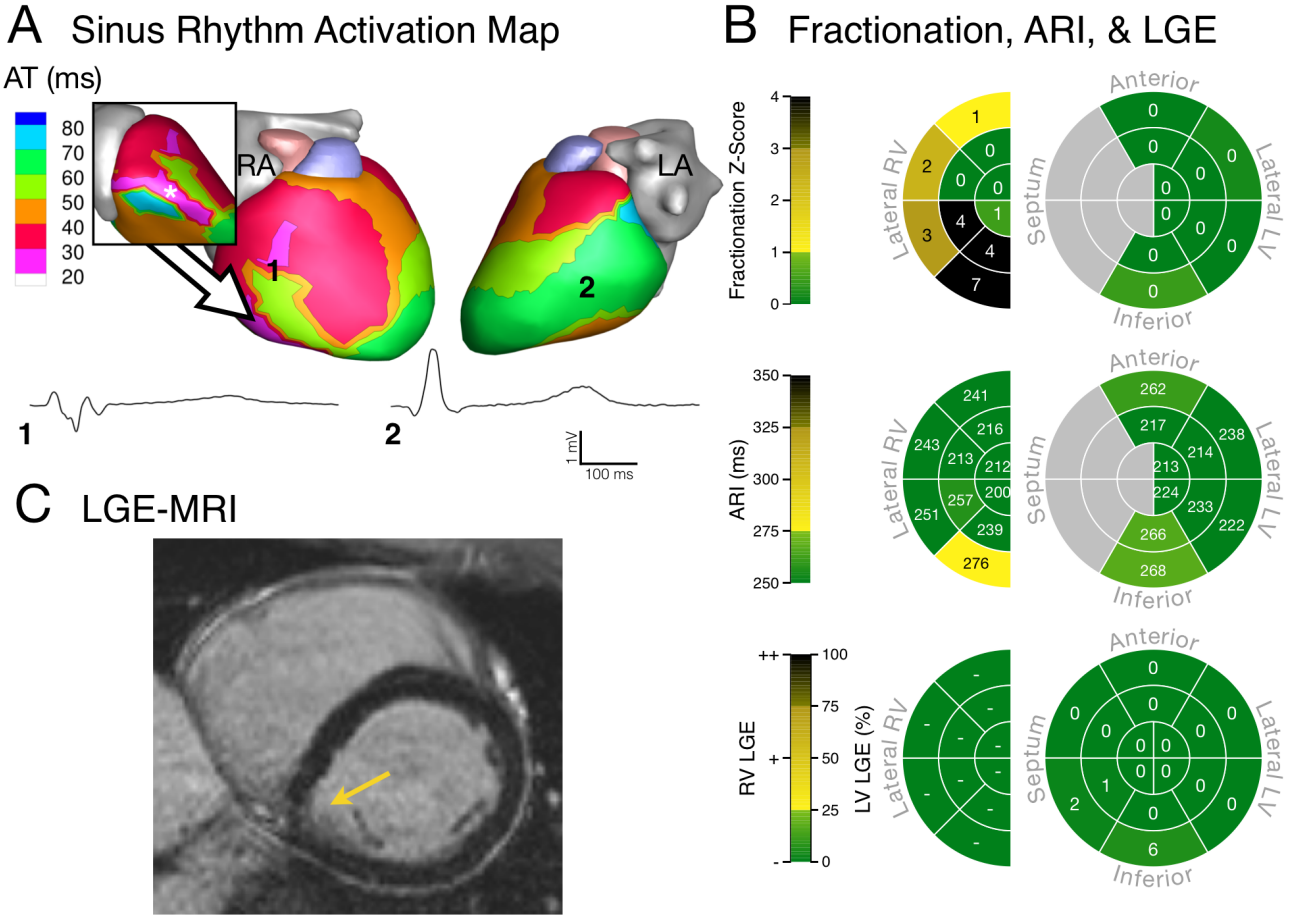

Figure 38. Electrical substrate of a 26 year-old male (Pt 13) with early disease and no recorded ectopy. (**A**) abnormal activation in the inferolateral RV (inferolateral breakthrough marked by asterisk in inset is seen. (**B**) Substrate showed prolonged ARI in both ventricles, significantly increased fractionation, but no/minimal LGE. (**C**) MRI revealed very small amounts of LV LGE, with no visible RV LGE.

When compared to controls patients (Table 9), ARVC patients displayed statistically longer total duration of epicardial activation (p = 0.007, Control: 42 [36-47] ms, ARVC: 52 [44-64] ms) and steeper mean epicardial gradients of AT (p = 0.018, Control: 0.24 [0.21-0.28] ms/mm, ARVC: 0.31 [0.26-0.37] ms/mm). Mean ventricular ARIs during sinus rhythm were significantly longer than control values (p = 0.014, Control: 241 [230-262] ms, ARVC: 275 [238-300] ms). While ARIs were prolonged in ARVC patients, increased spatial gradients of repolarization or total duration of epicardial depolarization were not observed. The presence of T-wave inversion on clinical ECG was a strong predictor of ARI prolongation (Table 10). ARVC patients with T-wave inversion had significantly longer mean ARI values than those without inversion (p = 0.010, With Inversion: 300 [269-313] ms, Without Inversion: 238 [231-262] ms).

Table 9. Electrical findings at baseline of controls vs ARVC patients

	Control			ARVC				
Parameter	**Median**	**Q1**	**Q3**	**Median**	**Q1**	**Q3**	**P**	**Significance**
Total Activation Time (msec)	42	36	47	52	44	64	0.007	**
Total Recovery Time (msec)	134	126	152	129	120	146	0.273	
Mean Epicardial ARI (msec, Fridericia Rate-Correction)	241	230	262	275	237	300	0.014	*
Mean Epicardial EGM Amplitude (mV)	2.28	2.00	3.03	2.58	1.69	2.96	0.735	
Mean Deflections Per-Electrogram	1.06	1.03	1.06	1.09	1.03	1.18	0.086	
Mean Epicardial Activation Time Gradient (ms/mm)	0.24	0.21	0.28	0.31	0.26	0.37	0.018	*
Mean Epicardial Recovery Time Gradient (ms/mm)	1.06	0.95	1.22	0.93	0.85	1.05	0.060	
Mean Epicardial ARI Gradient (msec, Fridericia Rate-Correction)	1.17	1.07	1.38	1.21	1.05	1.48	1.000	

Median, quartiles, and Wilcoxon rank sum comparison of ECGI EP parameters in healthy adults (Controls) and ARVC patients. Highlighted rows (yellow) indicate statistically significant differences between Control and ARVC groups.

Significance levels:
*** p < 0.001
** p < 0.01
* p < 0.05

Q1: First Quartile
Q3: Third Quartile

Table 10. ARI findings control patients vs ARVC with and without T-wave inversion

Controls					ARVC: T-Wave Inversion					ARVC: No T-Wave Inversion				
Median	**Q1**	**Q3**	**Min**	**Max**	**Median**	**Q1**	**Q3**	**Min**	**Max**	**Median**	**Q1**	**Q3**	**Min**	**Max**
241	230	262	206	274	300	269	313	218	330	238	231	262	226	285

Median, quartiles, Range, and Wilcoxon rank sum comparison of resting ARI (Fridericia rate-correction applied) in Controls and ARVC patients with and without T-Wave Inversion. Group difference ARVC with T-Wave Inversion is significantly different than controls at p < 0.001 level and ARVC without T-Wave Inversion at p < 0.01 level.

Q1: First Quartile
Q3: Third Quartile
Min: Minimum value observed in group
Max: Maximum value observed in group

8.5.2. Effect of Exercise

Mean epicardial ARI shortened during and post exercise ($p < 0.001$, Rest: 275 [235-313] ms, Exercise: 186 [173-203] ms). Total RT ($p < 0.001$, Rest: 130 [120-150] ms, Exercise: 186 [173-203] ms) and mean epicardial RT gradients ($p = 0.002$, Rest: 0.94 [0.87-1.06] ms/mm, Exercise: 0.70 [0.60-0.88] ms/mm) also decreased. Total AT, mean epicardial AT gradients, and fractionation were unaffected by exercise. Comparing patients with two or more major diagnostic criteria against patients with less than two major diagnostic criteria for ARVC, there was no significant change in the AT shortening on exercise (delta of mean AT) (-3.8ms vs -6.8ms, <2 vs >2, $p =0.13$), but a significantly different delta of ARI (-29ms in <2 major criteria patients, vs -68ms in >2 major criteria patients, $p=0.001$) and a significantly different delta RT (-59ms in <2 major criteria patients vs -138ms in >2 major criteria patients, $p<0.001$).

8.5.3. MRI Findings

LGE was found in 72% of ARVC patients. Three patients had isolated RV LGE, seven had isolated LV LGE, three had biventricular LGE, and five had no scar. Six patients in the study cohort had no Task Force CMR defects. Of these six, three had visible LV LGE. Electrical substrate correlations to the MRI findings are shown in Table 11.

Table 11. ECGI electrical substrate correlations to CMRI Late Gadolinium Enhancement

LV

Parameter	CC	P	Significance
EGM Amplitude	-0.42	< 0.001	***
Deflections Per-EGM	0.52	< 0.001	***
AT Spatial Gradient	0.24	0.001	**
Resting ARI	0.29	< 0.001	***
Exercise ARI	0.10	0.190	
RT Spatial Gradient	-0.09	0.232	
ARI Spatial Gradient	0.05	0.485	
Exercise ARI Shortening	0.31	< 0.001	***

RV

Parameter	CC	P	Significance
EGM Amplitude	-0.02	0.755	
Deflections Per-EGM	-0.05	0.472	
AT Spatial Gradient	-0.15	0.051	
Resting ARI	0.30	< 0.001	***
Exercise ARI	0.17	0.027	*
RT Spatial Gradient	-0.05	0.502	
ARI Spatial Gradient	-0.10	0.197	
Exercise ARI Shortening	0.36	< 0.001	***

Spearman correlation coefficients of LV LGE and EP substrate parameters. Highlighted rows (yellow) indicate statistically significant correlations between LV LGE and EP substrate parameters.

Significance levels:
*** $p < 0.001$
** $p < 0.01$
* $p < 0.05$

8.5.4. Ectopy

Ventricular ectopy occurred more frequently as heart rate increased following exercise. PVCs were observed in fifteen of twenty ARVC patients, with a total of 41 distinct morphologies. The sites of earliest epicardial activation of the PVCs were spread across both ventricles, with greater involvement of RV and basal locations. Figure 39 shows the location of the ectopy and the number of ectopics within regions of the heart in all patients.

The PVC rate within anatomical segments correlated with repolarization abnormalities and RV scar. There was a positive correlation between resting ARI and PVC rate. Figures 40 and 41 show the temporal and spatial location and propagation of PVCs in two patients.

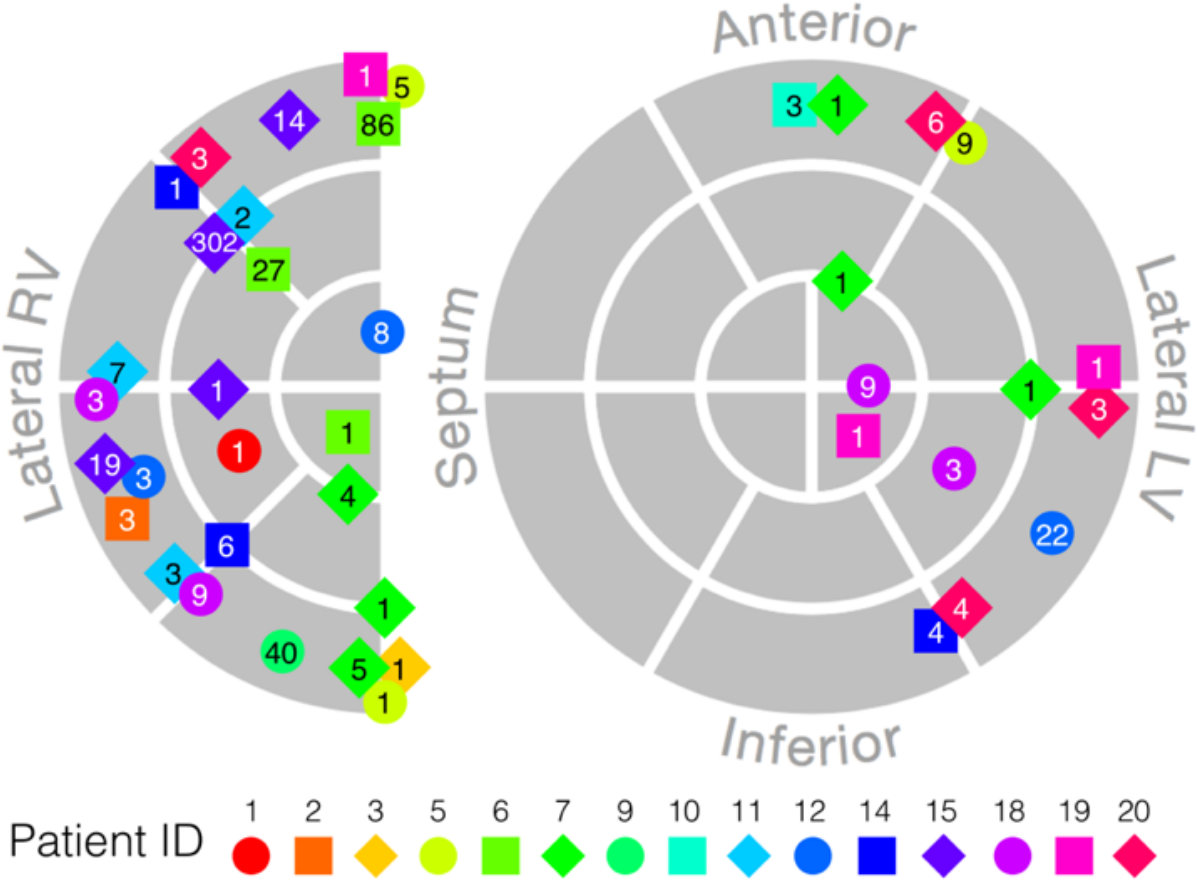

Figure 39. Number and location of ventricular ectopics seen in each patient within the study.

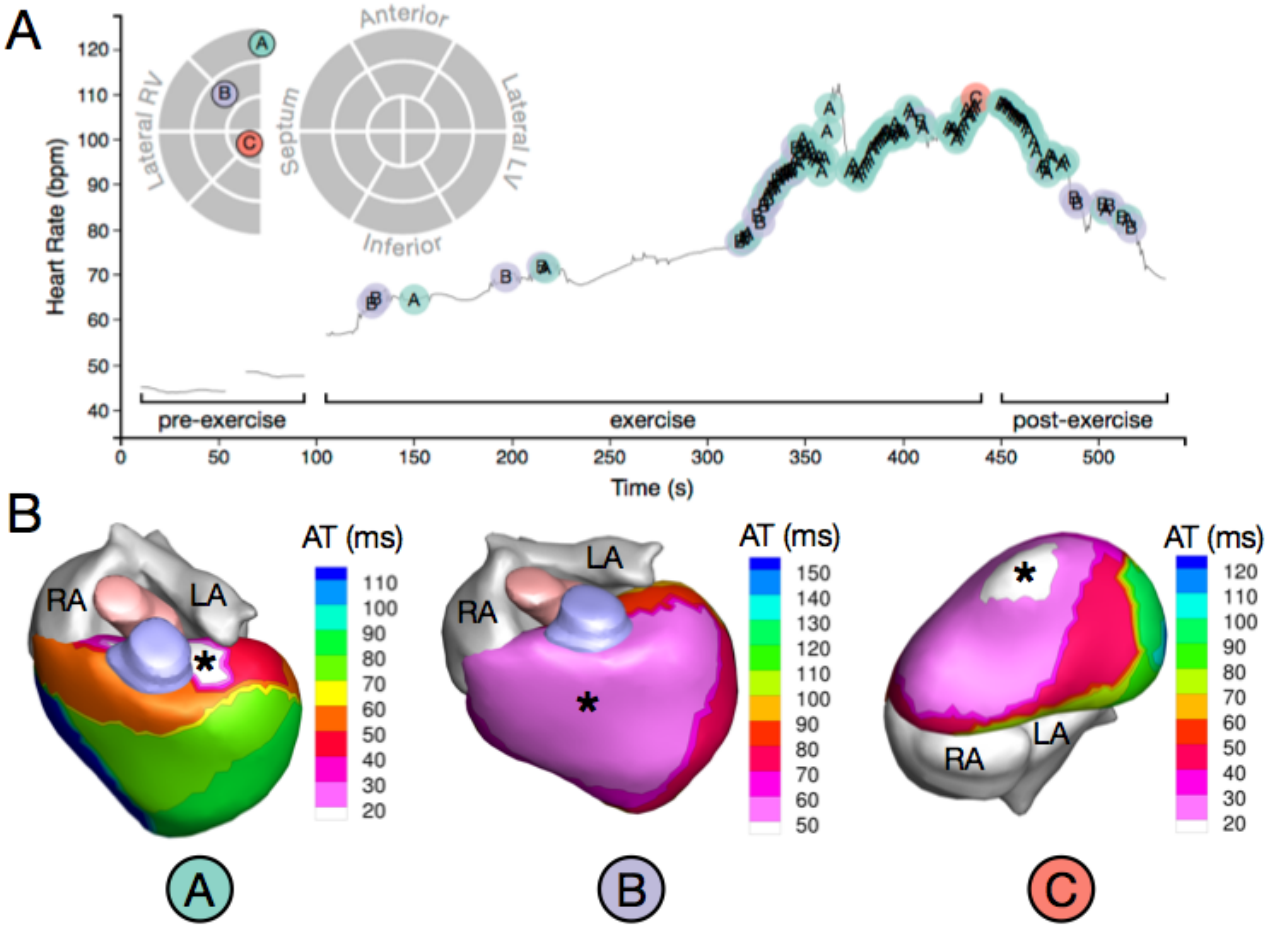

Figure 40. PVC onset and initiation sites of a patient (Patient 6) with a PVC burden 18.69% at rest on Holter monitoring (**A**). (**B**) The different PVC initiation sites are labeled A, B, and C. PVCs occurred only after the onset of exercise as seen in the timeline graph. Morphology B showed very a broad region of early epicardial activation, indicating a possible sub-epicardial origin and possible conduction system involvement. PVC: premature ventricular contraction. HR: heart rate. AT: activation time. RA: right atrium. LA: left atrium. RV: right ventricle. LV: left ventricle. Asterisks indicate PVC initiation sites.

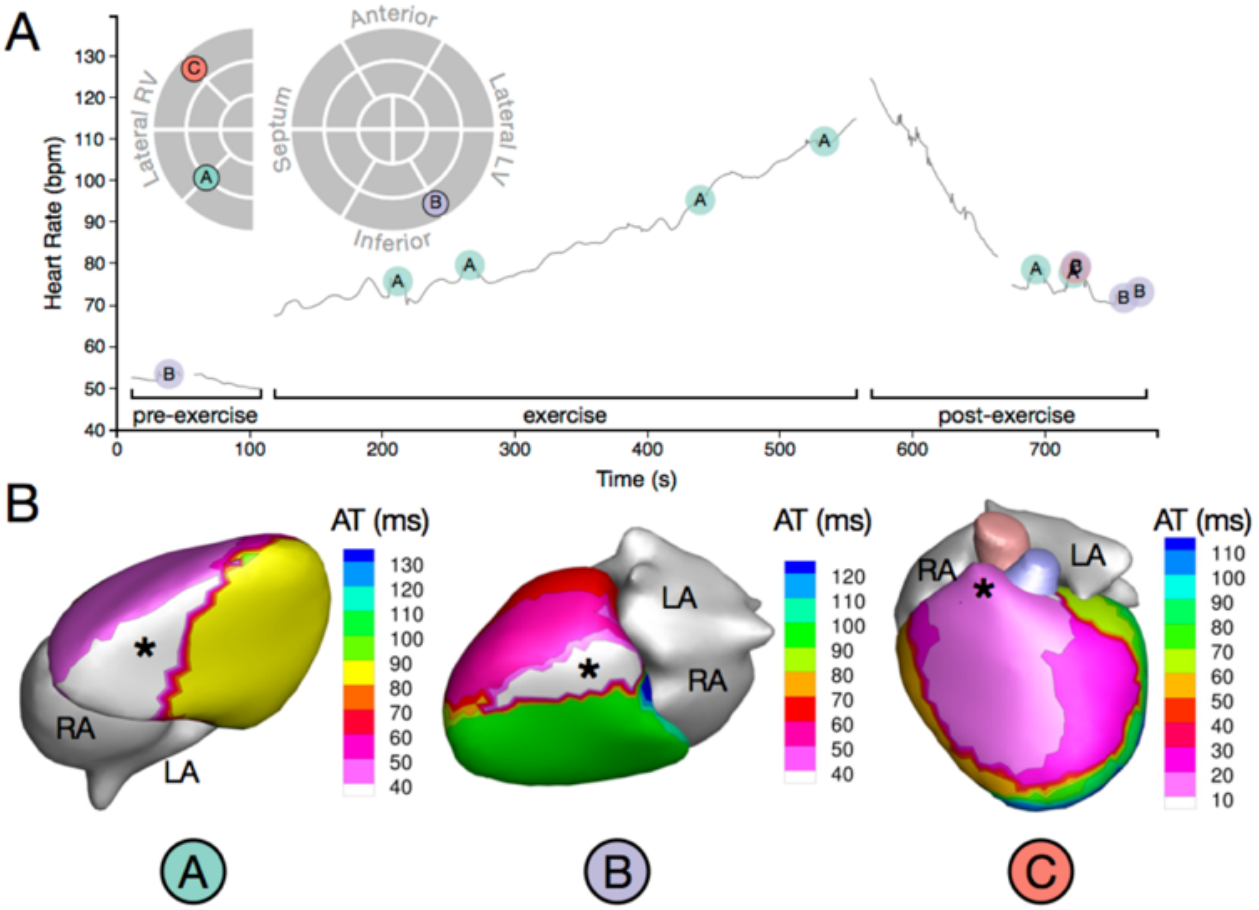

Figure 41. PVC onset and initiation sites of a patient (Patient 14) with a PVC burden 1% at rest on Holter monitoring. (**A**) The different PVC initiation sites are labeled A, B, and C. (**B**) Activation isochrone maps of the three distinct PVC morphologies observed in this patient. PVC: premature ventricular contraction. HR: heart rate. AT: activation time. RA: right atrium. LA: left atrium. RV: right ventricle. LV: left ventricle. Asterisks indicate PVC initiation sites.

8.6. Discussion

This is the first study of ECGI with anatomical MRI in patients with ARVC to characterize the electrophysiological and scar substrates in ARVC patients with a broad spectrum of disease expression. When compared to controls ARVC patients had significant prolongation in activation and depolarization time. We also highlight the role of exercise in increasing PVC rate and initiating PVC triggers, perhaps highlighting the mechanism of ayrrhythmogrenisis in this disease.

8.6.1. Prolongation Of AT And ARI

Dynamic conduction and repolarization delay have previously been demonstrated in patients with ARVC (Gomes et al. 2012; Finlay et al. 2014). The data are consistent with these findings demonstrating prolongation of activation and ARI in these patients when compared to controls. The mechanism for conduction delay is likely a combination of reduced expression of Cx43 (Gomes et al. 2012) and a loss of sodium channel density as a result of poor trafficking (Lodder & Rizzo 2012; Delmar & McKenna 2010). Prolongation of ARI may also occur as a result of abnormalities in trafficking of channels that are responsible for regulation of repolarization. It is known that Kv1.5 channels localise to the intercalated disc, and associate with Na1.5 (Mays et al. 1995; Milstein et al. 2012). Additionally function of Kv1.5 is dependant on N-cadherin, an intercalated disc protein (Cheng et al 2011). Thus this abnormal trafficking may prolong ARI, in a similar manner to mutations in KCNE2 which cause similar Kv1.5 trafficking inhibition and result in prolonged APD (Roepke et al. 2008). This may certainly explain the clinical finding of arrhythmia in patients without significant structural disease in ARVC.

In patients with more advanced disease, heart failure induced abnormal calcium handling may play a more important role in ARI prolongation (Aiba et al. 2009), through a decrease in the amplitude and a reduction in the rate of decay of the calcium transient (Roepke et al. 2008, Aiba et al. 2009). Additionally a significant amount of potassium channel remodelling occurs in heart failure, including a reduction in the inward rectifier I_{K1} (Rose et al. 2005), downregulaiton of Ito (Beuckelmann et al. 1993), and reductions in both I_{Kr} and I_{Ks} (Tsuji et al. 2000). Additionally cellular uncoupling may also prolong

ARI through a reduction in electronic forces (Viswanathan et al. 1999) secondary to fibrofatty replacement within cells and a reduction in the number and size of gap junctions within the intercalated disc (Delmar & McKenna 2010).

In this study ARI prolongation correlated with the presence of LGE suggesting that the uncoupling effect of scar plays a major role. This may also explain the significant ARI shortening on exercise as both increased heart rate and sympathetic activation of the myocardium have a greater effect in electrically uncoupled tissue.

8.6.2. PVC's With Exercise

ECGI allowed localisation of PVCs in a single beat, through the ability to map panoramically in ARVC. The overall rate of PVCs was increased by exercise. It was found that PVC rate correlated with local ARI prolongation, especially ARI at elevated HR after exercise. We also found that RV LGE was correlated with local PVC rate. All six patients with visible RV scar had at least one PVC with earliest epicardial activation in the RV. Low voltage and LV LGE both trended toward increased PVC rate, but the correlations were not statistically significant. No relationship between EGM fractionation and PVC rate was found.

Previous studies have demonstrated conduction slowing at elevated heart rates in ARVC patients (Finlay et al. 2014). The combination of scar, slow conduction and prolonged ARI could facilitate unidirectional block and reentrant arrhythmia.. In the present study, we found evidence of slow conduction in the form of longer total activation times and steeper activation gradients relative to controls. However, we did not demonstrate the dynamic conduction slowing at elevated heart rates previously reported (Finlay et al. 2014). This is likely due to the fact that Finlay et al (Finlay et al. 2014), were able to invoke conduction velocity restitution at rates close to the ERP of the ventricle, whereas we limited exercise to a maximum heart rate of 120bpm.

EGM fractionation and late potentials are commonly seen in reentrant VT circuits as part of the critical isthmus. We did not observe late potentials in the reconstructed EGMs . This is in contrast to ECGI studies of post-infarction scar-related VT, which found a high prevalence of late potentials with re-

entry circuits closely related to the EP substrate (Zhang et al. 2016). This may reflect significant differences in the anatomy of the scar in each population. Post-infarction scar is heterogeneous, with large islands of surviving myocardium, especially and border zone. In ARVC scar substrate accumulates over time and is often diffuse, originating initially from the epicardium. Additionally patients with ARVC may be prone to VF and fixed scar substrate initiating re-entrant VT may not predominate in these patients. It is possible our findings highlight the dynamic APD changes that occur with ARVC; particularly in early disease where sudden death is the predominant phenotype due to VF; that may promote wave break in the steep portion of the restitution curve and chaotic electrical activity that promotes VF due to non linear dynamics. It is possible that the lower regional density of surviving myocardium in ARVC scar makes it difficult to resolve late potentials in ECGI mapping of ARVC patients. This may be a limitation of the ECGI technique in such substrates as it may not be possible to resolve fractionated electrograms in this disease with ECGI technology. There are clear limitations and assumptions made with this technology, whereby the inverse solution is applied without accounting for different compositions of the body tissue, and error in lead positions and geometry may be magnified by the mathematical equations involved. Additionally in global low voltage tissue as seen in some patients with ARVC there may be limitations in the resolution of the electrograms in delineation of fractionation.

It is likely that focal mechanisms may cause arrhythmia triggers in ARVC patients. Focal triggered activity is commonly observed in isolated myocytes. EADs at plateau potentials are caused by recovery and re-activation of Ica, with the delayed rectifier currents, Ikr and Iks, playing an important role (Aiba et al. 2009). It was observed that PVC rate correlated with regions of prolonged ARI, especially during exercise when Ica is augmented by beta-adrenergic stimulation. APD prolongation increases the window for Ica re-activation and EAD formation. In the intact heart, electrotonic coupling between myocytes prevent conduction of EAD and DAD activity. Reduced coupling, caused by scar and gap junction abnormalities in ARVC, can increase the likelihood of focal activity. The observed correlation between RV scar and PVC rate suggests that an uncoupling effect is present at the PVC initiation sites.

8.6.3. Clinical Implications

This study has important clinical implications through demonstrating the ability to non invasively study the electrical substrate in patients with ARVC. We were able to demonstrate changes in AT and ARI in patient with both clinically manifest and pre-clinical disease. Given the challenge in diagnosing these patients this may prove to be a valuable method in distinguishing patients with disease and an aid to the present task force criteria (Marcus et al. 2010). This may prove useful in assessing disease progression with long term follow up, through the ability to perform repeat scanning and assess changes to the electrical phenotype. Finally, dynamic assessment of large scale cohorts of patients, with follow up data may help provide better electrical markers of risk prediction which may guide ICD implantation.

Additionally we were able to accurately locate the site of ventricular ectopy using a single beat non-invasively. This may prove useful in patients with ventricular arrhythmia where targeted ablation of critical substrate is required.

8.7. Limitations And Conclusions

The patients selected are a wide spread cohort with a varied clinical and genetic phenotype. However, larger scale studies are required to assess both the individual patient electrical characteristics, but also to try to highlight differences in electrical phenotype based on clinical features and genetic mutations. It may be that electrical parameters vary with genetic mutation, as well as progression and changes in electrical substrate over time. Additionally this pilot study was not powered to assess risk stratification, and indeed none of the patients in this study had a prior history of ventricular arrhythmia or ICD implantation. Therefore larger scale studies are needed both to segregate the electrical phenotype in more detail but also to look at risk markers in detail.

This is the first study of ECGI in ARVC and involved looking at a broad spectrum of disease. The main findings were of prolongation of AT and ARI in patients with both clinical and pre-clinical or early disease. Additionally we were able to localise sites of ventricular ectopy in these patients. Larger scale studies are required to delineate the role of ECGI in these patients, both in terms of assessing the

electrical phenotype and its progression to aid diagnosis, but also to understand its role in risk prediction.

Chapter 9

Overall Discussion

9.1. Summary Of Achievements

This thesis sought to bridge the gap between our basic cellular understanding of cardiac electrical activity and in-vivo contact intracardiac electrogram findings in order to better understand the surface ECG. The aim was to better understand intracardiac repolarization and its relation the surface ECG T-wave in order to identify potential biomarkers of cardiac risk.

Human studies in normal heart patients, enabled me to define the normal regional AT, APD and RT response to varying activation wavefronts within the heart. I was able to demonstrate that epicardial APD was shorter than endocardial APD, and that there were small difference in APD between the base and apex of the heart, with the base having a shorter APD, in both the right and left ventricle. During normal endocardial stimulation of the heart this resulted in minimal transmural and apicobasal repolarization differences. However, epicardial stimulation of the heart created significant transmural as well as apicobasal RT differences within nearby regions, primarily driven by the interplay between APD differences and AT delay during epicardial stimulation. These findings have important implications both as valuable data for animal experimental and computational modelling within the heart (Bergfeldt et al. 2017); as there is a paucity of true intact human data within the literature; but also in understanding the mechanism of arrhythmogenesis in patients with structurally normal hearts and additionally the potential acute changes to the cardiac AT-RT coupling during ectopy and CRT pacing (Lopez et al 2017).

I have then used this data to understand the association between intacardiac repolarization and the body surface T-wave, by simultaneously recording the body surface 12-lead ECG in patients. Though several markers of repolarization including QT interval (Chugh et al. 2009; Kinoshita et al. 2012; Zhang et al. 2011), JT interval (Crow et al. 2003) and Tpeak-Tend(TpTe) (Panikkath et al. 2011; Letsas et al. 2010; M. Shimizu et al. 2002), have been associated with an increased risk of cardiac events, little is known about how they reflect actual repolarization in the intact heart. Apicobasal repolarization wavefronts differences within the heart have been shown in several studies (Burgess et al. 1972; Cohen et al. 1976; T. Watanabe et al. 1985; Autenrieth et al. 1975; Franz et al. 1987) and are thought to form

the morphology of the body surface T-wave, however, others studies have demonstrated transmural gradients (Spach & Barr 1975; Antzelevitch et al. 1998; Yan & Antzelevitch 1998; Franz et al. 1987), and have suggested that T-peak and T-end of the surface ECG represents this transmural dispersion of repolarization (Yan & Antzelevitch 1998). I have shown that the morphology of the T-wave on the precordial leads of the body surface ECG is governed by the predominant morphology of the unipolar T-wave in the underlying myocardium of the precordial leads, with V1-2 predominantly displaying a similar T-wave morphology to the unipolar contact electrograms recorded in the right ventricle, and V5-6 predominantly displaying a similar morphology to the unipolar electrograms recorded in the left ventricle. With this being the case, when using the Wyatt method (Haws & Lux 1990) to measure intracardiac repolarization, it would seem logical that local intracardiac repolarization times would lie along the upslope of the precordial body surface T-wave as I have demonstrated. Thus the upslope of the T-wave in V1-2 reflects intracardiac repolarization in the right ventricle, while the upslope in V5-6 represents intracardiac repolarizaiton in the left ventricle regardless of polarity as I have demonstrated. There was no good correlation between the T-wave and transmural or apicobasal differences within the heart. The reason for this discrepancy between our study and previous work lies in the experimental methods. I have used intact human heart studies, where the upslope of the body surface T wave represents a summation of local repolarization in the underlying myocardium, while the downslope represents a summation of far field components. The polarity of the body surface T-wave is thus governed by the balance between the repolarization times of the far-field tissue and the near field tissue; where the far field depolarises earlier, there is an initial downslope followed by an upslope resulting in an inverted body surface T-wave, while early local repolarization results in an initial upslope and an upright T-wave. Other experimental setups have used wedge tissue, where there is no true far field versus near field influence on the surface ECG T-wave, or animal preparations where there are predominant apicobasal differences which I have shown are not present in the intact human heart.

I then went on to study the APD characteristics of patients with abnormal ventricular myocardium, to discern what happens to APD in patients with myocardial scar, and how this interacts with AT to influence RT and possibly arrhythmogenicity. I have demonstrated that regardless of pathology

myocardial scar results in a prolongation of APD compared to tissue with normal voltage in individual patients. Additionally the pattern of scar therefore determines the transmural APD differences across the tissue, but in general scar predominantly decreases the transmural differences in APD, due to preferential epicardial APD lengthening. This therefore results in significant regional and transmural differences in repolarization, which may provide the mechanism for arrhythmia initiation through the creation of functional block. This was demonstrated in one patient, where extra-stimuli testing resulted in an increase in repolarization dispersion both across the epicardium in closely separated neighbouring locations and also transmurally. In this patient sustained monomorphic VT was mapped to this region of repolarization dispersion and epicardial and endocardial ablation of this region resulted in non-inducablilty of VT. Although not powered to assess the role of repolarization dispersion in initiating arrhythmogenisis, the findings of this work confirm our conceptual understandings from previous experimental work while aiding future experimental and modelling studies in providing a reference for expected APD changes in the intact structurally abnormal human heart. The role of repolarization dispersion in arrhythmia initiation requires further assessment in clinical studies but provides an interesting target for substrate modification in patients where VT is non-inducible or too unstable to map.

Finally I used non-invasive ECGI mapping to study patients with ARVC with a spectrum of disease phenotypes. In keeping with my invasive studies I have demonstrated prolonged APD in regions of structural tissue abnormalities. An important finding was the ability to show prolonged APD in patients where there was an absence of myocardial scar on CMRI imaging, and also in regions of the heart where there was an absence of scar detected on CMRI. This may therefore prove to be an important tool in the diagnosis and assessment of disease progression in patients with ARVC. Further studies are require to assess the role of the body surface ECG and ECGI in both disease screening/progression and also risk prediction. I also showed that APD was prolonged in regions where ventricular ectopy occurred on exercise. Again this is in keeping with my invasive mapping study in VT where VT initiation occurred in a region of dynamic APD prolongation, and may again provide a useful mechanism to predict ventricular ectopy for targeted ablation.

As part of of my work, I have also been involved in the creation of a computational program for large volume data analysis, as well as advanced statistical and data analysis methods which not only serve as a guide for further such research, but can be developed further and implemented into clinical software tools to improve patient care.

9.2. Further Work

This thesis provides a basic understanding of the APD properties of the normal and structurally abnormal heart in the intact human. In addition an explanation of the polarity of the body surface precordial ECG T-wave is provided, along with evidence correlating the upslope of the T-wave to intracardic repolarization. Finally a novel non-invasive electroanatomic mapping method ECGI has been demonstrated as a method of non-invasive ECG assessment of disease. All of these four pillars of work, have scope to be further developed and will form the cornerstone of my further work.

Although I have provided assessment of APD differences within the normal and abnormal ventricle, the data has been limited by the fact that I have used decapolar catheters in strategic positions to make linear assessments of APD and have been unable to provide panoramic mapping of the ventricle. The next step to take this work further will be to integrate the Wyatt method into 3D electroanatomic mapping systems directly, to allow integrated mapping of AT and APD, thus providing assessment of total repolarization time. Electroanatomic mapping systems take several thousand points within the ventricle, and this assessment would provide a far better spatial representation of repolarization differences within the ventricle than the present linear studies I have performed. The pioneering work of Alessie et al (Allessie et al. 1976) and the group of Moe (Han & Moe 1964), has shown that APD heterogeneity which is critical to development of functional block and reentry, occurs over relatively small areas of space often in the region of 25mm^2 (Allessie et al. 1976). Present mapping systems lack this resolution, either because they use conventional wide spaced mapping catheters where the assessment of myocardial scar in inaccurate and the bipolar signal is often different to those of narrow

spaced bipolar (Anter et al. 2015), or because they use mapping catheters such as the PentaRay® (Biosense Webster, Baldwin Park, CA), where the operator has no control over spline orientation and therefore any meaningful assessment of directionality is lost. This dependance of the bipolar electrogram on orientation may be obviated by the use of omnipolar mapping strategies (Magtibay et al. 2017), with newer catheters such as the HD Grid (Abbott, St. Paul, MN), which contains 16 electrodes in a 4-by-4 unipolar electrode array, containing 1mm diameter electrodes at 4mm equidistant spacing. The design of this catheter not only allows the operator to map at the regional planar density specified by Alessie et al. (Allessie et al. 1976), but also contains narrow 4mm spacing and the capacity to incorporate omnipolar bipolar maps in order to determine the 'true' bipolar signal. Future iterations of this catheter involving 56 electrodes may provide the further density that is required to map small channels of conduction within critical isthmus'. This data could be incorporated into vector and conduction velocity algorithms, along with integration of unipolar APD data, to provide a more in-depth assessment of the myocardial substrate, potentially delineating critical isthmus' without the need to induce VT in patients. Our group is currently in the process of collecting pilot data using this system in order to provide assessment of global ventricular repolarization. Additionally this global mapping data could be coupled with body surface ECG data to further validate my work of the relationship of the body surface T-wave to intracardiac repolarization.

Given my findings relating to the regionality of the surface T-wave to intracardiac repolarization, I am currently assessing a risk marker based on this relating to dispersion of repolarization, on a cohort of patients with Brugada syndrome who underwent ajmaline testing. I will also test this marker on a cohort of patients with Long-QT syndrome who underwent exercise stress testing. Additionally I will also begin assessing this marker in patients with ischemic heart disease, both those who are due for ICD implant, but also assessing patients who present with out-of-hospital cardia arrest and have a pre arrest or first ambulance presentation ECG. Finally, although I have shown that the precordial 12-lead body surface ECG T-wave represents right to left dispersion of repolarization, I have also shown that the apical region of the ventricle and the posterior ventricle have poor repolarization representation on the 12-lead ECG T-wave. Thus in order to find a true body surface T-wave representation of global

ventricular repolarization, I have developed a modified ECG containing fifteen bespoke precordial ECG leads, which I will validate during global ventricular mapping studies using the HD Grid (Abbott, St. Paul, MN) mapping catheter, to show that these additional leads can be used to provide a more global field of cover. This may then be used to provide a more in-depth body surface representation of global ventricular repolarizaiton, without the need for expensive, MRI/CT studies and commercial ECGI mapping vests, and may improve the accuracy of my body surface repolarization dispersion index as a risk marker.

Finally given the work assessing ARVC substrate using non-invasive ECGI, the next step is to assess patients in large scale disease cohorts, not only to look at non-invasive electrical phenotypes and disease characterisation, but also to look at dynamic substrate behaviour as a marker of risk of arrhythmic events. At present, the research platform of ECGI is too slow to allow mass analysis of such a large scale clinical study and the commercial platform is both too expensive and lacks useable clinical features that can be integrated to assess risk. However, as with all technological advances, the speed of computing and the features will only advance with time, while costs will decrease.

We are on the precipice of being able to understand the role of dynamic APD heterogeneity invasively and non-invasively in disease substrate, and its rightful role as the forgotten important critical player in the genesis of lethal arrhythmia is about to be revealed.

10. Bibliography

Acar, B. et al., 1999. Spatial, temporal and wavefront direction characteristics of 12-lead T-wave morphology. *Medical & Biological Engineering & Computing*, 37(5), pp.574–584.

Adabag, A.S. et al., 2010. Sudden cardiac death: epidemiology and risk factors. *Nature Reviews Cardiology*, 7(4), pp.216–225.

Aiba, T. et al., 2009. Electrophysiological Consequences of Dyssynchronous Heart Failure and Its Restoration by Resynchronization Therapy. *Circulation*, 119(9), pp.1220–1230.

Aimond, F. et al., 1999. Ionic basis of ventricular arrhythmias in remodeled rat heart during long-term myocardial infarction. *Cardiovascular Research*, 42(2), pp.402–415.

Akar, F.G., 2002. Unique Topographical Distribution of M Cells Underlies Reentrant Mechanism of Torsade de Pointes in the Long-QT Syndrome. *Circulation*, 105(10), pp.1247–1253.

Allessie, M.A., Bonke, F.I. & Schopman, F.J., 1976. Circus movement in rabbit atrial muscle as a mechanism of tachycardia. II. The role of nonuniform recovery of excitability in the occurrence of unidirectional block, as studied with multiple microelectrodes. *Circulation Research*, 39(2), pp.168–177.

Allessie, M.A., Bonke, F.I. & Schopman, F.J., 1977. Circus movement in rabbit atrial muscle as a mechanism of tachycardia. III. The "leading circle" concept: a new model of circus movement in cardiac tissue without the involvement of an anatomical obstacle. *Circulation Research*, 41(1), pp.9–18.

Anderson, K.P. et al., 1993. Criteria for local myocardial electrical activation: effects of electrogram characteristics. *IEEE Transactions on Biomedical Engineering*, 40(2), pp.169–181.

Anter, E., Tschabrunn, C.M. & Josephson, M.E., 2015. High-Resolution Mapping of Scar-Related Atrial Arrhythmias Using Smaller Electrodes with Closer Interelectrode Spacing. Circulation: Arrhythmia and Electrophysiology, 8(3), pp.*CIRCEP*.114.002737–545.

Anter, E., Tschabrunn, C.M. & Josephson, M.E., 2015. High-Resolution Mapping of Scar-Related Atrial Arrhythmias Using Smaller Electrodes with Closer Interelectrode Spacing. *Circulation: Arrhythmia and Electrophysiology*, 8(3), pp.CIRCEP.114.002737–545.

Antzelevitch, C., 2000. Electrical Heterogeneity, Cardiac Arrhythmias, and the Sodium Channel. *Circulation Research*, 87(11), pp.964–965.

Antzelevitch, C., 2001. Transmural dispersion of repolarization and the T wave. *Cardiovascular Research*, 50(3), pp.426–431.

Antzelevitch, C. & Dumaine, R., 2011. *Electrical Heterogeneity in the Heart: Physiological, Pharmacological and Clinical Implications*, Hoboken, NJ, USA: John Wiley & Sons, Inc.

Antzelevitch, C. et al., 1998. Cellular basis for QT dispersion. *Journal of Electrocardiology*, 30 Suppl, pp.168–175.

Antzelevitch, C. et al., 1991. Heterogeneity within the ventricular wall. Electrophysiology and pharmacology of epicardial, endocardial, and M cells. *Circulation Research*, 69(6), pp.1427–1449.

Antzelevitch, C. et al., 2009. Is there a significant transmural gradient in repolarization time in the intact heart?: Cellular Basis of the T Wave: A Century of Controversy. *Circulation: Arrhythmia and Electrophysiology*, 2(1), pp.80–88.

Anversa, P. and Nadal-Ginard, B., 2002. Myocyte renewal and ventricular remodelling. *Nature*, 415(6868), p.240.

Attwell, D. et al., 1979. The steady state TTX-sensitive (?window?) sodium current in cardiac Purkinje fibres. *Pflgers Archiv European Journal of Physiology*, 379(2), pp.137–142.

Autenrieth, G., Surawicz, B. & Kuo, C.S., 1975. Sequence of repolarization on the ventricular surface in the dog. *American Heart Journal*, 89(4), pp. 463–469.

AVID Investigators, 1997. A comparison of antiarrhythmic-drug therapy with implantable defibrillators in patients resuscitated from near-fatal ventricular arrhythmias. The Antiarrhythmics versus Implantable Defibrillators (AVID) Investigators. *New England Journal of Medicine*, 337(22), pp.1576–1583.

Baba, S. et al., 2005. Remodeling in cells from different regions of the reentrant circuit during ventricular tachycardia. *Circulation*, 112(16), pp. 2386–2396.

Bacharova, L. et al., 2005. Where is the central terminal located? In search of understanding the use of the Wilson central terminal for production of 9 of the standard 12 electrocardiogram leads. *Journal of Electrocardiology*, 38(2), pp.119–127.

Bardy, G.H., 2005. Sudden Cardiac Death in Heart Failure Trial (SCD-HeFT) Investigators : Amiodarone or an implantable cardioverter-defibrillator for congestive heart failure. *New England Journal of Medicine*, 352, pp. 225–237.

Barthel, P. et al., 2003. Risk stratification after acute myocardial infarction by heart rate turbulence. *Circulation*, 108(10), pp.1221–1226.

Bass, B.G., 1975. Restitution of the action potential in cat papillary muscle. *The American journal of physiology*, 228(6), pp.1717–1724.

Basso, C. et al., 1996. Arrhythmogenic right ventricular cardiomyopathy. Dysplasia, dystrophy, or myocarditis? *Circulation*, 94(5), pp.983–991.

Bauer, A. et al., 2006. Deceleration capacity of heart rate as a predictor of mortality after myocardial infarction: cohort study. *Lancet*, 367(9523), pp.1674–1681.

Bean, B.P., 1985. Two kinds of calcium channels in canine atrial cells. Differences in kinetics, selectivity, and pharmacology. *The Journal of General Physiology*, 86(1), pp.1–30.

Behrens, S. et al., 1996. Dispersion of repolarization in the voltage domain: A novel approach to measure ventricular dispersion. Journal of the American College of Cardiology, 27(2), p.209.

Behrens, S. et al., 1998. Dispersion of Ventricular Repolarization in the Voltage Domain. Pacing and Clinical Electrophysiology, 21(1), pp.100–107.

Benharash, P. et al., 2015. Quantitative Analysis of Localized Sources Identified by Focal Impulse and Roter Modulation Mapping in Atrial Fibrillation. *Circulation: Arrhythmia and Electrophysiology*, 8(3), pp.CIRCEP. 115.002721–561.

Benoist, D. et al., 2017. Proarrhythmic remodelling of the right ventricle in a porcine model of repaired tetralogy of Fallot. *Heart*, 103(5), pp.347–354.

Bergfeldt, L. et al., 2017. Ventricular repolarization duration and dispersion adaptation after atropine induced rapid heart rate increase in healthy adults. Journal of Electrocardiology, 50(4), pp.424–432

Bers, D.M., 2002. Cardiac excitation–contraction coupling. *Nature*, 415(6868), pp.198–205.

Beuckelmann, D.J., Näbauer, M. & Erdmann, E., 1993. Alterations of K+ currents in isolated human ventricular myocytes from patients with terminal heart failure. Circulation Research, 73(2), pp.379–385.

Bloomfield, D.M. et al., 2004. Microvolt T-wave alternans distinguishes between patients likely and patients not likely to benefit from implanted cardiac defibrillator therapy: a solution to the Multicenter Automatic Defibrillator Implantation Trial (MADIT) II conundrum. *Circulation*, 110(14), pp.1885–1889.

Bode, F. et al., 2002. Upstream stimulation versus downstream stimulation: arrhythmogenesis based on repolarization dispersion in the human heart. Journal of the American College of Cardiology, 40(4), pp.731–736.

Bogun, F. et al., 2006. Isolated potentials during sinus rhythm and pace-mapping within scars as guides for ablation of post-infarction ventricular tachycardia. *Journal of the American College of Cardiology*, 47(10), pp.2013–2019.

Boukens, B.J. et al., 2015. Transmural APD gradient synchronizes repolarization in the human left ventricular wall. *Cardiovascular Research*, p.cvv202.

Boyle, N.G. & Shivkumar, K., 2012. Epicardial interventions in electrophysiology. *Circulation*, 126(14), pp.1752–1769.

Brink, A.J. & Goodwin, J.F., 1952. The pericardial T deflection of the electrocardiogram. *British heart journal*, 14(3), pp.331–338.

Bueno-Orovio, A. et al., 2012. In vivo human left-to-right ventricular differences in rate adaptation transiently increase pro-arrhythmic risk

following rate acceleration. R. G. Katare, ed. *PLoS ONE*, 7(12), p.e52234.

Burdon-Sanderson, J., 1884. On the Electrical Phenomena of the Excitatory Process in the Heart of the Frog and of the Tortoise, as investigated Photographically. *The Journal of physiology*, 4(6), pp.327–386.15.

Burger, H.C., 1955. The zero of potential: a persistent error. *American Heart Journal*, 49(4), pp.581–586.

Burgess, M.J. et al., 1972. The sequence of normal ventricular recovery. *American Heart Journal*, 84(5), pp.660–669.

Burnes, J.E., Kaelber, D.C., Taccardi, B., Lux, R.L., Ershler, P.R. and Rudy, Y., 1998. A field-compatible method for interpolating biopotentials. *Annals of biomedical engineering,* 26(1), pp.37-47.

Buxton, A.E., 2005. Should everyone with an ejection fraction less than or equal to 30% receive an implantable cardioverter-defibrillator? Not everyone with an ejection fraction < or = 30% should receive an implantable cardioverter-defibrillator. *Circulation*, 111(19), pp.2537–49–discussion 2537–49.

Buxton, A.E. et al., 1999. A Randomized Study of the Prevention of Sudden Death in Patients with Coronary Artery Disease. *New England Journal of Medicine*, 341(25), pp.1882–1890.

Buxton, A.E. et al., 2007. Limitations of ejection fraction for prediction of sudden death risk in patients with coronary artery disease: lessons from the MUSTT study. *Journal of the American College of Cardiology*, 50(12), pp. 1150–1157.

Castro Hevia, J. et al., 2006. Tpeak-Tend and Tpeak-Tend Dispersion as Risk Factors for Ventricular Tachycardia/Ventricular Fibrillation in Patients With the Brugada Syndrome. *Journal of the American College of Cardiology*, 47(9), pp.1828–1834.

Chen, P.S. et al., 1991. Epicardial activation and repolarization patterns in patients with right ventricular hypertrophy. *Circulation*, 83(1), pp.104–118.

Cheng, L. et al., 2011. Cortactin is required for N-cadherin regulation of Kv1.5 channel function. Journal of Biological Chemistry, 286(23), pp. 20478–20489.

Child, N. et al., 2015. An activation-repolarization time metric to predict localized regions of high susceptibility to reentry. *Heart Rhythm*, 12(7), pp.1644–1653.

Chinushi, M. et al., 2001. Correlation between the effective refractory period and activation-recovery interval calculated from the intracardiac unipolar electrogram of humans with and without dl-sotalol treatment. *Japanese circulation journal*, 65(8), pp.702–706.

Chow, A.W.C. et al., 2004. Mechanism of pacing-induced ventricular fibrillation in the infarcted human heart. *Circulation*, 110(13), pp.1725–1730.

Chugh, S.S. et al., 2009. Determinants of prolonged QT interval and their contribution to sudden death risk in coronary artery disease: the Oregon Sudden Unexpected Death Study. *Circulation*, 119(5), pp.663–670.

Chugh, S.S. et al., 2008. Epidemiology of sudden cardiac death: clinical and research implications. *Progress in cardiovascular diseases*, 51(3), pp.213–228.

Cohen, I., Giles, W. & Noble, D., 1976. Cellular basis for the T wave of the electrocardiogram. *Nature*, 262(5570), pp.657–661.

Connolly, S.J. et al., 2000. Canadian implantable defibrillator study (CIDS) : a randomized trial of the implantable cardioverter defibrillator against amiodarone. *Circulation*, 101(11), pp.1297–1302.

Conrath, C.E. & Opthof, T., 2006. Ventricular repolarization: an overview of (patho)physiology, sympathetic effects and genetic aspects. *Progress in biophysics and molecular biology*, 92(3), pp.269–307.

Cori, A.D. et al., 2005. New-Onset Ventricular Tachycardia After Cardiac Resynchronization Therapy. *Journal of interventional cardiac electrophysiology : an international journal of arrhythmias and pacing*, 12(3), pp.231–235.

Coronel, R. et al., 2006. Monophasic action potentials and activation recovery intervals as measures of ventricular action potential duration: Experimental evidence to resolve some controversies. *Heart Rhythm*, 3(9), pp.1043–1050.

Corrado, D. et al., 2008. Three-Dimensional Electroanatomical Voltage Mapping and Histologic Evaluation of Myocardial Substrate in Right Ventricular Outflow Tract Tachycardia. Journal of the American College of Cardiology, 51(7), pp.731–739.

Corrado, D. et al., 2011. Molecular biology and clinical management of arrhythmogenic right ventricular cardiomyopathy/dysplasia. *Heart*, 97(7), pp.530–539.

Corrado, D. et al., 2015. Treatment of arrhythmogenic right ventricular cardiomyopathy/dysplasia: an international task force consensus statement. European heart journal, 36(46), pp.3227–3237.

Cowan, J.C. et al., 1988. Sequence of epicardial repolarisation and configuration of the T wave. *British heart journal*, 60(5), pp.424–433.

Crow, R.S., Hannan, P.J. & Folsom, A.R., 2003. Prognostic significance of corrected QT and corrected JT interval for incident coronary heart disease in a general population sample stratified by presence or absence of wide QRS complex: the ARIC Study with 13 years of follow-up. *Circulation*, 108(16), pp.1985–1989.

Cuculich, P.S et al., 2011. The electrophysiological cardiac ventricular substrate in patients after myocardial infarction: noninvasive characterization with electrocardiographic imaging. *Journal of the American College of Cardiology*, 58(18), pp.1893-1902.

de Bakker, J.M.T. & Wittkampf, F.H.M., 2010. The pathophysiologic basis of fractionated and complex electrograms and the impact of recording techniques on their detection and interpretation. *Circulation: Arrhythmia and Electrophysiology*, 3(2), pp.204–213.

Delacretaz, E. & Stevenson, W.G., 2001. Catheter ablation of ventricular tachycardia in patients with coronary heart disease: part I: Mapping. *Pacing and Clinical Electrophysiology*, 24(8 Pt 1), pp.1261–1277.

Delmar, M. et al., 1991. Dynamics of the background outward current of single guinea pig ventricular myocytes. Ionic mechanisms of hysteresis in cardiac cells. Circulation Research, 69(5), pp.1316–1326.

Delmar, M. & McKenna, W.J., 2010. The cardiac desmosome and arrhythmogenic cardiomyopathies: from gene to disease. *Circulation Research*, 107(6), pp.700–714.

Dhamoon, A.S. & Jalife, J., 2005. The inward rectifier current (IK1) controls cardiac excitability and is involved in arrhythmogenesis. *Heart Rhythm*, 2(3), pp.316–324.

Di Diego, J.M. et al., 2002. Ionic and cellular basis for the predominance of the Brugada syndrome phenotype in males. *Circulation*, 106(15), pp. 2004–2011.

Di Diego, J.M., Sun, Z.Q. & Antzelevitch, C.A., 1996. I(to) and action potential notch are smaller in left vs. right canine ventricular epicardium. *American Journal of Physiology - Heart and Circulatory Physiology*, 271(2), pp.H548–H561.

Diness, T.G. et al., 2006. Frequency-dependent modulation of KCNQ1 and HERG1 potassium channels. *Biochemical and Biophysical Research Communications*, 343(4), pp.1224–1233.

Dorenkamp, M. et al., 2013. Long-term prognostic value of restitution slope in patients with ischemic and dilated cardiomyopathies. A. A. Sovari, ed. *PLoS ONE*, 8(1), p.e54768.

Dun, W. & Boyden, P.A., 2005. Diverse phenotypes of outward currents in cells that have survived in the 5-day-infarcted heart. *AJP: Heart and Circulatory Physiology*, 289(2), pp.H667–73.

Dun, W. et al., 2004. Dynamic remodeling of K+ and Ca2+ currents in cells that survived in the epicardial border zone of canine healed infarcted heart. *AJP: Heart and Circulatory Physiology*, 287(3), pp.H1046–54.

Durrer, D. & van der Twell, L.H., 1953. Spread of activation in the left ventricular wall of the dog. I. *American Heart Journal*, 46(5), pp.683–691.

Durrer, D. et al., 1970. Total excitation of the isolated human heart. *Circulation*, 41(6), pp.899–912.

Earley, M.J., Abrams, D. & Sporton, S.C., 2006. Validation of the noncontact mapping system in the left atrium during permanent atrial fibrillation and sinus rhythm. *Journal of the American College Of Cardiology, 1;48(3): 485-491*

Ebinger, M.W., Krishnan, S. & Schuger, C.D., 2005. Mechanisms of ventricular arrhythmias in heart failure. *Current Heart Failure Reports*, 2(3), pp.111–117.

Estes, N.A.M., 2011. Predicting and preventing sudden cardiac death. *Circulation*, 124(5), pp.651–656.

Fabritz, C.L. et al., 1994. *The vulnerable period equals the range of dispersion of repolarization in the intact heart*, Eur Heart J.

Finlay, M.C. et al., 2014. Dynamic conduction and repolarisation changes in early arrhythmogenic right ventricular cardiomyopathy versus benign outflow tract ectopy demonstrated by high density mapping & paced surface ECG analysis. B. Rodriguez, ed. *PLoS ONE*, 9(7), p.e99125.

Fish, J.M., Brugada, J. & Antzelevitch, C., 2005. Potential proarrhythmic effects of biventricular pacing. *Journal of the American College of Cardiology*, 46(12), pp.2340–2347.

Fozzard, H.A. & Hanck, D.A., 1996. Structure and function of voltage-dependent sodium channels: comparison of brain II and cardiac isoforms. *Physiological reviews*, 76(3), pp.887–926.

Franz, M. & Franz, M.R., 1999. Current status of monophasic action potential recording: theories, measurements and interpretations. *Cardiovascular Research*, 41(1), pp.25–40.

Franz, M.R., 1983. Long-Term Recording of Monophasic Action-Potentials From Human Endocardium. *The American Journal of Cardiology*, 51(10), pp.1629–1634.

Franz, M.R., 1991a. Method and theory of monophasic action potential recording. *Progress in Cardiovascular Diseases*, 33(6), pp.347–368.

Franz, M.R., 1991b. Method and theory of monophasic action potential recording. *Progress in cardiovascular diseases*, 33(6), pp.347–368.

Franz, M.R., 2003. The Electrical Restitution Curve Revisited:. Steep or Flat Slope-Which is Better? *Journal of Cardiovascular Electrophysiology*, 14(s10), pp.S140–S147.

Franz, M.R., 2001. Ventricular Repolarization, T-Wave Genesis, and Risk Prediction. *Annals of Noninvasive Electrocardiology*, 6(1), pp.1–4.

Franz, M.R. et al., 1988. Cycle length dependence of human action potential duration in vivo. Effects of single extrastimuli, sudden sustained rate acceleration and deceleration, and different steady-state frequencies. *The Journal of clinical investigation*, 82(3), pp.972–979.

Franz, M.R. et al., 1983. Electrical and mechanical restitution of the human heart at different rates of stimulation. *Circulation Research*, 53(6), pp.815–822.

Franz, M.R. et al., 1986. In vitro validation of a new cardiac catheter technique for recording monophasic action potentials. *European heart journal*, 7(1), pp.34–41.

Franz, M.R. et al., 1987. Monophasic action potential mapping in human subjects with normal electrocardiograms: direct evidence for the genesis of the T wave. *Circulation*, 75(2), pp.379–386.

Gamble, J.H.P. et al., 2013. Left ventricular endocardial pacing via the interventricular septum for cardiac resynchronization therapy: First report. *Heart Rhythm*, 10(12), pp.1812–1814.

Gardner, P.I. et al., 1985. Electrophysiologic and anatomic basis for fractionated electrograms recorded from healed myocardial infarcts. *Circulation*, 72(3), pp.596–611.

Garfinkel, A. et al., 2000. Preventing ventricular fibrillation by flattening cardiac restitution. *Proceedings of the National Academy of Sciences of the United States of America*, 97(11), pp.6061–6066.

Garfinkel, A. et al., 1997. Quasiperiodicity and chaos in cardiac fibrillation. *The Journal of clinical investigation*, 99(2), pp.305–314.

Glukhov, A.V. et al., 2012. Conduction remodeling in human end-stage nonischemic left ventricular cardiomyopathy. *Circulation*, 125(15), pp. 1835–1847.

Glukhov, A.V. et al., 2010. Transmural dispersion of repolarization in failing and nonfailing human ventricle. *Circulation Research*, 106(5), pp.981–991.

Gold, M.R. et al., 2000. A comparison of T-wave alternans, signal averaged electrocardiography and programmed ventricular stimulation for arrhythmia risk stratification. *Journal of the American College of Cardiology*, 36(7), pp.2247–2253.

Gomes, J. et al., 2012. Electrophysiological abnormalities precede overt structural changes in arrhythmogenic right ventricular cardiomyopathy

due to mutations in desmoplakin-A combined murine and human study. 33(15), pp.1942–1953.

Grant, A.O. & Starmer, C.F., 1987. Mechanisms of closure of cardiac sodium channels in rabbit ventricular myocytes: single-channel analysis. *Circulation Research*, 60(6), pp.897–913.

Grunnet, M., 2010. Repolarization of the cardiac action potential. Does an increase in repolarization capacity constitute a new anti-arrhythmic principle? *Acta physiologica (Oxford, England)*, 198 Suppl 676(s676), pp.1–48.

Grunnet, M. et al., 2003. KCNQ1 Channels Sense Small Changes in Cell Volume. *The Journal of physiology*, 549(2), pp.419–427.

Guiraudon, G.M. et al., 1994. Encircling endocardial cryoablation for ventricular tachycardia after myocardial infarction: Experience with 33 patients. *American Heart Journal*, 128(5), pp.982–989.

Guo, W. et al., 1999. Molecular basis of transient outward K current diversity in mouse ventricular myocytes. *The Journal of physiology*, 521(3), pp.587–599.

Haigney, M.C. et al., 2004. QT interval variability and spontaneous ventricular tachycardia or fibrillation in the Multicenter Automatic Defibrillator Implantation Trial (MADIT) II patients. *Journal of the American College of Cardiology*, 44(7), pp.1481–1487.

Hayase, J. et al., 2013. A case of a human ventricular fibrillation rotor localized to ablation sites for scar-mediated monomorphic ventricular tachycardia. Heart Rhythm 10(12), pp.1913–1916.

Han, J. & Moe, G.K., 1964. Nonuniform Recovery Of Excitability In Ventricular Muscle. *Circulation Research*, 14(1), pp.44–60.

Hanson, B. et al., 2009. Interaction of Activation-Repolarization Coupling and Restitution Properties in Humans. *Circulation: Arrhythmia and Electrophysiology*, 2(2), pp.162–170.

Harris, L. et al., 1987. Activation sequence of ventricular tachycardia: Endocardial and epicardial mapping studies in the human ventricle. *Journal of the American College of Cardiology*, 10(5), pp.1040–1047.

Haws, C.W. & Lux, R.L., 1990. Correlation between in vivo transmembrane action potential durations and activation-recovery intervals from

electrograms. Effects of interventions that alter repolarization time. *Circulation*, 81(1), pp.281–288.

Hayashi, M. et al., 2008. Ventricular repolarization restitution properties in patients exhibiting type 1 Brugada electrocardiogram with and without inducible ventricular fibrillation. *Journal of the American College of Cardiology*, 51(12), pp.1162–1168.

Hirano, Y., Moscucci, A. & January, C.T., 1992. Direct measurement of L-type Ca2+ window current in heart cells. *Circulation Research*, 70(3), pp. 445–455.

Hoffman, B.F. et al., 1959. Comparison of cardiac monophasic action potentials recorded by intracellular and suction electrodes. *The American journal of physiology*, 196(6), pp.1297–1301.

Horie, M., Hayashi, S. & Kawai, C., 1990. Two types of delayed rectifying K channels in atrial cells of guinea pig heart. The Japanese Journal of Physiology, 40(4), pp.479–490.

Hua, F., 2004. Contribution of IKr to Rate-Dependent Action Potential Dynamics in Canine Endocardium. *Circulation Research*, 94(6), pp.810–819.

Imanishi, S. & Surawicz, B., 1976. Automatic activity in depolarized guinea pig ventricular myocardium. Characteristics and mechanisms. *Circulation Research*, 39(6), pp.751–759.

Ino, T. et al., 1988. Relation of monophasic action potential recorded with contact electrode to underlying transmembrane action potential properties in isolated cardiac tissues: a systematic microelectrode validation study. *Cardiovascular Research*, 22(4), pp.255–264.

Isomoto, S. & Kurachi, Y., 1997. Function, Regulation, Pharmacology, and Molecular Structure of ATP-Sensitive K Channels in the Cardiovascular System. *Journal of Cardiovascular Electrophysiology*, 8(12), pp.1431–1446.

Jaïs, P. et al., 2012. Elimination of local abnormal ventricular activities: a new end point for substrate modification in patients with scar-related ventricular tachycardia. *Circulation*, 125(18), pp.2184–2196.

Janse, M.J., 1986. Electrophysiology and electrocardiology of acute myocardial ischemia. *The Canadian journal of cardiology*, Suppl A, pp.46A–52A.

Janse, M.J. et al., 2005. Repolarization gradients in the canine left ventricle before and after induction of short-term cardiac memory. *Circulation*, 112(12), pp.1711–1718.

Janse, M.J. et al., 2012. Repolarization gradients in the intact heart: transmural or apico-basal? *Progress in biophysics and molecular biology*, 109(1-2), pp.6–15.

Jia, P., Punske, B., Taccardi, B. and Rudy, Y., 2002. Endocardial mapping of electrophysiologically abnormal substrates and cardiac arrhythmias using a noncontact nonexpandable catheter. *Journal of cardiovascular electrophysiology*, 13(9), pp.888-895.

Jiang, M. et al., 2000. Delayed rectifier K currents have reduced amplitudes and altered kinetics in myocytes from infarcted canine ventricle. *Cardiovascular Research*, 48(1), pp.34–43.

Jochim, K., Katz, L.N. & Mayne, W., 1935. The monophasic electrogram obtained from the mammalian heart. *The American journal of physiology*, 111(1), pp.177–186.

Kadish, A. et al., 2004. Prophylactic defibrillator implantation in patients with nonischemic dilated cardiomyopathy. *New England Journal of Medicine*, 350(21), pp.2151–2158.

Kaltenbrunner, W. et al., 1991. Epicardial and endocardial mapping of ventricular tachycardia in patients with myocardial infarction. Is the origin of the tachycardia always subendocardially localized? *Circulation*, 84(3), pp.1058–1071.

Karma, A., 1994. Electrical alternans and spiral wave breakup in cardiac tissue. *Chaos (Woodbury, N.Y.)*, 4(3), pp.461–472.

Kellman, P. & Arai, A.E., 2012. Cardiac imaging techniques for physicians: late enhancement. *Journal of magnetic resonance imaging : JMRI*, 36(3), pp. 529–542.

Kinoshita, T. et al., 2012. Time course and prognostic implications of QT interval in patients with coronary artery disease undergoing coronary

bypass surgery. *Journal of Cardiovascular Electrophysiology*, 23(6), pp.645–649.

Koller, B.S. et al., 1995. Relation Between Repolarization and Refractoriness During Programmed Electrical Stimulation in the Human Right Ventricle: Implications for Ventricular Tachycardia Induction. Circulation, 91(9), pp.2378–2384.

Koller, M.L., Riccio, M.L. & Gilmour, R.F., 1998. Dynamic restitution of action potential duration during electrical alternans and ventricular fibrillation. *American Journal of Physiology - Heart and Circulatory Physiology*, 275(5), pp.H1635–1642.

Kondo, M., Nesterenko, V. & Antzelevitch, C., 2004. Cellular basis for the monophasic action potential. Which electrode is the recording electrode? *Cardiovascular Research*, 63(4), pp.635–644.

Kongstad, O. et al., 2002. Global and local dispersion of ventricular repolarization: endocardial monophasic action potential mapping in

swine and humans by using an electro-anatomical mapping system. *Journal of Electrocardiology*, 35(2), pp.159–167.

Korsgren, M. et al., 1966. Intracardiac recording of monophasic action potentials in the human heart. *Scandinavian journal of clinical and laboratory investigation*, 18(5), pp.561–564.

Kuck, K.H. et al., 2000. Randomized comparison of antiarrhythmic drug therapy with implantable defibrillators in patients resuscitated from cardiac arrest : the Cardiac Arrest Study Hamburg (CASH). *Circulation*, 102(7), pp.748–754.

Kurz, R.W., Ren, X.L. & FRANZ, M.R., 1994. Dispersion and delay of electrical restitution in the globally ischaemic heart. *European heart journal*, 15(4), pp.547–554.

Laurita, K.R. et al., 1998. Modulated dispersion explains changes in arrhythmia vulnerability during premature stimulation of the heart. *Circulation*, 98(24), pp.2774–2780.

Laurita, K.R., Girouard, S.D. & Rosenbaum, D.S., 1996. Modulation of Ventricular Repolarization by a Premature Stimulus: Role of Epicardial

Dispersion of Repolarization Kinetics Demonstrated by Optical Mapping of the Intact Guinea Pig Heart. *Circulation Research*, 79(3), pp. 493–503.

Letsas, K.P. et al., 2010. Tpeak-Tend interval and Tpeak-Tend/QT ratio as markers of ventricular tachycardia inducibility in subjects with Brugada ECG phenotype. *Europace*, 12(2), pp.271–274.

Li, G.-R. et al., 2004. Ionic current abnormalities associated with prolonged action potentials in cardiomyocytes from diseased human right ventricles. *Heart Rhythm*, 1(4), pp.460–468.

Li, G.R. et al., 1998. Transmural heterogeneity of action potentials and Ito1 in myocytes isolated from the human right ventricle. *The American journal of physiology*, 275(2 Pt 2), pp.H369–77.

Litwin, S.E. & Bridge, J.H., 1997. Enhanced Na(+)-Ca2+ exchange in the infarcted heart. Implications for excitation-contraction coupling. *Circulation Research*, 81(6), pp.1083–1093.

Liu, D.W., Gintant, G.A. & Antzelevitch, C., 1993. Ionic bases for electrophysiological distinctions among epicardial, midmyocardial, and

endocardial myocytes from the free wall of the canine left ventricle. Circulation Research, 72(3), pp.671–687.

Liu, D.W. & Antzelevitch, C., 1995. Characteristics of the delayed rectifier current (IKr and IKs) in canine ventricular epicardial, midmyocardial, and endocardial myocytes. A weaker IKs contributes to the longer action potential of the M cell. *Circulation Research*, 76(3), pp.351–365.

Liu, M., Yang, K.-C. & Dudley, S.C., 2014. Cardiac sodium channel mutations: why so many phenotypes? *Nature Reviews Cardiology*, 11(10), pp.607–615.

Lodder, E.M. & Rizzo, S., 2012. Mouse Models in Arrhythmogenic Right Ventricular Cardiomyopathy. *Frontiers in Physiology*, 3.

Lopez, C. et al., 2017. Polymorphic ventricular arrhythmia triggered by temporary epicardial right ventricular stimulation after cardiac surgery. HeartRhythm Case Reports, 3(12), pp.571–573.

Magtibay, K. et al., 2017. Physiological Assessment of Ventricular Myocardial Voltage Using Omnipolar Electrograms. *Journal of the American Heart Association*, 6(8), p.e006447.

Marban, E., Robinson, S.W. & Wier, W.G., 1986. Mechanisms of arrhythmogenic delayed and early afterdepolarizations in ferret ventricular muscle. *The Journal of clinical investigation*, 78(5), pp.1185–1192.

Marchlinski, F.E. et al., 2000. Linear Ablation Lesions for Control of Unmappable Ventricular Tachycardia in Patients With Ischemic and Nonischemic Cardiomyopathy. *Circulation*, 101(11), pp.1288–1296.

Marcus, F.I. et al., 2010. Diagnosis of Arrhythmogenic Right Ventricular Cardiomyopathy/Dysplasia: Proposed Modification of the Task Force Criteria. *Circulation*, 121(13), pp.1533–1541.

Marrus, S.B. et al., 2012. Repolarization changes underlying long-term cardiac memory due to right ventricular pacing: noninvasive mapping with electrocardiographic imaging. *Circulation: Arrhythmia and Electrophysiology*, 5(4), pp.773–781.

Martinez, J.P. & Olmos, S., 2005. Methodological principles of T wave alternans analysis: a unified framework. *IEEE Transactions on Biomedical Engineering*, 52(4), pp.599–613.

Mayer, A.G., 1906. *Rhythmical pulsations in Scyphomedusae: Rhythmical pulsation in scyphomedusae (No. 47). Carnegie institution of Washington.*

Mays, D.J. et al., 1995. Localization of the Kv1.5 K+ channel protein in explanted cardiac tissue. *The Journal of clinical investigation*, 96(1), pp.282–292.

Mäkikallio, T.H. et al., 2005. Prediction of sudden cardiac death after acute myocardial infarction: role of Holter monitoring in the modern treatment era. *European heart journal*, 26(8), pp.762–769.

Medina-Ravell, V.A., 2003. Effect of Epicardial or Biventricular Pacing to Prolong QT Interval and Increase Transmural Dispersion of Repolarization: Does Resynchronization Therapy Pose a Risk for Patients Predisposed to Long QT or Torsade de Pointes? *Circulation*, 107(5), pp.740–746.

Meijborg, V.M.F. et al., 2014. Electrocardiographic T wave and its relation with ventricular repolarization along major anatomical axes. *Circulation: Arrhythmia and Electrophysiology*, 7(3), pp.524–531.

Millar, C.K., Kralios, F.A. & Lux, R.L., 1985. Correlation between refractory periods and activation-recovery intervals from electrograms: effects of rate and adrenergic interventions. *Circulation*, 72(6), pp.1372–1379.

Milstein, M.L. et al., 2012. Dynamic reciprocity of sodium and potassium channel expression in a macromolecular complex controls cardiac excitability and arrhythmia. *Proceedings of the National Academy of Sciences of the United States of America*, 109(31), pp.E2134–43.

Mines, G.R., 1914. On circulating excitations in heart muscle and their possible relation to tachycardia and fibrillation. *Trans R Soc Can,* 8, pp. 43-52.

Mines, G.R., 1913. On dynamic equilibrium in the heart. *The Journal of physiology*, 46(4-5), pp.349–383.

Ming, Z., Nordin, C. & Aronson, R.S., 1994. Role of L-type calcium channel window current in generating current-induced early afterdepolarizations. *Journal of Cardiovascular Electrophysiology*, 5(4), pp. 323–334.

Moran, J.M. et al., 1982. Extended Endocardial Resection for the Treatment of Ventricular Tachycardia and Ventricular Fibrillation. *The Annals of Thoracic Surgery*, 34(5), pp.538–552.

Morgan, J.M., Cunningham, D. & Rowland, E., 1992. Dispersion of monophasic action potential duration: Demonstrable in humans after premature ventricular extrastimulation but not in steady state. *Journal of the American College of Cardiology*, 19(6), pp.1244–1253.

Moss, A.J., 2005. Should everyone with an ejection fraction less than or equal to 30% receive an implantable cardioverter-defibrillator? Everyone with an ejection fraction < or = 30% should receive an implantable cardioverter-defibrillator. *Circulation*, 111(19), pp.2537–49– discussion 2537–49.

Moss, A.J. et al., 2009. Cardiac-resynchronization therapy for the prevention of heart-failure events. *New England Journal of Medicine*, 361(14), pp. 1329–1338.

Moss, A.J. et al., 1996. Improved survival with an implanted defibrillator in patients with coronary disease at high risk for ventricular arrhythmia.

Multicenter Automatic Defibrillator Implantation Trial Investigators. *New England Journal of Medicine*, 335(26), pp.1933–1940.

Moss, A.J. et al., 2002. Prophylactic implantation of a defibrillator in patients with myocardial infarction and reduced ejection fraction. *New England Journal of Medicine*, 346(12), pp.877–883.

Moss, A.J. et al., 2001. Survival benefit with an implanted defibrillator in relation to mortality risk in chronic coronary heart disease. *The American Journal of Cardiology*, 88(5), pp.516–520.

Moubarak, J.B. et al., 2000. High dispersion of ventricular repolarization after an implantable defibrillator shock predicts induction of ventricular fibrillation as well as unsuccessful defibrillation. *Journal of the American College of Cardiology*, 35(2), pp.422–427.

Myerburg, R.J. et al., 1982. Cellular electrophysiology in acute and healed experimental myocardial infarction. *Annals of the New York Academy of Sciences*, 382, pp.90–115.

Myerburg, R.J., Reddy, V. & Castellanos, A., 2009. Indications for implantable cardioverter-defibrillators based on evidence and judgment. *Journal of the American College of Cardiology*, 54(9), pp.747–763.

Myles, R.C. et al., 2010. Effect of activation sequence on transmural patterns of repolarization and action potential duration in rabbit ventricular myocardium. *American Journal of Physiology - Heart and Circulatory Physiology*, 299(6), pp.H1812–1822.

Nademanee, K. et al., 2011. Prevention of ventricular fibrillation episodes in Brugada syndrome by catheter ablation over the anterior right ventricular outflow tract epicardium. *Circulation*, 123(12), pp.1270–1279.

Nanthakumar, K. et al., 2004. Prophylactic implantable cardioverter-defibrillator therapy in patients with left ventricular systolic dysfunction: A pooled analysis of 10 primary prevention trials. *Journal of the American College of Cardiology*, 44(11), pp.2166–2172.

Narayan, S.M. et al., 2007. T-wave alternans, restitution of human action potential duration, and outcome. *Journal of the American College of Cardiology*, 50(25), pp.2385–2392.

Nash, M.P. et al., 2006. Whole heart action potential duration restitution properties in cardiac patients: a combined clinical and modelling study. *Experimental physiology*, 91(2), pp.339–354.

Nayyar, S. et al., 2014. High Density Mapping of Ventricular Scar: A Comparison of Ventricular Tachycardia Supporting Channels with Channels That Do Not Support VT. *Circulation: Arrhythmia and Electrophysiology*, 7(1), pp.90–98.

Nerbonne, J.M. & Kass, R.S., 2005. Molecular physiology of cardiac repolarization. *Physiological reviews*, 85(4), pp.1205–1253.

Nicolson, W.B. et al., 2012. A novel surface electrocardiogram-based marker of ventricular arrhythmia risk in patients with ischemic cardiomyopathy. *Journal of the American Heart Association*, 1(4), pp.e001552.

Nilius, B. et al., 1985. A novel type of cardiac calcium channel in ventricular cells. *Nature*, 316(6027), pp.443–446.

Noble, D. & Cohen, I., 1978. The interpretation of the T wave of the electrocardiogram. *Cardiovascular Research*, 12(1), pp.13–27.

Nolasco, J.B. & Dahlen, R.W., 1968. A graphic method for the study of alternation in cardiac action potentials. *Journal of applied physiology*, 25(2), pp.191–196.

O'Hara, T. et al., 2011. Simulation of the undiseased human cardiac ventricular action potential: model formulation and experimental validation. A. D. McCulloch, ed. *PLoS computational biology*, 7(5), p.e1002061.

Ohara, T. et al., 2001. Increased wave break during ventricular fibrillation in the epicardial border zone of hearts with healed myocardial infarction. *Circulation*, 103(10), pp.1465–1472.

Olsson, S.B. et al., 1991. Effect of pentisomide (CM 7857) on myocardial excitation, conduction, repolarization, and refractoriness. An electrophysiological study in humans. *Journal of cardiovascular pharmacology*, 18(6), pp.849–854.

Olsson, S.B. et al., 1995. The dispersion of repolarization in patients with ventricular tachycardia: A study using simultaneous monophasic action

potential recordings from two sites in the right ventricle. 16(1), pp.68–76.

Opthof, T. et al., 2007. Dispersion of repolarization in canine ventricle and the electrocardiographic T wave: Tp-e interval does not reflect transmural dispersion. *Heart Rhythm*, 4(3), pp.341–348.

Opthof, T., Coronel, R. & Janse, M.J., 2009. Is there a significant transmural gradient in repolarization time in the intact heart?: Repolarization Gradients in the Intact Heart. *Circulation: Arrhythmia and Electrophysiology*, 2(1), pp.89–96.

Orini, M. et al., 2014. Comparative evaluation of methodologies for T-wave alternans mapping in electrograms. *IEEE Transactions on Biomedical Engineering*, 61(2), pp.308–316.

Ostermeyer, J. et al., 1984. Surgical treatment of ventricular tachycardias. Complete versus partial encircling endocardial ventriculotomy. *The Journal of thoracic and cardiovascular surgery*, 87(4), pp.517–525.

Ozgen, N. & Rosen, M.R., 2009. Cardiac memory: a work in progress. *Heart Rhythm*, 6(4), pp.564–570.

Panikkath, R. et al., 2011. Prolonged Tpeak-to-tend interval on the resting ECG is associated with increased risk of sudden cardiac death. *Circulation: Arrhythmia and Electrophysiology*, 4(4), pp.441–447.

Pastore, J.M. et al., 1999. Mechanism linking T-wave alternans to the genesis of cardiac fibrillation. *Circulation*, 99(10), pp.1385–1394.

Pastore, J.M., Laurita, K.R. & Rosenbaum, D.S., 2006. Importance of spatiotemporal heterogeneity of cellular restitution in mechanism of arrhythmogenic discordant alternans. *Heart Rhythm*, 3(6), pp.711–719.

Patberg, K.W. et al., 2005. Cardiac memory: mechanisms and clinical implications. *Heart Rhythm*, 2(12), pp.1376–1382.

Patel, C. et al., 2009. Is there a significant transmural gradient in repolarization time in the intact heart? Cellular basis of the T wave: a century of controversy. *Circulation: Arrhythmia and Electrophysiology*, 2(1), pp.80–88.

Perez-Reyes, E., 2003. Molecular Physiology of Low-Voltage-Activated T-type Calcium Channels. *Physiological reviews*, 83(1), pp.117–161.

Peters, N.S. et al., 1993. Reduced content of connexin43 gap junctions in ventricular myocardium from hypertrophied and ischemic human hearts. *Circulation*, 88(3), pp.864–875.

Pinto, J.M. et al., 1997. Regional gradation of L-type calcium currents in the feline heart with a healed myocardial infarct. *Journal of Cardiovascular Electrophysiology*, 8(5), pp.548–560.

Pogwizd, S.M., McKenzie, J.P. & Cain, M.E., 1998. Mechanisms underlying spontaneous and induced ventricular arrhythmias in patients with idiopathic dilated cardiomyopathy. *Circulation*, 98(22), pp.2404–2414.

Potse, M. et al., 2009. Validation of a simple model for the morphology of the T wave in unipolar electrograms. *AJP: Heart and Circulatory Physiology*, 297(2), pp.H792–H801.

Priori, S.G. et al., 2013. HRS/EHRA/APHRS expert consensus statement on the diagnosis and management of patients with inherited primary arrhythmia syndromes: document endorsed by HRS, EHRA, and APHRS in May 2013 and by ACCF, AHA, PACES, and AEPC in June 2013. *Heart Rhythm*, 10(12), pp.1932–1963.

Qu, Z., Weiss, J.N. & Garfinkel, A., 1999. Cardiac electrical restitution properties and stability of reentrant spiral waves: a simulation study. *The American journal of physiology*, 276(1 Pt 2), pp.H269–83.

R Core Team (2013). R: A language and environment for statistical computing. R Foundation for Statistical Computing, Vienna, Austria. URL http://www.R-project.org/.

Ramanathan, C. et al., 2006. Activation and repolarization of the normal human heart under complete physiological conditions., 103(16), pp. 6309–6314.

Ramanathan, C. et al., 2004. Noninvasive electrocardiographic imaging for cardiac electrophysiology and arrhythmia. *Nature Medicine*, 10(4), pp. 422–428.

Rea, T.D. & Page, R.L., 2010. Community approaches to improve resuscitation after out-of-hospital sudden cardiac arrest. *Circulation*, 121(9), pp.1134–1140.

Reddy, V.Y. et al., 2003. Short-term results of substrate mapping and radiofrequency ablation of ischemic ventricular tachycardia using a

saline-irrigated catheter. *Journal of the American College of Cardiology*, 41(12), pp.2228–2236.

Roepke, T.K. et al., 2008. Targeted deletion of kcne2 impairs ventricular repolarization via disruption of I(K,slow1) and I(to,f). The FASEB Journal, 22(10), pp.3648–3660.

Rojas, A. & Calkins, H., 2015. Present understanding of the relationship between exercise and arrhythmogenic right ventricular dysplasia/ cardiomyopathy. *Trends in cardiovascular medicine*, 25(3), pp.181–188.

Rose, J. et al., 2005. Molecular correlates of altered expression of potassium currents in failing rabbit myocardium. *American Journal of Physiology - Heart and Circulatory Physiology*. 288(5), p.H2077.

Rosen, M.R., 2009. Why T waves change: A reminiscence and essay. *Heart Rhythm*, 6(11), pp.S56–S61.

Rosen, M.R. & Cohen, I.S., 2006. Cardiac memory ... new insights into molecular mechanisms. *The Journal of physiology*, 570(Pt 2), pp.209–218.

Rosenbaum, M.B. et al., 1982. Electrotonic modulation of the T wave and cardiac memory. 50(2), pp.213–222.

Rosenbaum, M.B. et al., 1983. Electrotonic Modulation of Ventricular Repolarization and Cardiac Memory. In *Frontiers of Cardiac Electrophysiology*. Developments in Cardiovascular Medicine. Dordrecht: Springer Netherlands, pp. 67–99.

Rudy, Y 2013. Noninvasive electrocardiographic imaging of arrhythmogenic substrates in humans. *Circulation Research*, 112(5), 863-74.

Sacher, F. et al., 2015. Substrate mapping and ablation for ventricular tachycardia: the LAVA approach. *Journal of Cardiovascular Electrophysiology*, 26(4), pp.464–471.

Salama, G. & Choi, B.-R., 2007. Imaging ventricular fibrillation. *Journal of Electrocardiology*, 40(6 Suppl), pp.S56–61.

Sanguinetti, M.C., 1990. Two components of cardiac delayed rectifier K current. Differential sensitivity to block by class III antiarrhythmic agents. *The Journal of General Physiology*, 96(1), pp.195–215.

Sanguinetti, M.C. & Tristani-Firouzi, M., 2006. hERG potassium channels and cardiac arrhythmia. *Nature*, 440(7083), pp.463–469.

Scacchi, S. et al., 2009. A reliability analysis of cardiac repolarization time markers. *Mathematical biosciences*, 219(2), pp.113–128.

Scheffer, M.G., Ramanna, H. & van Gelder, B.M., 2014. Left Ventricular endocardial pacing by the interventricular septum route. *Europace*, 16(10), pp.1520–1520.

Schwartz, P.J. et al., 2009. Why T waves change: A reminiscence and essay. 6(11), pp.S56–S61.

Shimizu, M. et al., 2002. T-peak to T-end interval may be a better predictor of high-risk patients with hypertrophic cardiomyopathy associated with a cardiac troponin I mutation than QT dispersion. *Clinical Cardiology*, 25(7), pp.335–339.

Shimizu, W. et al., 1991. Early afterdepolarizations induced by isoproterenol in patients with congenital long QT syndrome. *Circulation*, 84(5), pp. 1915–1923.

Shipsey, S.J., Bryant, S.M. & Hart, G., 1997. Effects of hypertrophy on regional action potential characteristics in the rat left ventricle: a cellular basis for T-wave inversion? *Circulation*, 96(6), pp.2061–2068.

Shukla, G. et al., 2005. Potential proarrhythmic effect of biventricular pacing: fact or myth? *Heart Rhythm*, 2(9), pp.951–956.

Sicouri, S. et al., 2010. Transseptal dispersion of repolarization and its role in the development of Torsade de Pointes arrhythmias. *Journal of Cardiovascular Electrophysiology*, 21(4), pp.441–447.

Soejima, K. et al., 2002. Electrically Unexcitable Scar Mapping Based on Pacing Threshold for Identification of the Reentry Circuit Isthmus. *Circulation*, 106(13), pp.1678–1683.

Spach, M.S. & Barr, R.C., 1975. Ventricular intramural and epicardial potential distributions during ventricular activation and repolarization in the intact dog. *Circulation Research*, 37(2), pp.243–257.

Srinivasan, N.T. et al., 2016. Ventricular stimulus site influences dynamic dispersion of repolarization in the intact human heart. *American Journal of Physiology - Heart and Circulatory Physiology*, 311(3), pp.H545–54.

Steinhaus, B.M., 1989a. Estimating cardiac transmembrane activation and recovery times from unipolar and bipolar extracellular electrograms: a simulation study. *Circulation Research*, 64(3), pp.449–462.

Steinhaus, B.M., 1989b. Estimating cardiac transmembrane activation and recovery times from unipolar and bipolar extracellular electrograms: a simulation study. *Circulation Research*, 64(3), pp.449–462.

Stevenson, W.G., 2009. Ventricular scars and ventricular tachycardia. *Transactions of the American Clinical and Climatological Association*, 120, pp. 403–412.

Stevenson, W.G. & Soejima, K., 2007. Catheter ablation for ventricular tachycardia. *Circulation*, 115(21), pp.2750–2760.

Stevenson, W.G. et al., 1997. Exploring postinfarction reentrant ventricular tachycardia with entrainment mapping. *Journal of the American College of Cardiology*, 29(6), pp.1180–1189.

Stühmer, W. et al., 1989. Structural parts involved in activation and inactivation of the sodium channel. *Nature*, 339(6226), pp.597–603.

Subramanian, A. et al., 2011. Modulated dispersion of activation and repolarization by premature beats in patients with cardiomyopathy at risk of sudden death. *AJP: Heart and Circulatory Physiology*, 300(6), pp.H2221–H2229.

Sun, Y. & Weber, K.T., 2000. Infarct scar: a dynamic tissue. *Cardiovascular Research*. 46(2), pp.250-256

Szél, T. & Antzelevitch, C., 2014. Abnormal repolarization as the basis for late potentials and fractionated electrograms recorded from epicardium in experimental models of Brugada syndrome. *Journal of the American College of Cardiology*, 63(19), pp.2037–2045.

Taggart, P., 2001. Transmural repolarisation in the left ventricle in humans during normoxia and ischaemia. *Cardiovascular Research*, 50(3), pp.454–462.

Taggart, P. et al., 2003. Effect of adrenergic stimulation on action potential duration restitution in humans. *Circulation*, 107(2), pp.285–289.

Taggart, P. et al., 2000. Inhomogeneous transmural conduction during early ischaemia in patients with coronary artery disease. *Journal of molecular and cellular cardiology*, 32(4), pp.621–630.

Tandri, H. et al., 2009. Prolonged RV endocardial activation duration: a novel marker of arrhythmogenic right ventricular dysplasia/cardiomyopathy. Heart Rhythm, 6(6), pp.769–775.

Tang, A.S.L. et al., 2010. Cardiac-resynchronization therapy for mild-to-moderate heart failure. *New England Journal of Medicine*, 363(25), pp. 2385–2395.

Tayeh, O. et al., 2013. Potential pro-arrhythmic effect of cardiac resynchronization therapy. *Journal of the Saudi Heart Association*, 25(3), pp.181–189.

Thomsen, M.B. et al., 2004. Increased short-term variability of repolarization predicts d-sotalol-induced torsades de pointes in dogs. *Circulation*, 110(16), pp.2453–2459.

Tolkacheva, E.G., Anumonwo, J.M.B. & Jalife, J., 2006. Action Potential Duration Restitution Portraits of Mammalian Ventricular Myocytes: Role of Calcium Current. Biophysical Journal, 91(7), pp.2735–2745.

Tsuji, Y. et al., 2000. Pacing-induced heart failure causes a reduction of delayed rectifier potassium currents along with decreases in calcium and transient outward currents in rabbit ventricle. Cardiovascular Research, 48(2), pp.300–309.

van Duijvenboden, S. et al., 2015. Accuracy of measurements derived from intracardiac unipolar electrograms: A simulation study. *2015 37th Annual International Conference of the IEEE Engineering in Medicine and Biology Society (EMBC)*, pp.76–79.

Varró, A., Nánási, P.P. & Lathrop, D.A., 1993. Potassium currents in isolated human atrial and ventricular cardiocytes. *Acta Physiologica Scandinavica*, 149(2), pp.133–142.

Venlet, J. et al., 2017. Unipolar Endocardial Voltage Mapping in the Right Ventricle: Optimal Cutoff Values Correcting for Computed

Tomography-Derived Epicardial Fat Thickness and Their Clinical Value for Substrate Delineation. *Circulation: Arrhythmia and Electrophysiology*, 10(8), p.e005175.

Verma, A. et al., 2005. Relationship Between Successful Ablation Sites and the Scar Border Zone Defined by Substrate Mapping for Ventricular Tachycardia Post-Myocardial Infarction. *Journal of Cardiovascular Electrophysiology*, 16(5), pp.465–471.

Volders, P.G. et al., 1999. Repolarizing K+ currents ITO1 and IKs are larger in right than left canine ventricular midmyocardium. *Circulation*, 99(2), pp.206–210.

Volders, P.G. et al., 1997. Similarities between early and delayed afterdepolarizations induced by isoproterenol in canine ventricular myocytes. *Cardiovascular Research*, 34(2), pp.348–359.

Wang, N.C. et al., 2008. Clinical implications of QRS duration in patients hospitalized with worsening heart failure and reduced left ventricular ejection fraction. *JAMA*, 299(22), pp.2656–2666.

Wang, S. et al., 2004. Activation properties of Kv4.3 channels: time, voltage and [K+]o dependence. *The Journal of physiology*, 557(Pt 3), pp.705–717.

Wang, Y. et al., 2011. Noninvasive electroanatomic mapping of human ventricular arrhythmias with electrocardiographic imaging. *Science Translational Medicine*, 3(98), pp.98ra84–98ra84.

Watanabe, M., Otani, N.F. & Gilmour, R.F., 1995. Biphasic restitution of action potential duration and complex dynamics in ventricular myocardium. *Circulation Research*, 76(5), pp.915–921.

Watanabe, T., Rautaharju, P.M. & McDonald, T.F., 1985. Ventricular action potentials, ventricular extracellular potentials, and the ECG of guinea pig. *Circulation Research*, 57(3), pp.362–373.

Weiss, J.N. et al., 1999. Chaos and the transition to ventricular fibrillation: a new approach to antiarrhythmic drug evaluation. *Circulation*, 99(21), pp. 2819–2826.

Weiss, J.N. et al., 2002. Electrical Restitution and Cardiac Fibrillation. *Journal of Cardiovascular Electrophysiology*, 13(3), pp.292–295.

Weiss, J.N. et al., 2000. Ventricular fibrillation: how do we stop the waves from breaking? *Circulation Research*, 87(12), pp.1103–1107.

Weissenburger, J., Nesterenko, V.V. & Antzelevitch, C., 2000. Transmural heterogeneity of ventricular repolarization under baseline and long QT conditions in the canine heart in vivo: torsades de pointes develops with halothane but not pentobarbital anesthesia. Journal of Cardiovascular Electrophysiology, 11(3), pp.290–304.

Western, D., Hanson, B. & Taggart, P., 2015. Measurement bias in activation-recovery intervals from unipolar electrograms. *American Journal of Physiology - Heart and Circulatory Physiology*, 308(4), pp.H331–8.

Wickenden, A.D., Kaprielian, R., Kassiri, Z., Tsoporis, J.N., Tsushima, R., Fishman, G.I. and Backx, P.H., 1998. The role of action potential prolongation and altered intracellular calcium handling in the pathogenesis of heart failure. *Cardiovascular research*, 37(2), pp.312-323.

Wilson, F.N. et al., 1934. Electrocardiograms that represent the potential variations of a single electrode. *American Heart Journal*, 9(4), pp.447–458.

Wilson, L.D. & Rosenbaum, D.S., 2007. Mechanisms of arrythmogenic cardiac alternans. *Europace*, 9(suppl_6), pp.vi77–vi82.

Wyatt, R.F. et al., 1981. Estimation of ventricular transmembrane action potential durations and repolarization times from unipolar electrograms, *American Journal of Cardiology*, 47, p.488.

Xia, Y. et al., 2005. Tpeak-Tend Interval as an Index of Global Dispersion of Ventricular Repolarization: Evaluations Using Monophasic Action Potential Mapping of the Epi- and Endocardium in Swine. *Journal of interventional cardiac electrophysiology : an international journal of arrhythmias and pacing*, 14(2), pp.79–87.

Xu, H., 1999. Four Kinetically Distinct Depolarization-activated K Currents in Adult Mouse Ventricular Myocytes. *The Journal of General Physiology*, 113(5), pp.661–678.

Yan, G.-X. et al., 2004. Phase 2 reentry as a trigger to initiate ventricular fibrillation during early acute myocardial ischemia. *Circulation*, 110(9), pp.1036–1041.

Yan, G.X. & Antzelevitch, C., 1998. Cellular basis for the normal T wave and the electrocardiographic manifestations of the long-QT syndrome. *Circulation*, 98(18), pp.1928–1936.

Yu, F.H. & Catterall, W.A., 2003. Overview of the voltage-gated sodium channel family. *Genome biology*, 4(3), p.207.

Yuan, S. et al., 1995. The dispersion of repolarization in patients with ventricular tachycardia. *European heart journal*, 16(1), pp.68–76.

Yue, A.M., 2005. Global Dynamic Coupling of Activation and Repolarization in the Human Ventricle. *Circulation*, 112(17), pp.2592–2601.

Yue, A.M. et al., 2004. Determination of human ventricular repolarization by noncontact mapping: validation with monophasic action potential recordings. *Circulation*, 110(11), pp.1343–1350.

Yue, A.M. et al., 2005. Global Endocardial Electrical Restitution in Human Right and Left Ventricles Determined by Noncontact Mapping. *Journal of the American College of Cardiology*, 46(6), pp.1067–1075.

Zabel, M. et al., 2000. Analysis of 12-lead T-wave morphology for risk stratification after myocardial infarction. Circulation, 102(11), pp.1252–1257.

Zabel, M. et al., 2013. Long-Term Prognostic Value of Restitution Slope in Patients with Ischemic and Dilated Cardiomyopathies A. A. Sovari, ed. *PLoS ONE*, 8(1), p.e54768.

Zaitsev, A.V. et al., 2003. Wavebreak formation during ventricular fibrillation in the isolated, regionally ischemic pig heart. *Circulation Research*, 92(5), pp.546–553.

Zeng, J. & Rudy, Y., 1995. Early afterdepolarizations in cardiac myocytes: mechanism and rate dependence. *Biophysical journal*, 68(3), pp.949–964.

Zhang, Y. et al., 2011. Electrocardiographic QT interval and mortality: a meta-analysis. *Epidemiology (Cambridge, Mass.)*, 22(5), pp.660–670.

Zhang, J. et al., 2016. Electrophysiologic Scar Substrate in Relation to VT: Noninvasive High−Resolution Mapping and Risk Assessment with ECGI. Pacing and clinical electrophysiology : PACE, 39(8), pp.781–791.

Zipes, D.P. et al., 2006. ACC/AHA/ESC 2006 Guidelines for Management of Patients With Ventricular Arrhythmias and the Prevention of Sudden Cardiac Death: a report of the American College of Cardiology/American Heart Association Task Force and the European Society of Cardiology Committee for Practice Guidelines (writing committee to develop Guidelines for Management of Patients With Ventricular Arrhythmias and the Prevention of Sudden Cardiac Death): developed in collaboration with the European Heart Rhythm Association and the Heart Rhythm Society. *Circulation*, 114(10), pp.e385–484.

Zipes, D.P., Jalife, J. & Stevenson, W.G., 2017. Cardiac Electrophysiology: from Cell to Bedside, Elsevier.

Zorzi, A. et al., 2013. Electrocardiographic Predictors of Electroanatomic Scar Size in Arrhythmogenic Right Ventricular Cardiomyopathy: Implications for Arrhythmic Risk Stratification. Journal of Cardiovascular Electrophysiology, 24(12), pp.1321–1327.

Zygmunt, A.C., Goodrow, R.J. & Antzelevitch, C., 2000. I NaCa contributes to electrical heterogeneity within the canine ventricle. *American Journal of Physiology - Heart and Circulatory Physiology*, 278(5), pp.H1671–H1678.